Identification of small molecule inhibitors targeting *Plasmodium falciparum* Hsp70-Hop pathway

A thesis submitted in fulfilment of the requirements for the degree of

Master of Science in Biochemistry

School of Mathematical and Natural Sciences

University of Venda

By

Muthelo Tshifhiwa

11621047

Supervisor: Prof. A. Shonhai

Co-supervisor: Dr. T. Zininga

June 2020

ABSTRACT

Malaria is caused by protozoan parasites of the *Plasmodium* genus. An estimated 405 000 million deaths due to malaria were reported in 2018. *Plasmodium falciparum* (*P. falciparum*) accounts for the deadliest form of the disease in Sub-Saharan Africa. *P. falciparum* has a complex life cycle spanning across both the mosquito vector and human hosts. During the lifecycle, the parasite is thus subjected to various physiological conditions. Therefore the parasite generally survives under stressful conditions and in response it upregulates its own molecular chaperones mainly the heat shock proteins (Hsps) in order to protect its protein constituents for survival. Heat shock protein 70 (Hsp70) together with heat shock protein 90 (Hsp90) are regarded as the most abundant cellular chaperones. Hsp70 and Hsp90 cooperate in order to exchange peptide substrates for folding and maturation. The cooperation of Hsp90 and Hsp70 is known to be facilitated by a co-chaperone, Hsp70-Hsp90 organizing protein (HOP) which serves as a module to facilitate interaction of the two chaperones. *P. falciparum* Hop (PfHop; PF3D7_1434300) brings together PfHsp70-1 and PfHsp90 into a functional complex. PfHop interacts with PfHsp70-1 (PF3D7_0818900) and PfHsp90 (PF3D7_0708400) through its tetracopeptide repeats (TPR) domains. PfHsp70-1 and PfHsp90 possess C-terminal EEVD and MEEVD motifs, respectively. The TPR1 and TPR2A of PfHop bind to the EEVD motif of PfHsp70-1 while TPR2B binds to the MEEVD motif of PfHsp90. It is thought that PfHsp70-1, PfHop and PfHsp90 form a functional complex that facilitates the folding of specific parasite proteins. Both PfHsp70-1 and PfHsp90 are essential molecules that could be specifically inhibited by potential antimalarial drugs. Therefore, this study evaluated the inhibition of the functional partnership between PfHop and PfHsp70-1 by colistin sulfate and pifithrin μ. In order to carry out in vitro assays, both PfHop and PfHsp70-1 were heterologously expressed in *E. coli* XL1 Blue cells and further purified by nickel affinity chromatography. Using ELISA, it was observed that the inhibition of the interaction between PfHsp70-1 and PfHop was more pronounced in the presence of colistin sulfate as compared to pifithrin μ. In addition, using surface plasmon resonance (SPR) assay, it was demonstrated that colistin sulfate and pifithrin μ directly bind to to PfHsp70-1 in nanomolar range. Furthermore, both colistin sulfate and pifithrin μ inhibited the PfHsp70-1 and PfHop interaction. Taken together, the findings from this study broadens the search for small molecule inhibitors of Hsp70 including repurposing some known antimicrobials such as colistin sulfate towards targeting malaria parasite.

Keywords: *Plasmodium falciparum*, molecular chaperone, PfHsp70-1, PfHop, inhibitor, colistin sulfate, pifithrin μ

DECLARATION

I, Tshifhiwa Muthelo hereby declare that this thesis for Master of Science degree in Biochemistry at the University of Venda, hereby submitted, is my original work and has not been submitted for any degree at any other University or institution. This thesis does not contain any other person's writings unless specifically acknowledged and referenced accordingly.

Signature  **Date:** 26/ 06/ 2020

DEDICATION

This thesis is dedicated to my parents, Maluta Richard Muthelo and Luambo Alice Thagwana, and to my late grandmothers, Tshisevhe Khuba Thagwana and Tshinondiwa Muthelo.

ACKNOWLEDGEMENTS

I am thankful for the opportunity that God has granted me with. Mighty God above everything.

I would like to express my special thanks of gratitude to my amazing supervisors Prof A. Shonhai and Dr T. Zininga for all the support, guidance and mentorship throughout the course of the project. I am very grateful that they never gave up on me.

I also wish to extend my acknowledgement to the following:

- National Research Council (NRF South Africa) for funding this research project.
- University of Venda Research Committee (South Africa) for research funding.

I also wish to thank Dr NE. Madala for proof-reading my thesis.

Lastly, many thanks to my incredible members of protein biochemistry and malaria research team (ProBioM) and staff members at the department of Biochemistry (University of Venda) for all the support and research conversations.

TABLE OF CONTENTS

Appendix C: Supplementary data

List of figures

List of tables

LIST OF OUTPUTS

Conference presentations:

Muthelo, T., Zininga, T., Shonhai, A. Identification of small molecule inhibitors targeting *Plasmodium falciparum* Hsp70-Hop pathway. 5th Annual Southern Africa Malaria Research Conference. "Co-operation for Elimination". 30 July-1 August 2019. University of Pretoria (Future Africa campus; South Africa).

Muthelo, T. NRF and British Council FAME LAB. Treatment of malaria using small molecules inhibitors targeting *Plasmodium falciparum* (PfHsp70-1-PfHop) pathway. November 2019. University of Venda, South Africa.

List of Symbols and Abbreviations

A320	absorbance at 320 nanometres
A600	absorbance at 600 nanometres
bp	base pair
kDa	kilodalton
%	percent
µl	microlitre
µM	micromolar
nM	nanometres
°C	degree celsius
µl	microlitre
ml	milliliter
l	litres
µg	microgram
ng	nanogram
g	gram
α	alpha
β	beta
DMSO	dimethyl sulphoxide
ER	endoplasmic reticulum
HPD	histidine-proline-asparatic acid
IPTG	isopropyl β-D-1 thiogalactopyranoside
NEF	nucleotide exchange factor
PMSF	Phenylmethylsufonyl fluoride
SBD	substrate binding domain
SDS-PAGE	sodium dodecyl sulphate polyacrylamide gel electrophoresis
NN	no nucleotide
ADP	adenosine diphosphate

ATP	adenosine triphosphate
TPR	tetratricopeptide repeat
ANOVA	analysis of varience

CHAPTER 1: INTRODUCTION

1.1. The Global burden of Malaria

Malaria is a life-threatening disease that is transmitted to humans during the bite of an infected female *Anopheles* mosquito. According to World Health Organization (WHO), an estimated 228 million malaria cases were recorded worldwide for the year 2018 which resulted in approximately 405 000 deaths globally (WHO, 2019). Malaria is endemic in the Sub-saharan Africa and India, accounted for almost 85 % of the global malaria burden (WHO, 2019). In addition, WHO also reported an increase in number of malaria cases in some Sub-saharan Africa countries like Nigeria, Madagascar and the Democratic Republic of Congo (WHO, 2018). This upsurge in cases shows that malaria is still a public health burden. There are five species of *Plasmodium* genus that are responsible for causing malaria in human namely *P. falciparum*, *P. vivax*, *P. ovale*, *P. malariae* and *P. knowlesis* (WHO, 2019). *P. falciparum* accounts for the most severe cases of malaria, accounting for 99.7 % of cases in the African region in 2018 (WHO, 2018).

1.2. *P. falciparum* life cycle

The protozoan parasite, *P. falciparum* has a complex life cycle that spans across both the mosquito vector and human host (Tuteja, 2007; Figure 1.1). Infection in humans begins with bite by an infected female *Anopheles* mosquito (Figure 1.1). This initiates the release of sporozoites into the blood stream of the human host and further migrate to the liver (Seraphim *et al*., 2014). Within the hepatocyte, the parasite differentiates and undergoes asexual reproduction which results in the release of thousands of merozoites that burst from the hepatocyte (Sturm *et al*., 2006; Tuteja, 2007). The merozoites get released into the blood stream and further invade red blood cells (RBCs). The transformation continues by allowing the parasite to replicate and form schizonts. As a result, mature schizonts rupture, releasing merozoites in the blood stream to infect additional RBCs (Fujioka *et al*., 2002; Tuteja, 2007). During this process, not all merozoites develop into schizonts, some merozoites develop into male and female gametocytes. These gametocytes are taken up by the mosquito during the blood meal (Boyle *et al*., 2010). This aids the differentiation of gametes in the mosquito's mid gut (Boyle *et al*., 2010). The flagellated microgametes produced

as a result of nuclear division by male gametocyte fertilizes the macrogametes to form a zygote. The zygote develops into an ookinete which penetrates the mosquito gut wall and develops into an oocyst (Boyle *et al*., 2010). The oocyst ruptures, and release sporozoites, which migrate to the salivary glands of the mosquito. The mosquito eventually infects a human and the life cycle continues. Mostly, drugs that are involved in the treatment of malaria targets the parasite during its development at the red blood cells stage.

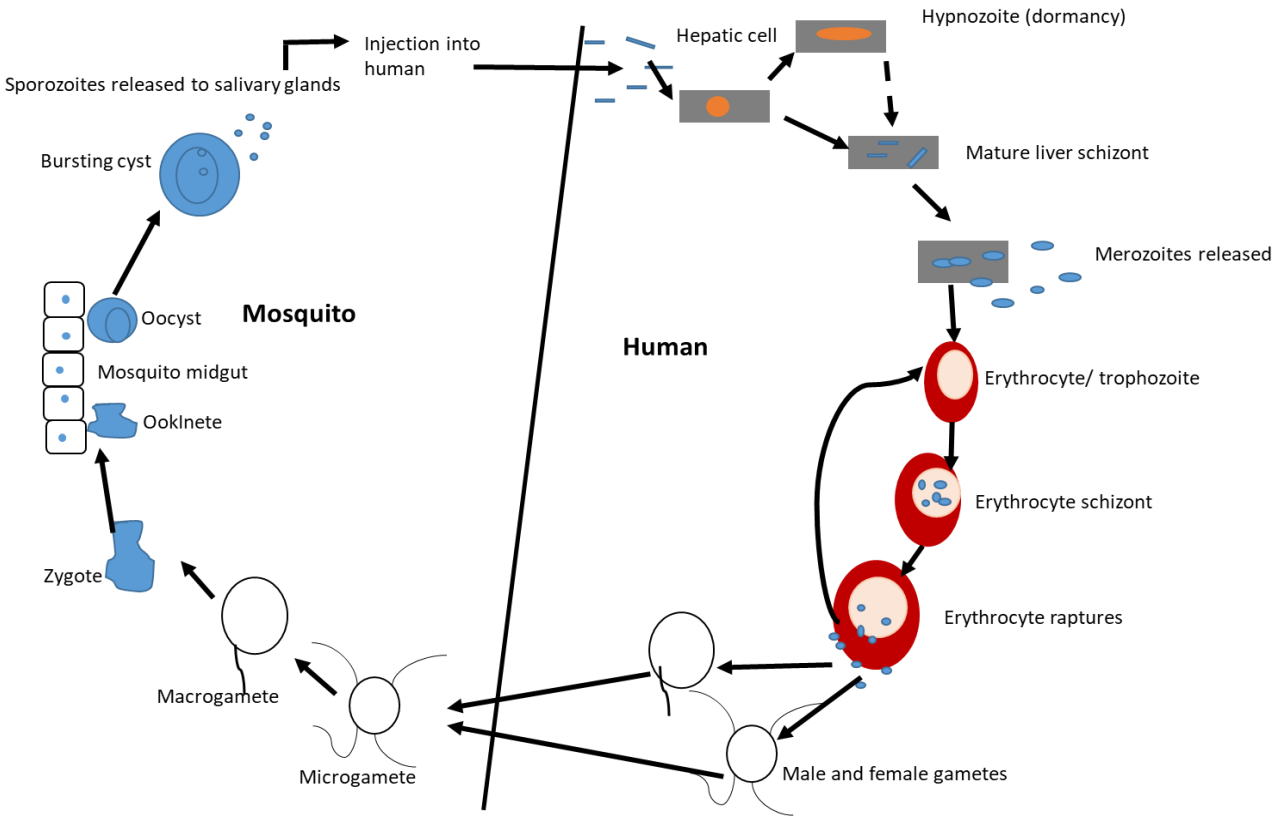

Figure 1.1: Parasite life cycle of *P. falciparum*. The schematic representation of *Plasmodium* life cycle showing the mosquito stage, the human stage which consists of the liver stage and the erythrocytic cycle stage. Adapted from Seraphim *et al*., (2014).

1.3. Antimalarial therapeutic agents and drug resistance

There are several interventions to reduce malaria cases, this include development of vaccines, vector control, chemoprophylaxis and antimalarial chemotherapy (Rappuloi and Aderem, 2011). Antimalarial chemotherapy is mostly based on natural products, semi-synthetic and synthetic

compounds that have been developed since the 1940s. The three main classes of currently used drugs in the treatment of malaria include quinolone derivatives, antifolates and artemisinin derivates (Staines and Krishna, 2012; Heise *et al*., 2013).

Quinolines are regarded as the first widely used drugs in the treatment of malaria. In the beginning of the 17th century, quinine was the first drug to be used in the treatment of malaria. Quinine (QN) is an alkaloid from the bark of *Cinochona* trees. This drug became common for malaria treatment from the mid-19th to 20th century. QN acts by blocking the parasite from polymerization of the heme to non-toxic haematin crystals (Hobbs and Duffy, 2011). The use of QN in the treatment of malaria was later abolished due to resistance of *P. falciparum.* The ineffectiveness of QN was associated with multi-drug resistance-like proteins, for example P-glycoprotein homologue 1 (*pgh1*; a product of *pfmdr1* gene) that is found in *P. falciparum* (Price *et al*., 1999; Cui *et al*., 2015). The function of pgh1 is to modulate the vulnerability of parasites to QN and other drugs, for example, mefloquine, chloroquine and artemisinin (Cowman *et al*., 1991; Rubio and Cowman, 1996; Gavigan *et al*., 2007). Resistance of *P. falciparum* to QN was speculated to be associated with pharmacokinetic profiles of the drug itself. The therapeutic responses and pharmacokinetic properties varies with age, pregnancy, immunity and severity of malaria (Reed *et al*., 2000). Nevertheless, QN is occasionally still used in combination with a second agent that minimizes the duration of therapy and adverse effects (Achan *et al*., 2011).

Chloroquine was also amongst the drugs widely used for the treatment of malaria for several years (Cui *et al*., 2015). It was regarded as the first-line antimalarial chemotherapy in the year 1947 (Cunico *et al*., 2008; Kaur *et al*., 2010). Chloroquine is a 4-aminoquinoline derivative of quinine, with high efficacy, low cost, and tolerable drug (Kraffs *et al*., 2012; O'Neill *et al*., 2012; Teixeira *et al*., 2014). Unfortunately, the parasite also developed resistance to chloroquine. The resistance was associated with a spontaneous mutation of *Pfmdr1* and *Pfcrt* (Price *et al*., 1999). An increase of *P. falciparum* resistance to quinolones derivatives led to synthesis of new derivatives with fewer modifications, such derivatives include amodiaquine, a 4-phenylamino-quinoline (Teixerira *et al*., 2014).

Piperaquine is a bis-4-aminoquinoline that was developed in the 1960s in France. Piperaquine was reported to have activity against chloroquine-resistant strains. The resistance to chloroquine was due to multiple mutation in 'chloroquine resistance transporter' gene (*pfcrt*). The *pfcrt* is required

in digestive vacuoles transport processes that are important for the parasite (Rowena and Kiaran, 2004). Furthermore, it was postulated that the resistance could be a result of phenotypic and genotypic alterations (Bunnet *et al*., 2007). The structure of piperaquine, a member of the quinolines class is similar to that of chloroquine, as such it is thought to inhibit transporter-mediated drug efflux pathway and protect other drugs against chloroquine resistance (Cunico *et al*., 2008).

Other drugs such as pyronaridine and mefloquine were also developed for the treatment of malaria. Both pyronaridine and mefloquine fall under the class of quinolones. Pyronaride was discovered and synthesized in China in the 1970s and its clinical use only started in the 1980s. Pyronaridine was very effective against *P. falciparum*, chloroquine-resistant strains. Pyronaridine acts by inhibiting b-hematin formation, which prevents the malarial parasite from neutralizing heme. Heme is toxic to the parasite, pyronaridine also inhibits the glutathione-dependent degradation of hematin. This increases hematin-induced lysis of RBCs. Both actions resulted in the death of the parasite (Cunico *et al*., 2008). Mefloquine was developed and synthesized by the United States Army in 1970. Mefloquine was also used in the fight against chloroquine-resistant strains (Cunico *et al*., 2008).

Antifolate derivatives were also an important class of antimalarial drugs. Antifolates were developed in 1940 and are classified into two categories (I and II). The classification was based on the mechanisms of action. Type I includes sulfodoxines, and type II includes proguanil and pyrimethamine. Type I class was responsible for blocking dihydrofolic acid production by inhibiting an essential enzyme dihydropteroate synthase (DHPS). On the other hand, type II class was considered to be very effective and responsible for inhibiting another enzyme called dihydrofolate reductase (DHFR). Proguanil was the first antimalarial antifolate reported and studies from the 1940s showed that proguanil was more active than quinine against the avian malaria (Curd *et al*., 1945; Wichmann *et al*,, 2003). Pyrimethamine was developed in 1952 and its clinical use started in 1953. Both proguanil and pyrimethamine of type II were regarded as powerful schizonticidal agents, because they act on asexual forms of the parasite (Figure 1.1; Bioland, 2001; Hyde, 2005). Generally, the antifolate derivatives are toxic to humans and have very low oral tolerance. The use of this class of drugs was eliminated due to a rapid increase of resistance in parasites (Nzila, 2012; Barnett and Guy, 2014). The resistance is thought to be

associated with specific gene mutations that encode for the enzyme DHPS and DHFR (Cunico *et al*., 2008; Cui *et al*., 2015).

The third class of derivatives is artemisinin (ART) that are natural products of sesquiterpene. Artemisinin derivatives were isolated from a Chinese medicinal plant *Artemisia annua* in 1971 (Ashton *et al*., 1998; Hobbs and Duffs, 2011). Since then, ART and its derivatives were used as first-line drugs for the treatment of malaria (Franac *et al.*, 2008; Cui *et al*., 2009; Mishra *et al*., 2014). In addition, ART gained more attention worldwide as chemotherapy against malaria. ART and its derivatives; dihydroartemisinin (DHA), artemether, arteether and artesunate act by killing the parasite at an early stage phase of development. However, drug resistance to these derivatives as monotherapies is associated with nucleotide polymorphisms in parasite's *kelch13* gene (Miotto *et al*., 2015). The role of Kelch13 protein in resistance is not clear. However, in a recent study done by Birnbau *et al*., (2020), they have found that eight other proteins that resides within the Kelch13 compartments are responsible for endocytosis of hemoglobin. In addition, the mutation in Kelch13 led to reduction of its activity. As a result, the reduced activity caused the resistance (Birnbau *et al*., 2020).

The resistance of the parasite to ART led to the development of artemisinin-based combination therapy (ACT; Hobbs and Duffy, 2011; WHO, 2015). ACT is the first-line therapy recommended to treat uncomplicated malaria with two extra drugs to reduce development of resistance (WHO, 2016). The use of ACT was implemented worldwide, especially in areas where *P. falciparum* infection results in severe outcomes. ACT is considered very effective and fast-acting than some of the quinolines drugs (Cui *et al*., 2015). ACT acts by clearing most parasites rapidly, while the partner drug clears the remains of the parasites from the blood (Butler *et al*., 2010). Therefore, ACT has provided a platform to produce novel drugs that can be used in combination with other drugs or just as monotherapies.

The capability of the parasite to survive under drug pressure is facilitated by molecular chaperones that assist proteins to fold natively despite the drug pressure (reviewed in Shonhai, 2010; Zininga and Shonhai, 2014). These molecular chaperones that are employed by the parasite are referred to as stress proteins. Some of these stress proteins are thought to be involved in drug resistance and interestingly, their expression levels were raised in artemisinin-resistant *P. falciparum* strain (Witkowski *et al.*, 2010). In a study done by Famin and Ginsburg (2003), it was shown that the

stress proteins interact with ferriprotoporphyrin IX, a malarial protein. Ferriprotoporphyrin IX is involved in the evolution of chloroquine resistance (Fitch, 1989). This suggests that the molecular chaperones may possibly be involved in the folding of some parasite proteins that are under drug pressure. Therefore; this explains the urgent need of novel antimalarial compounds that target these important chaperones only or in combination with other malarial proteins that are attractive drug targets.

1.4. Molecular chaperones

Molecular chaperones are proteins that play an important role of folding other proteins (Young *et al*., 2004; Bukau *et al*., 2006). In addition, they are responsible for assembly of client proteins, translocation and facilitate protein degradation (Wang *et al*., 2004). Molecular chaperones are also known to assist with stabilization of proteins and membranes, as well as aiding protein refolding under stressful conditions (Wang *et al*., 2004). Some molecular chaperones such as heat shock proteins (Hsp; section 1.5) are upregulated in response to cellular stress (Hartl and Hayer-Hartl, 2002). Hsps are crucial for the survival of parasites in the human host and their inhibition has been reported to result in the disruption of parasite growth (Pallavi *et al*., 2010).

1.5. Heat shock proteins as molecular chaperones

The term “heat shock proteins” (Hsps) was first described by Ritosa in fruit fly *Drosophila* which was subjected to heat stress (Ritosa, 1962). Ritossa observed that expression of chromosomal puffs in the salivary glands of *Drosophila* were due to heat shock treatment (Ritossa, 1962, 1963). This discovery led to the identification of heat shock proteins. Since then, many studies started to focus on the structures and functions of these groups of proteins. Most Hsps are highly expressed molecules that are present in all living organisms (Feder and Hofmann, 1999). In addition, Hsps are involved in many biological processes such as transcription, translation and posttranslational modification (Maio and Santoro, 2012).

1.5.1. Major heat shock protein groups of *P. falciparum*

Hsps are grouped into several families of proteins that carry out different functions (Table 1.1; Bukau *et al*., 2006). Hsps are categorized according to their molecular weights in kilodaltons (kDa) (Table 1.1: Bukau *et al*., 2006).

Table 1.1: Heat shock proteins families in *P. falciparum* and their functions

Protein family	**M.W (kDa)**	**Cellular localization**	**Function**	**References**
Hsp110	100-150	ER, cytoplasm	act as NEFs for Hsp70, inhibit protein folding	Dragovic *et al*., 2006; Vos *et al*., 2008; Muralidharan, 2012; Zininga *et al*., 2016; Kudyba *et al*., 2019
Hsp100	80-110	nucleus, cytosol, nucleolus, chloroplast, apicoplast, parasitophorous vacuole	folding and degradation of protein	Bosl *et al*., 2006; Barends *et al*., 2010; Nowicki, 2012; Bakkouri *et al*., 2010
Hsp90	82-96	cytosol, nucleus, ER, mitochondria, apicoplast	protein folding and maturation of steroid hormone receptors and kinases	Achrya *et al*., 2007; Hahn, 2009; Shonhai *et al*., 2011; Yang *et al*., 2015; Mora'n and Luengo, 2018
Hsp70	66-78	mitochondria, cytosol, ER, nucleus	serves as cytoprotection; folding and refolding of protein	Vos *et al*., 2008; Hartl and Hayer-Hartl, 2009; Chen *et al*., 2018
Hsp60	58-65	mitochondria	folding and assembling of protein	Sato and Wilson, 2005; Zhang *et al*., 2010
Hsp40	40-100	cytosol	recruits substrate for Hsp70; regulates Hsp70 activity	Botha *et al*., 2007; Njunge *et al*., 2013
sHsps	10-40	cytosol, nucleus	prevent protein aggregation	Vos *et al*., 2008; Mchaourab *et al*., 2009

Table legend: MW-molecular weight**,** ER- endoplasmic reticulum

1.5.2. Hsp40 family

Hsp40, (also known as DnaJ) in prokaryotes is made up of a highly conserved J-domain (Hennessy *et al*., 2005; Kampinga and Craig, 2009). The J-domain consists of 70 amino acids residues (Lie *et al*., 2009). The Hsp40s are grouped into four types (type I, II, III and IV) according to their structures and functions (Botha *et al*., 2011). The Hsp40s distribution vary across species. There are at least 50 Hsp40s in humans and 51 in *P. falciparum* (Kampinga *et al*., 2009; Njunge *et al*., 2013).

P. falciparum Hsp40s are classified into four subclasses; type I, type II, type III and type IV. The Type I has an N-terminal J-domain with G/F rich region, CRR domain and C-terminal SBD, type II has the same domains that type I has except for the zinc finger region. Type I and Type II are responsible for binding of substrates and directing them to Hsp70 (section 1.5.5) and further stimulate ATP hydrolysis for folding of proteins (Walsh *et al*., 2004; Hennessy *et al*., 2005). Type III are different from type I and type II as they only share the conserved J-domain with HPD motif (Xiao *et al*., 2006). Type IV members are similar to Type IIIs, however type IV possess a J-domain that lacks both the HPD motif and a C-terminal domain (Figure 1.3; Botha *et al*., 2007).

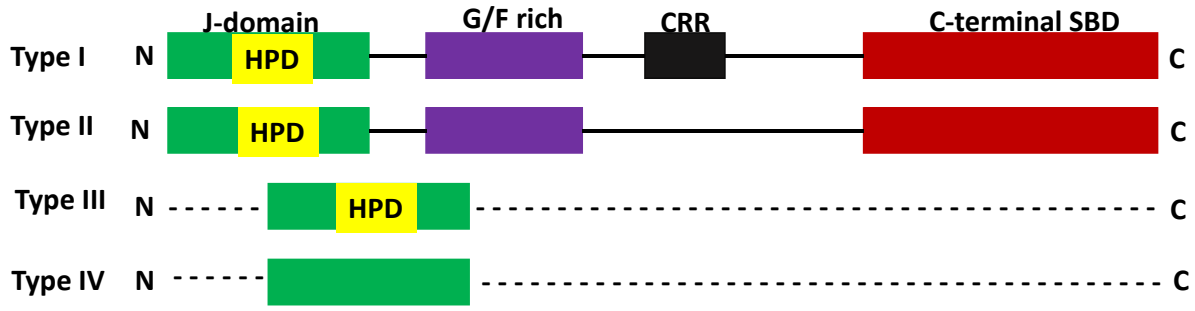

Figure 1.2: Classification of Hsp40 according to their domain organization. The different subdomains illustrated here are as follows: the J-domain with conserved HPD (His-Pro-Asp motif) glycine/phenylalanine rich region (G/F), CRR region and C-terminal SBD. The N-terminus is shown as 'N'. Adapted from Botha *et al* (2007).

Hsp40 is a well-known co-chaperone of Hsp70 (section 1.5.5). Hsp40 binds to substrates and hand over them to Hsp70 for proper folding (Figure 1.3; Botha *et al*., 2007, 2011). In addition, the association of Hp40 with Hsp70 modulates and stimulates Hsp70 ATPase activity (Botha *et al*.,

2007, 2011; Cockburn *et al*., 2014; Njunge *et al*., 2015). The complex formation of Hsp40 with Hsp70 is facilitated by the J-domain of Hsp40. The Hsp40-Hsp70 folding pathway begins when Hsp40 recruits unfolded protein to an Hsp70 that is bound to ATP with low affinity (Figure 1.3). Upon Hsp40 binding to Hsp70-ATP bound, the ATP hydrolysis of Hsp70 is stimulated by Hsp40 resulting in Hsp70-ADP-substrate complex with high affinity (Kampinga and Craig, 2010; Figure 1.3). This is followed by binding of nucleotide exchange factors (NEFs) that are required for ADP dissociation from Hsp70 to ATP state. As a result, the folded protein gets released (Figure 1.3; Evans *et al*., 2010).

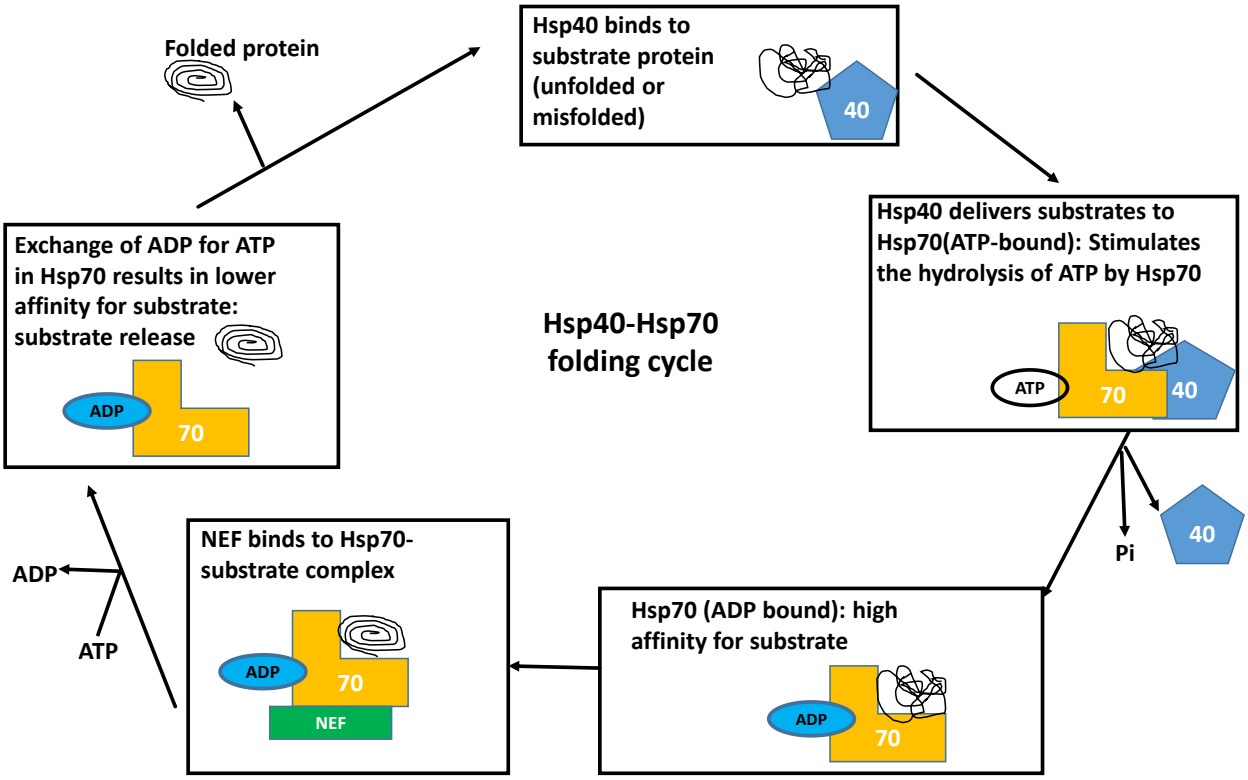

Figure 1.3: The Hsp40-Hsp70 folding cycle. The cycle is regulated by the Hsp40 and nucleotide exchange factors (NEFs), Adapted from Hennessy *et al*., (2005); Evans *et al* (2010).

Some of the Hsp40s that are encoded in *P. falciparum* contain *Plasmodium* export element (PEXEL) motif which enables them to get exported to the erythrocyte cytosol (Botha *et al*., 2007; Njunge *et al*., 2013). Amongst the exported Hsp40s, type IV Hsp40-like described as 'ring-infected erythrocyte surface antigen '(RESA) has been shown to be essential during malaria pathogenesis and for the survival of the parasite (Silva *et al*., 2005; Njunge *et al*., 2013). Type I and Type II

PfHsp40s associate with PfHsp70 to modulate and activate ATPase activity of Hp70 (Njunge *et al*., 2015). In addition, Botha and colleagues (2011) showed that PfHsp40 (PF3D7_1437900), a type I member forms a functional complex in the parasite cytoplasm with PfHsp70-1. Furthermore, type I Hsp40s are thought to independently function as holdase (protein misfolding suppressing) chaperones and are capable of forming a functional complex with Hsp70 chaperones as compared to their type II counterparts (Lu and Cyr, 1998; Rosser and Cyr, 2007).

Studies have shown that plasmodial and human Hsp40 and Hsp70 chaperone systems can be selectively modulated by small molecules inhibitors. For example, an Hsp70 inhibitor pyrimidinone was reported to selectively inhibit PfHsp40-PfHsp70 partnership without affecting the human Hsp40-Hsp70 system (Botha *et al*., 2011). In addition, Cockburn and colleagues (2011, 2014) reported that malanganenone A, B, C and lapachol inhibited the Hsp40-stimulated ATPase activity of PfHsp70-1. These observations make Hsp40-Hsp70 partnership an attractive drug target (Botha *et al*., 2011; Cockburn *et al*., 2011; Zininga and Shonhai, 2014, 2019).

1.5.3. Hsp90 family

The Hsp90 family is a cellular signaling hub and a highly abundant chaperone composed of several biological functions (Saibil, 2013). Hsp90 is required for activation and stabilization of many client proteins that are involved in cellular process like signal transduction (Li *et al*., 2011). Hsp90 functions include, preventing the aggregation of polypeptides and facilitating the folding of proteins involved in transcription regulation (Bagetell and Whites, 2004, Saibil, 2013). Hsp90 is made up of three highly conserved subdomains (Figure 1.3); a 25 kDa N-terminal ATP-binding domain (NBD), 35 kDa middle domain which is involved in ATP hydrolysis and substrate binding. Notably, in Hsp90, the ATP hydrolysis is fairly slow. The C-terminal domain is required for dimerization of the protein (Ciglia *et al*., 2014). In the C-terminal there is a dimerization domain, responsible for Hsp90 dimer formation. Dimerization is essential for *in vivo* functioning of Hsp90 (Wayne and Bolon, 2007). The C-terminal is also made of an MEEVD motif that facilitates the binding of peptide and TPR containing co-chaperones such as Hop (section 1.6; Figure 1.7; Tarasawa *et al*., 2005).

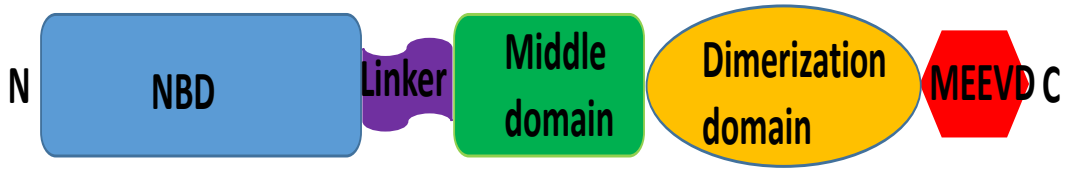

Figure 1.4: Diagrammatic representation of Hsp90, showing the N-terminal (NBD), flexible linker region, the middle domain and C-terminal (dimerization domain and an MEEVD). Adapted from Whitesell and Lindquist (2005).

The Hsp90 system is modulated by several co-chaperones and substrates (Krunkenberg *et al*., 2011). Co-chaperones that target Hsp90 include p50 (also known as CDC37), a set of prolyl isomerase activity such as immunophilin 52 kDa FK506-binding protein (FKBP52). The tetratricopeptide repeat (TPR) domains are responsible for the interaction of these co-chaperones (Prodromou *et al*., 1999; Lie *et al*., 2012). Hsp90 has several functional partners that regulate its structure and function, for example, Hsp40, Hsp70, p23 and TPR domain-containing co-chaperones (Ratzke *et al*., 2010; Jhaveri *et al*., 2012; Karagoz and Rudiger, 2015; Lie *et al*., 2018). In addition, Hsp90 coordinates with Hsp70 (section 1.5.5) through a Hop protein (section 1.6) to facilitate several Hsp90 client proteins (Shonhai *et al*., 2011; Lie *at al*., 2018). In general, Hsp90 is responsible for folding of some signal transduction proteins such as kinases, transcription factors and steroid hormone receptors (Krunkenberg *et al*., 2011; Wayne *et al*., 2011).

1.5.4. *P. falciparum* Hsp90

The *P. falciparum* genome encodes for four Hsp90 proteins, a cytosolic PfHsp90 (PF3D7_0708400), endoplasmic reticulum (ER) Hsp90 Grp94 (PF3D7_1222300), a mitochondrial TRAP1 (PF3D7_1118200) and an apicoplast Hsp90 (PF3D7_1443900) (Kumar *et al*., 2003). PfHsp90 is a stress-inducible protein. As such, it has been shown to be upregulated during heat stress (Pallavi *et al*., 2010). In addition, PfHsp90 is an essential chaperone in the parasite as it is involved in the latter development especially in fever stages (Banumathy *et al*., 2003; Pavithra *et al*., 2004). Therefore, this makes PfHsp90 a promising drug target as its inhibition leads to parasite death (Zininga and Shonhai, 2014). Several studies have identified inhibitors that target PfHsp90. Such inhibitors include a well-known Hsp90 inhibitor geldanamycin (GA). This inhibitor has been shown to bind and inhibit Hsp90 activity (Banuthamy *et al*., 2003). In another

study conducted by Pallavi and colleagues (2010), 17-allylaminogeldanamycin (17-AAG) was shown to inhibit the activity of Hsp90. This highlights the importance of the Hsp90 chaperone in the parasite. Furthermore, the cytosolic PfHsp90 (PF3D7_0708400) occurs in a functional complex with PfHsp70-1 (section 1.6.5.3.1; Gitau *et al*., 2012; Zininga *et al*., 2015a). This complex is linked by PfHop (section 1.6.2) to facilitate the transfer of substrates for further folding (Gitau *et al*., 2012).

1.5.5. Hsp70 family

The 70 kDa heat shock protein (Hsp70) is regarded as the most abundant chaperone family found in all major organelles. In *E. coli,* Hsp70s are known as 'DnaK' while in mammals they are referred to as 'HSPA' (Kampinga *et al*., 2009). Hsp70 family is ubiquitous, well conserved and falls under the best studied chaperone as it is involved in several roles in the cell (Kampinga *et al*., 2009; Saibil, 2013). Some members of Hsp70 family are expressed in the absence of heat stress and are referred to as cognate (Hsc70) while other members are expressed in the presence of cellular stress such as temperature changes and are referred to as heat shock proteins (Hsp70s) (Szabo *et al*., 1994; Botha *et al*., 2007). Both groups are virtually important for maintenance of cellular proteostasis under normal and stressful conditions. Hsp70s are responsible for protein folding, translocations across organelle membranes and disaggregation and signal transduction (Kabani and Martineau, 2008; Saibil, 2013). Hsp70 functional valency is expanded on account of its interaction with other chaperones and co-chaperones such as Hsp40, Hsp60, Hsp90, Hsp100 and Hsp110 (Mayer and Bukau, 2005; Mogk *et al*., 2015).

1.5.5.1. The structural features of Hsp70

Hsp70s are structurally divided into two major domains namely; a 45 kDa N-terminal nucleotide binding domain (NBD) that exhibits ATPase activity and a 25 kDa substrate binding domain (SBD). The SBD is composed of β-sheets and α-helical subdomains (Figure 1.5; Mayer and Bukau, 2005).

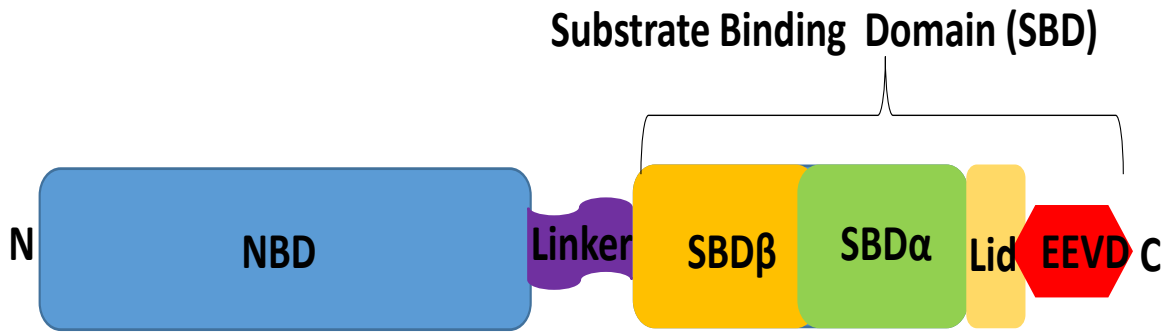

Figure 1.5: Structural domains of Hsp70. The N-terminal consists ATPase domain; NBD (45 kDa) and central substrate binding domain (SBD) are separated by a linker region. The C-terminal domain of cytosolic Hsp70 proteins typically contains a highly conserved EEVD motif. Adapted from Sharma and Masison (2009).

The NBD and SBD domains are connected by a highly charged flexible linker domain (Chakafana *et al*., 2019). The linker is responsible for allosteric regulation of NBD and SBD activities. In the C-terminal, there is a lid that is more alpha helical, and an EEVD motif. The EEVD motif enables this protein to communicate with co-chaperones (Assimon *et al*., 2015).

Hsp70s function depend on ATP hydrolysis. Generally, Hsp70s have high affinity for substrate when bound to ADP, but have low affinity when bound to ATP, thus allowing the substrate to be released (Evans *et al*., 2010). In a case where a co-chaperone and substrate are absent, ATP hydrolysis is rate limiting as Hsps70s display a low basal ATPase activity. Hsp70s cooperate with several co-chaperones such as Hp40s and nucleotide exchange factors (NEFs) (section 1.5.2) that primarily bind to its ATPase domain to facilitate binding of substrates and their release (Figure 1.3; Hennessy *et al*., 2005; Brodsky and Bracher, 2007). The functional partnership between Hsp70s and Hsp40s is thus crucial for successful substrate refolding (Figure 1.3).

1.5.5.2. *P. falciparum* Hsp70s

The *P. falciparum* genome encodes for six Hsp70 proteins that are localized in different cellular organelles of the parasite as summarized in a table below (Table 1.2; Shonhai *et al*., 2007).

Table 1.2: *P. falciparum* Hsp70s and their functions

Name	Molecular weight (kDa)	Localisation	Functions	References
PfHsp70-1 (PF3D7_0818900)	74	nucleus and cytosol	protein folding and aggregation	Shonhai *et al*., 2007; Pesce *et al*., 2008
PfHsp70-x (PF3D7_0917900)	76	exported to parasite infected RBC	parasite protein export and refolding in host red blood cell	Kulzer *et al*., 2012 ; Cobb *et al*., 2017; Charnaud *et al*., 2017
PfHsp70-2 (PF3D7_1134000)	73	ER	import of *P. falciparum* protein to the ER, protein folding and quality control in the ER	Njunge *et al*., 2013; Chen *et al*., 2018
PfHsp70-3 (PF3D7_0831700)	73	mitochondrion	import of proteins into the mitochondrial matrix	Shonhai *et al*., 2007; Njunge *et al*., 2013 ; Nyakundi *et al*., 2016
PfHsp70-y (PF3D7_1344200)	108	ER	NEF for PfHsp70-2	Shonhai *et al*.,2007; Njunge *et al*., 2013; Kudyba *et al*., 2019
PfHsp70-z (PF3D7_0708800)	100	cytoplasm	NEF of PfHsp70-1, suppresses protein aggregation	Muralidharan *et al*., 2012; Zininga *et al*., 2015b; Zininga *et al*., 2016

Table legend: NEF-nucleotide exchange factor, ER-endoplasmic reticulum, RBC-red blood cell

1.5.5.2.1. PfHsp70-1

PfHsp70-1 is highly expressed and is involved in the development of *P. falciparum* at all life stages (Matambo *et al*., 2004; Shonhai *et al*., 2008). PfHsp70-1 is induced by both stress and growth stage related factors (Sharma, 1992; Shonhai *et al*., 2007). PfHsp70-1 exhibits ATPase activity and is efficient at preventing heat-induced protein aggregation (Matambo *et al*., 2004; Shonhai *et al*.,

2005, 2008). PfHsp70-1 is involved in the cyto-protection of the parasite during stressful conditions, suggesting that it is essential for the survival of the parasite in the human host (Pesce *et al*., 2008; Shonhai *et al*., 2011). PfHsp70-1 has been shown to co-localize with PfHop (section 1.6.2) and PfHsp90 (section 1.5.4) in the parasite cytosol (Gitau *et al*., 2012). There is evidence that the three proteins form a functional complex that facilitates the folding of some select parasite proteins (Gitau *et al*., 2012; Zininga *et al*., 2015a).

It has become apparent that PfHsp70-1 is an attractive drug target (Shonhai *et al*., 2010, 2014). However, targeting *P. falciparum* proteins is a challenge, as these proteins share high sequence structural and functional conservation with their human homologs (Pesce *et al*., 2010; Shonhai, 2010). For example, the cytosolic PfHsp70-1 and the human HSP1A share over 72 % (sequence identity). Interestingly, a recent study showed that even though there is high conservation between the PfHsp70-1 and its human homologues, there are certain structure-function features of the protein that set it distinctly from its human homologues (Chakafana *et al*., 2019). Using bioinformatics tools, Chakafana *et al* (2019) identified the following motifs; Magic, Tedwlyee, GGMP and EKEK which seem to exist in the parasite Hsp70s, distinguishing the latter from their human homologues (Chakafana *et al*., 2019). However, the role of these motifs on the structure–function features of PfHsp70-1 have not been fully elucidated. Encouragingly, Lebepe *et al* (2020) demonstrated that PfHsp70-1 exhibits unique structure-function features compared to *E coli* DnaK. While the same study demonstrated that the functional specificity of PfHsp70-1 is dictated by its SBD, it was also demonstrated that interdomain communication between the NBD and the SBD also regulates functional specificity of the protein. Furthermore, Lepebe *et al* (2020) demonstrated that PfHsp70-1 is tailored to refold plasmodial proteins more effectively than DnaK. Altogether, this suggests that plasmodial Hsp70s are functionally unique. Not surprisingly, *P. falciparum* Hsp70s have been the focus in the development of novel antiplasmodial inhibitors. Some of the inhibitors that have been identified so far are summarized in (Section 1.7). Interestingly, novel inhibitors identified by Cockburn and colleagues (2014) showed selective inhibition of parasite Hsp70s without affecting their human counterparts.

1.6. Hsp70-Hsp90 organizing protein (Hop)

1.6.1. Structural features and function of Hop

Hop was first identified in yeast and it belongs to the most studied co-chaperone of Hsp70-Hsp90 complex (Nicolet and Craig, 1989). Hop is also known as stress inducible protein 1 (STI1), stress-inducible phosphoprotein 1 (STIP1 or p60; Johnson and Brown, 2009). Hop is a highly conserved eukaryotic protein. Hop is encoded in the genome of many organisms, for example humans, fruit flies (*Drosophilla*) (Grisgas *et al*, 1998), Zebrafish (Woods *et al*., 2005), parasites (Webb *et al*., 1997; Hombach *et al*., 1998).

Structurally, Hop is composed of three tetratricopeptide repeat (TPR) domains (TPR1, TPR2A and TPR2B) and two dipeptide repeats (DP1 and DP2) as shown (Figure 1.8; Odunuga *et al*., 2003). Hop functions by linking together Hsp70 and Hsp90 chaperones. Both Hsp70 and Hsp90 contain the EEVD motifs which are necessary for interaction with TPR domains of Hop (Flom *et al*., 2006). Thus, TPR domains are required for protein-protein interactions.

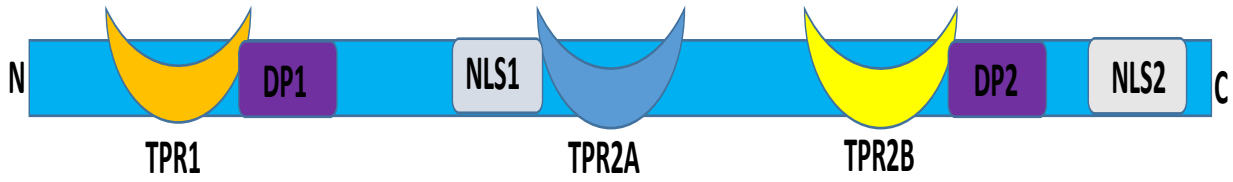

Figure 1.6: Schematic representation of Hop TPR domains. The structure shows Hop TPR domains (TPR1, TPR2A and TPR2B). Two aspartate-proline dipeptide repeats (DP1 and DP2) and nuclear localization signal (NLS1 and NLS2). Adapted from (Gitau *et al*., 2012).

The DP repeats are rich in aspartate-proline. DP1 is thought to be involved in the ATPase of Hop while DP2 is responsible for providing support to Hop in binding Hsp70 (Schmid *et al*., 2012; Yamamoto *et al*., 2014). Hop also possesses nuclear localization signal (NLS1 and NLS2) (Figure 1.8). Hop serves as a link between Hsp70 and Hsp90. In addition, Hop interacts with the EEVD motifs of Hsp90 and Hsp70 through the TPR domains. Hsp70 binds to TPR1 and TPR2B domains while Hsp90 binds to the TPR2A subdomain of Hop (Chang *et al*., 1997; Gitau *et al*., 2012; Yamamoto *et al*., 2014; Zininga *et al*., 2015a).

1.6.2. *P. falciparum* Hsp70-Hsp90 organizing protein (PfHop)

P. falciparum Hsp70-Hsp90 organizing protein (PfHop; PF3D7_1434300) is a conserved molecule across *Plasmodium* genus and is structurally divergent from human Hop (Odunuga *et al*., 2003; Gitau *et al*., 2012). PfHop contain conserved structural features of a general Hop protein, particularly TPR1 and TPR2A domains known to interact with the EEVD motifs of Hsp70 and Hsp90 are conserved (Scheufler *et al*., 2000; Odunuga *et al*., 2004; Gitau *et al*., 2012). PfHop is expressed at the erythrocyte stage and its expression is upregulated in response to heat stress (Gitau *et al*., 2012; Zininga *et al*., 2015a). PfHop is localized to the cytosol and is also found in the nucleus (Hajj *et al*., 2013). Furthermore, PfHop co-localizes with PfHsp70-1 and PfHsp90 in the parasite cytosol forming a PfHsp70-PfHop-PfHsp90 complex in the parasite cytosol (Gitau *et al*., 2012). This functional complex is thought to be essential for folding of some select parasite protein (Gitau *et al*., 2012). As such, it can be targeted towards development of antimalarial drugs.

The current model of Hsp70-Hop-Hsp90 indicates that newly synthesized polypeptide is partially folded by Hsp70 that is bound to TPR1 domain of Hop and then gets transferred to Hsp90 that is bound to TPR2A of Hop (Figure 1.9). The transfer of polypeptide from Hsp70 to Hsp90 through Hop ensures the correct folding and maturation of proteins. Binding of Hsp90 to TPR2A causes a conformational change which allows Hp70 to bind to TPR2B domain of Hop with high affinity (Figure 1.9; Seo, 2015). Thus Hsp90 presence facilitates high affinity binding of Hsp70 to Hop. Furthermore, the collaboration between Hsp70 and Hsp90 linked by Hop allows proteins to be fully folded into their functional state (Figure 1.9). For the interest of this study, it is assumed that the introduction of an inhibitor in the Hsp70-Hop-Hsp90 pathway will disrupt the folding of proteins (Figure 1.7). The inhibitor of interest is assumed to target Hsp70 function which will eventually inhibit the transfer of substrates from Hsp70 to Hsp90. As a result, substrates that require Hsp90 for further folding will be misfolded and later subjected to degradation (Figure 1.9).

Protein degradation is another process which is facilitated by a number of co-chaperones. For example, a C-terminal Hsp70 interacting protein (CHIP) is known to facilitate protein degradation (McDonough and Petterson, 2003). CHIP is a TPR containing molecule, just like Hop, it interacts with Hsp70 and Hsp90 through its TPR domains. The primary function of CHIP is to channel the chaperone complexes (Hsp70 and Hsp90) for degradation (Demand *et al*., 2001). CHIP interacts with Hsp70 and Hsp90 as a way of targeting their client proteins for ubiquitination and to

proteasome for degradation (Stankiewicz *et al*., 2010; Shiber and Ravid, 2014). This denotes a central role of CHIP in protein degradation. Taken together, the Hsp70-Hop-Hsp90 pathway is extremely attractive for novel drug design.

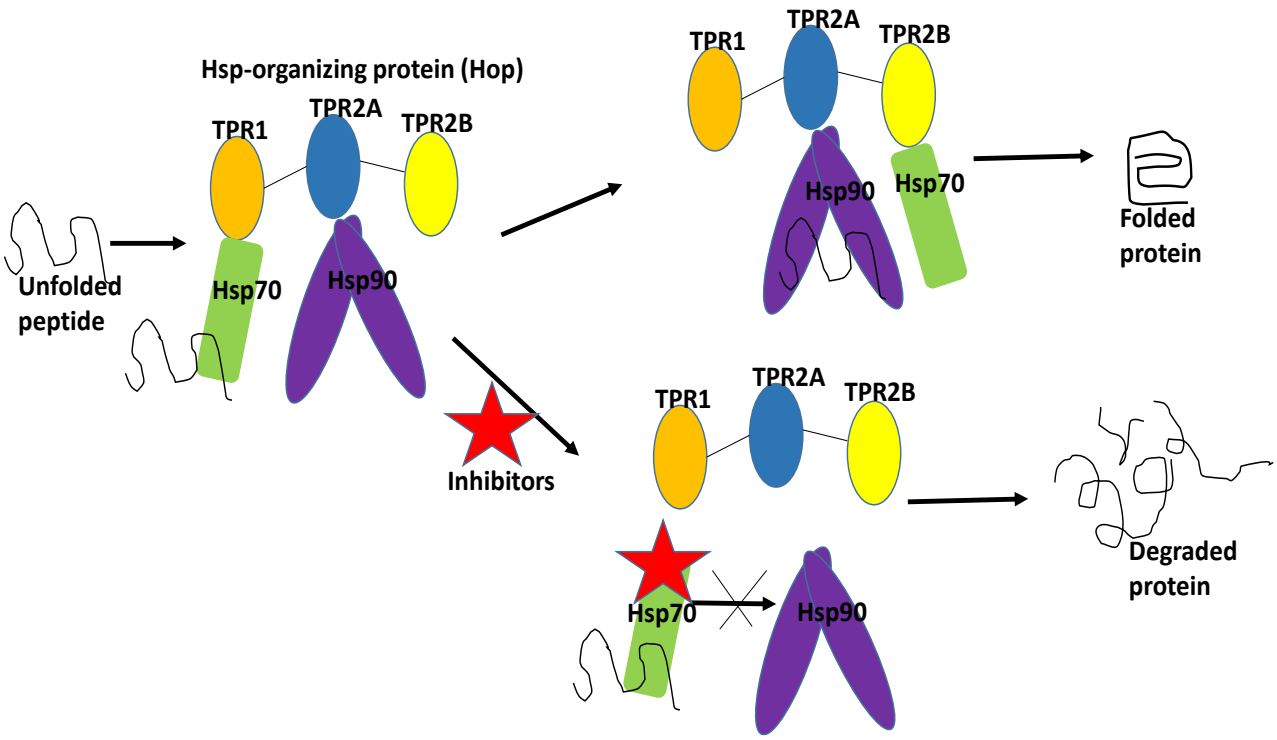

Figure 1.7: Schematic diagram of Hsp70-Hop-Hsp90 folding relay system. The figure shows the cooperation of Hsp70, Hsp90 and Hop in mediating protein folding. Hsp70 and Hsp90 are brought into proximity by Hop. The model assumes that a newly synthesized peptide is first chaperoned by Hsp70 bound to TPR1 and further transferred to Hsp90 bound to TPR2A for correct folding. The interaction between these three proteins form a multichaperone complex of Hsp70-Hop-Hsp90. The introduction of an inhibitor in the complex will prevent protein folding through this complex. As a result, some proteins will not be fully folded, hence they will undergo degradation. Adapted from Seo (2015).

1.7. Hsp70 inhibitors

Many studies have shown that Hsp70 is an attractive molecule in the development of novel drugs against malarial parasite. Some of the novel and repurposed inhibitors of Hsp70 are summarized in a table (Table 1.3; Zininga and Shonhai, 2019).

Table 1.3: Hsp70 inhibitors and their antimalarial effects

Inhibitor name	Target protein	Antimalarial effect	References
Malonganenone derivatives (A, B, C)	PfHsp70-1 and PfHsp70-x	Selectively inhibited the ATPase activity of both PfHsp70-1 and PfHsp70-x	Cockburn *et al*., 2011; Cockburn *et al*., 2014
Lapachol (1.4 naphthoquinone	PfHsp70-1 and PfHsp70-x	Selectively inhibited the ATPase activity of both PfHsp70-1 and PfHsp70-x	Cockburn *et al*.,2011
EGCG	PfHsp70-1 and PfHsp70-z	EGCG binds to NBD of PfHsp70-1. In addition, EGCG inhibited the chaperone and ATPase activities of both PfHsp70-1 and PfHsp70-z, in addition, EGCG inhibited parasite growth IC_{50}= 2.9 µM	Zininga *et al*., 2017b
PMB	PfHsp70-1 and PfHsp70-z	Inhibited the chaperone and ATPase activities of both PfHsp70-1 and PfHsp70-z	Zininga *et al*., 2017a
Apoptozole, MKT-077, VER-15008 (repurposed anticancer inhibitors)	PfHsp70-2	Apoptozole, MKT-077 and VER-15008 bind to PfHsp70-2, in addition, they have exhibited some antiplasmodial activities to *P. falciparum* 3D7 and W2 strains	Chen *et al*., 2018

Table legend: EGCG- Epigallocatechin-3-gallate, PMB- Polymyxin B, NBD- Nucleotide binding domain

This study focuses on repurposing two known Hsp70 inhibitors (colistin sulfate and pifithrin µ; Figure 1.8) towards their use in the treatment of malaria. Colistin sulfate is amongst different compounds of polymyxins (A-E). Colistin sulfate is also known as polymyxin E and its molecular formula is $C_5H_{102}N_{16}O_{17}S$ (Falagas and Kasiakou, 2005; Minagawa, 2012). Colistin sulfate is composed of decapeptide identified by the presence of five positively charged amine residues from Dab and a lipophilic tail (Falagas and Kasiakou, 2005; Minagawa, 2012). Colistin sulfate is a lipopeptide that was discovered in 1949 (Komura and Kurahashi, 1979). Colistin sulfate was synthesized from *Bacillas polymyxa*, subspecies *colistinus Koyama* (Komura and Kurahashi, 1979). Colistin sulfate targets the bacterial cell membrane by binding to anionic lipopolysaccharide molecules and alters bacterial outer membrane permeability. As a result, cell contents are released and this leads to bacterial death (Falagas and Kasiakou, 2005; Minagawa, 2012).

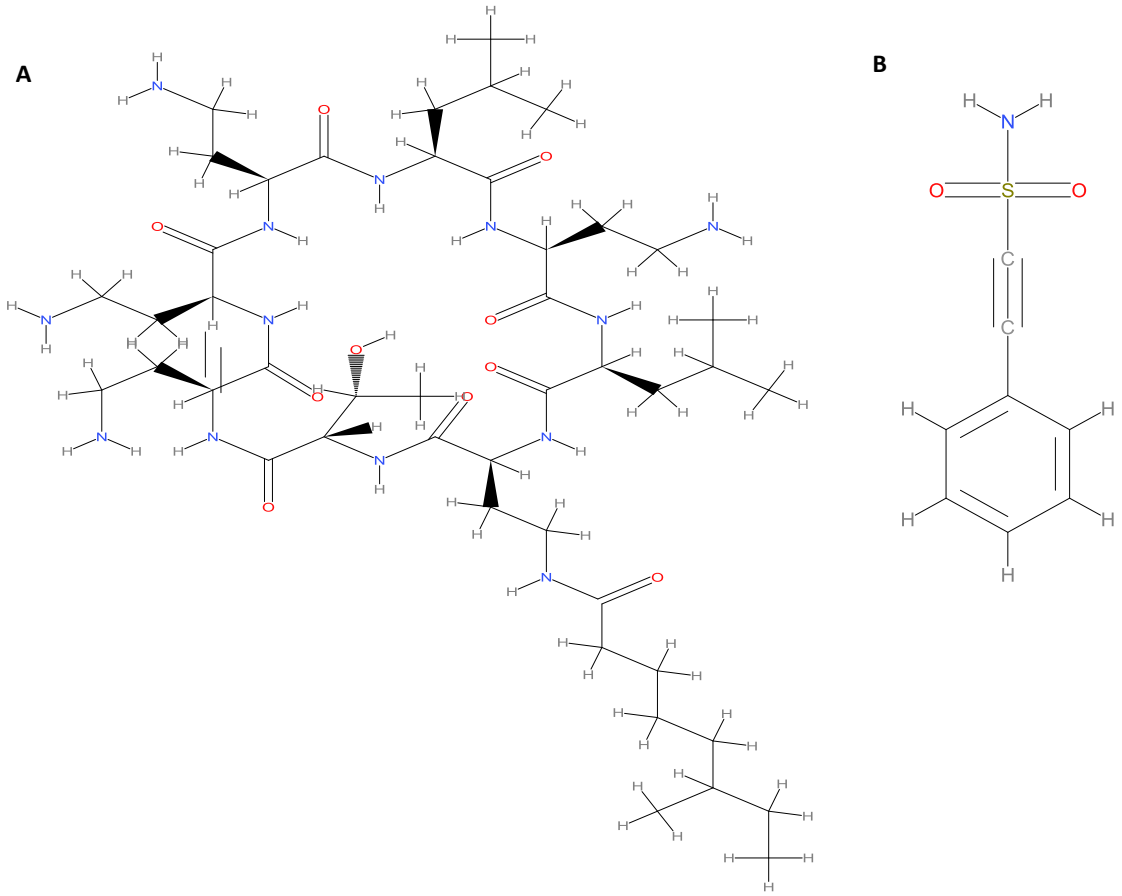

Figure 1.8: Chemical structures of colistin sulfate (A) and pifithrin μ (B). The structures were generated using Chem4Word version 3.1.

The use of colistin sulfate has been in the treatment of multidrug-resistance Gram-negative bacteria (Nation and Li, 2009). Colistin sulfate was initially used in cancer to target Hsp90. It was shown that it binds to the N-terminal of Hsp90 and inhibit its chaperone function (Bergen *et al*., 2006; Nation and Li, 2009; Minagawa *et al*., 2012). In addition, the derivative of colistin sulfate, PMB, has been shown to bind to Hsp70 and modulate its function (Zininga *et al*., 2017a). Furthermore, colistin sulfate and PMB share similar mechanism of action, thus making colistin sulfate a promising compound to target Hsp70.

Pifithrin μ also known as 2-phenylthynesulfonamide (PES) is a member of benzene family and its molecular formula is $C_8H_7NO_2S$ (Jemal *et al*., 2010; Wen *et al*., 2014). It was designed and identified as an inhibitor of tumor protein p53 (p53) which is referred to as nuclear transcription factor (Lacroix *et al*., 2006; Strom *et al*., 2006). The p53 is responsible for regulating cell cycle

and prevents tumor formation (Lacroix *et al*., 2006). In a study done by Liu *et al*., (2009), pifithrin μ was confirmed that it interacts with Hsp70 in the SBD and inhibit its function in cancer cells. Both colistin sulfate and pifithrin μ have not been tested if they possess any antimalarial activity, hence, this study sought to investigate their effect on *P. falciparum* proteins.

1.8. Problem statement

To date, malaria is still regarded as one of the main health burdens across the world affecting more than half of the world's population (WHO, 2019). To complicate the existing burden of malaria, there is an increase in antimalarial drug resistance, which further delays the efforts to eradicate this disease. Heat shock proteins which assist in maintaining the protein quality control in the parasites have been implicated in drug resistance (Bukau *et al*., 2006; Shonhai *et al*., 2008).). Both PfHsp70-1 and PfHsp90 are essential for parasite survival as they facilitate proper folding of parasite proteins unfolded and mutated under drug pressure into their native functional state (Shonhai *et al*., 2005; Shonhai *et al*., 2008; Taipale *et al*., 2010; Postai *et al*., 2018).).

Both PfHsp70-1 and PfHsp90 form a functional complex with PfHop that is responsible for folding of some parasite proteins (Gitau *et al*., 2012; Zininga *et al*., 2015a). There is high unmet need for novel antimalarials and inhibitors of Hsps are attractive drug candidates. There are efforts to screen for novel compounds to meet the high need for novel antimalarials. This study is part of efforts aimed at repurposing previously described drugs as potential antimalarials targeting the protein folding pathway (Shonhai, 2010). Our group has shown that epigallocatechin-3-gallate (EGCG) and polymyxin B (PMB) bind and inhibited PfHsp70-1 function (Zininga *et al*., 2017a, b). In addition, both compounds inhibited the interaction of PfHsp70-1 and PfHop (Zininga *et al*., 2017a, b). Therefore, this study sought to screen compounds that inhibit the formation of the PfHsp70-PfHop complex.

1.9. Hypothesis

Both colistin sulfate and pifithrin μ inhibit the association between *P. falciparum* Hsp70 and the adaptor protein Hop.

1.10. The aim of the study

The main aim of this study is to evaluate the inhibitory effects of colistin sulfate and pifithrin μ on PfHsp70-1-PfHop complex formation.

1.11. Specific Objectives

- To heterologously overexpress PfHsp70-1 and PfHop using *E. coli* XL1 Blue cells and purify the recombinant proteins using affinity chromatography
- Develop and optimize an enzyme-linked immunosorbent assay (ELISA) for PfHsp70-1-PfHop interaction
- To investigate the inhibitory effects of colistin sulfate and pifithrin μ on the direct association of PfHsp70-1 and PfHop using ELISA
- To evaluate the PfHsp70-1 binding affinity to the colistin sulfate and pifithrin μ using surface plasmon resonance (SPR) assay

CHAPTER 2: MATERIALS AND METHODS

2.1. Materials

The following restriction enzymes were used to confirm the integrity of the plasmid DNA; *Bam*HI, *Hind*III, *Sph*I and *Pst*I. Plasmids and *E. coli* strains used for the production of recombinant proteins are listed in a table below (Table 2.1). The following previously described antibodies were used to confirm the expression and purification of recombinant proteins; rabbit raised α-PfHsp70-1 (Shonhai *et al*., 2008), rabbit raised α-PfHop (Gitau *et al*., 2012), α-His antibody and HRP conjugated α-rabbit from Thermofischer Scientific (USA). The other reagents used in this study are listed in appendix section (Appendix A1).

Table 2.1: List of plasmids and *E. coli* strains used for recombinant protein expression

Plasmids and Recombinant protein expression strains	**Description**	**Supplier/Reference**
Plasmids		
pQE30/PfHsp70-1	encoding PfHsp70-1, Amp^R	Makumire *et al*., 2020; Lebepe *et al*., 2020
pQE30/PfHop	encoding PfHop, Amp^R	Gitau *et al*., 2012
Expression Strains		
E. coli XL1 Blue	recA1 endA1 gyrA96 thi1 hsdR17 supE44 relA1 lac (F' proAB laclqZM15 Tn10 (Tetr)	Thermofischer Scientific, USA
E. coli JM109	e14-(McrA-) recA1 endA1 gyrA96 thi-1 hsdR17 (rK-mK+) A1 Δ(lac-proAB) (F' traD36 proAB lacIqZΔM15)	Thermofischer Scientific, USA

2.2. Confirmation of PfHsp70-1 and PfHop expression constructs

E. coli JM109 competent cells were chemically prepared (Appendix B1) and used for transformation using the plasmid constructs, pQE30/PfHsp70-1 and pQE30/PfHop expressing PfHsp70-1 and PfHop respectively. Both plasmid constructs were purified using GeneJET Plasmid Miniprep Kit (Thermofischer Scientific, USA) as per manufacturer's instructions (Appendix B3).

The DNA integrity was confirmed by restriction digest for both pQE30/PfHsp70-1, using restriction enzymes *Bam*HI, *Hind*III, and pQE30/PfHop, using restriction enzymes, *Sph*I and *Pst*I (Thermofischer Scientific, USA). Samples were prepared and incubated at 37 °C incubator for 15 minutes to allow digestion by restriction enzymes (Appendix B; Table B1). The digested samples were analyzed by agarose gel electrophoresis (Appendix B4).

2.3. Expression of recombinant proteins

E. coli XL1 Blue chemically made competent cells were transformed with plasmid constructs, pQE30/PfHsp70-1 and pQE30/PfHop in 2YT media [1.6 % tryptone (w/v), 1 % yeast extract (w/v), 0.5 % NaCl (w/v), 1.5 % agar (w/v)] containing 100 µg/ml ampicillin (final concentration). The expression was done following a previously described protocol (Gitau *et al*., 2012; Zininga *et al*., 2015a). Briefly, single colonies were inoculated into 50 ml conical flasks with 100 µg/ml ampicillin overnight at 37 °C, shaking at 250 rpm using the FMH 200 (FMH Electronics, RSA). The overnight culture was subsequently diluted into 450 ml containing 100 µg/ml ampicillin. The cultures were then incubated until they reached a mid-log phase at OD_{600} = 0.6. Expression of recombinant protein was induced using 1 mM (final concentration) of isopropyl-β-D-1-thiogalactopyranoside (IPTG) and the cultures were incubated to allow expression up to 5 hours for PfHsp70-1 and 6 hours for PfHop. During expression, the hourly samples were collected and analyzed by 12 % sodium dodecyl sulfate-polyacrylamide gel electrophoresis (SDS-PAGE; Appendix B5) and visualized using Coomassie Blue. The remaining cultures were harvested by centrifugation at 5000 g for 20 minutes at 4 °C, supernatant was discarded and the remaining pellets were resuspended in 10 ml lysis buffer (10 mM Tris-HCl, pH 7.5, 300 mM NaCl and 10 mM Imidazole containing 1 mM EDTA, 1mM phenylmethylsufonyl fluoride (PMSF) and 1 mg/ml lysozyme). The prepared cell lysates were incubated at room temperature with shaking for 30 minutes and stored at -80 °C freezer for future use. The expression of recombinant proteins was confirmed by Western blot analysis using α-PfHsp70-1, α-PfHop and α-His antibodies (Appendix B6).

2.4. Purification of recombinant proteins

Recombinant proteins (PfHsp70-1 and PfHop) were successfully purified using sepharose nickel affinity chromatography. Purification of proteins followed a protocol previously described (Gitau *et al*., 2012; Zininga *et al*., 2015a). The cell lysates from -80 °C were thawed on ice for 1 hour. Polyethyleneimine (PEI; 0.1 % v/v) was added to the lysates to allow removal of nucleic acids by precipitation and to solubilize insoluble proteins. The cell lysates were then sonicated for a duration of 5 minutes, pulse; 15 seconds ON and 10 seconds OFF at an amplitude of 30 %. The cell lysates were centrifuged at 5000 g for 20 minutes at 4 °C. The supernatants were loaded onto Hispur Nickel-charged nitrilotriacetic acid (Ni-NTA) immobilized metal affinity chromatography (IMAC) (ThermoScientific, USA) for 4 hours on ice to allow His-tagged proteins to bind to Hispur Ni-NTA. The soluble fractions were allowed to run through the column and flow through fractions were collected. The unbound proteins were then washed off with wash buffer 1 (100 mM Tris pH 7.5, 300 mM NaCl, 25 mM Immidazole and 1 mM PMSF), followed by wash buffer 2 (100 mM Tris pH 7.5, 300 mM NaCl, 80 mM Immidazole and 1 mM PMSF). The bound proteins were then eluted with elution buffer 1 (100 mM Tris pH 7.5, 300 mM NaCl, 250 mM Immidazole and 1 mM PMSF), followed by elution buffer 2 (100 mM Tris pH 7.5, 300 mM NaCl, 500 mM Immidazole and 1 mM PMSF). Both wash and elution fractions were collected for analysis by SDS-PAGE (Appendix B5) and confirmed by Western blot analysis (Appendix B6).

The purified proteins were further dialyzed to remove imidazole and to avoid interference with any downstream applications. Dialysis was done using Amicon Ultra-10k centrifuge filter device (Merck Millipore, Germany) in dialysis buffer (300 mM NaCl, 10mM Immidazole, 10 mM Tris-HCl pH 7.5, 10 % (v/v) glycerol, 1 mM PMSF). The centrifugation was done for 15 minutes at 4000 g at 4 ° C. The concentrated proteins were removed from the filter device and stored in 2 ml Eppendorf tubes.

2.5. Analysis of PfHsp70-1 and PfHop interaction using ELISA

Enzyme-linked immunosorbent assay (ELISA) is a common plate-based assay that is used to detect and also quantify hormones, peptides, antibodies and proteins. ELISA is a protein-protein interaction technique. The ELISA was used for the development and optimization of high

throughput screening of compounds targeting the PfHsp70-1-PfHop pathway of the parasite. The ELISA used here was previously described by Mabate *et al*., (2018) and it was conducted as illustrated in Figure 2.1 below. PfHsp70-1 (5 µg/ml) was prepared as ligand in 5 mM sodium bicarbonate ($NaHCO_3$) at pH 9.5 and noncovalently immobilized on a 96 well plate. BSA (5 µg/ml) was used as a negative control. The immobilized proteins were incubated for overnight at 4 °C. The plate was washed once to remove any unbound protein. The washing was done using Tris - buffered saline (TBS; 20 mM, pH 7.5, 500 NaCl) with Tween-20 (TBS + 0.1 % Tween 20). To block the wells, 150 µL of 5 % non-fat skimmed milk was added to each well and then the plate was incubated at 25 °C for 1 hour. The wells were washed using TBST for a total of 10 minutes. Serial dilutions of recombinant PfHop (0-1000 nM) were prepared in 5 % non-fat skimmed milk prepared in TBST. The analyte (PfHop) was incubated with the ligands for 2 hours at 25 °C. To remove any unbound analytes, the plate was washed before addition of primary antibody. Primary antibody α-PfHop (1: 4000) was added into the wells at 100 µL/well and incubated at 25 °C for 1 hour. After incubation, the wells were washed before addition of secondary HRP conjugated goat raised α-rabbit antibody (1: 4000). The plate was then incubated for 45 minutes at 25 °C. The plate was washed three times prior to detection, 3, 3'5, 5' –tetramethylbenzidine (TMB) (Bio Scientific, USA) was added to the wells at 100 µL/well and was allowed to sit at room temperature for 2 minutes to allow the substrate reaction. To monitor color development, the Spectra max M3 Micro plate reader (Molecular Devices) was used. The absorbance readings were measured at 370 nm at time intervals (0, 5, 10, 15, 20, 25 and 30 minutes). The absorbance values were plotted against time. The assay was repeated in the presence of 5 mM ADP and ATP in order to investigate the effect of nucleotides on the interaction. In addition, to determine the effect of colistin sulfate or pifithrin µ on the PfHsp70-1 and PfHop interaction, the assay was repeated in the presence of 0.04, 0.2, 1, 5, 25 µM. Furthermore, the assay was repeated interchanging the ligand and analyte to validate data reproducibility.

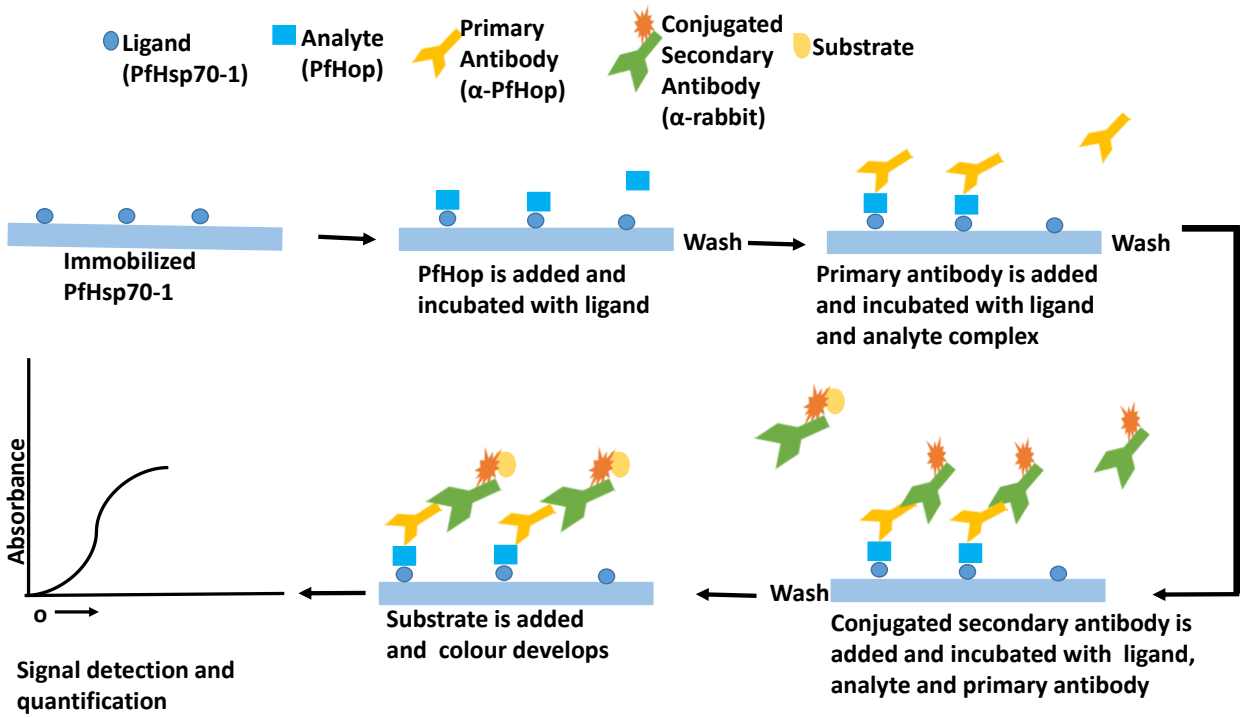

Figure 2.1: Schematic diagram of ELISA set up. In the assay, the ligand is immobilized onto a 96 well plate, and its interacting partner is added in solution. The interaction between the ligand and the analyte is detected by an antibody raised against the protein in solution, followed by conjugated secondary antibody. The signal is detected by adding a substrate that triggers colour development.

The analysis of data was done as follows, background absorbance values for each serial dilution of the analyte was determined from uncoated and BSA (5 µg/ml) negative control wells. After background subtraction, the resultant absorbance values at the highest concentration of each analyte was averaged as maximum (100 %) binding. Titration curves were then generated against a log scale of dilution concentrations using GraphPad prism 6.05 (GraphPad software, USA). The relative binding affinities for PfHsp70-1 versus PfHop under different conditions were normalized to the maximum absorbance value obtained at the highest concentration of PfHop.

2.6. Analysis of PfHsp70-1 and PfHop interaction using surface plasmon resonance (SPR)

SPR assay is a technique that measures the interaction affinity of two different molecules (Kusnezow and Hoheisel, 2003). The principle is based on the idea that one molecule (ligand) is fixed on a thin layer of gold and the other molecule (analyte) is mobile as illustrated (Figure 2.2). Gold immobilization is usually used because gold is an inert metal. As such, it allows an easy

immobilization (Lofas *et al*., 1991). Based on the figure mentioned, the interaction involves ligand immobilization onto the sensor chip which has carboxymethyl dextran (CMD) that is attached to a gold surface and varying concentrations of analyte are injected to allow binding (Ferraris *et al*., 2010). The binding of analyte to ligand causes a change in the refractive index on the gold sensor chip. Light passes through the glass and reflects back off the gold coating as seen in (Figure 2.2 A). The changes that take place as the light reflects back are measured in the resonance angle. The signal is then quantified in resonance units (RU) as a representation of a shift in resonance angle (Figure 2.2 B).

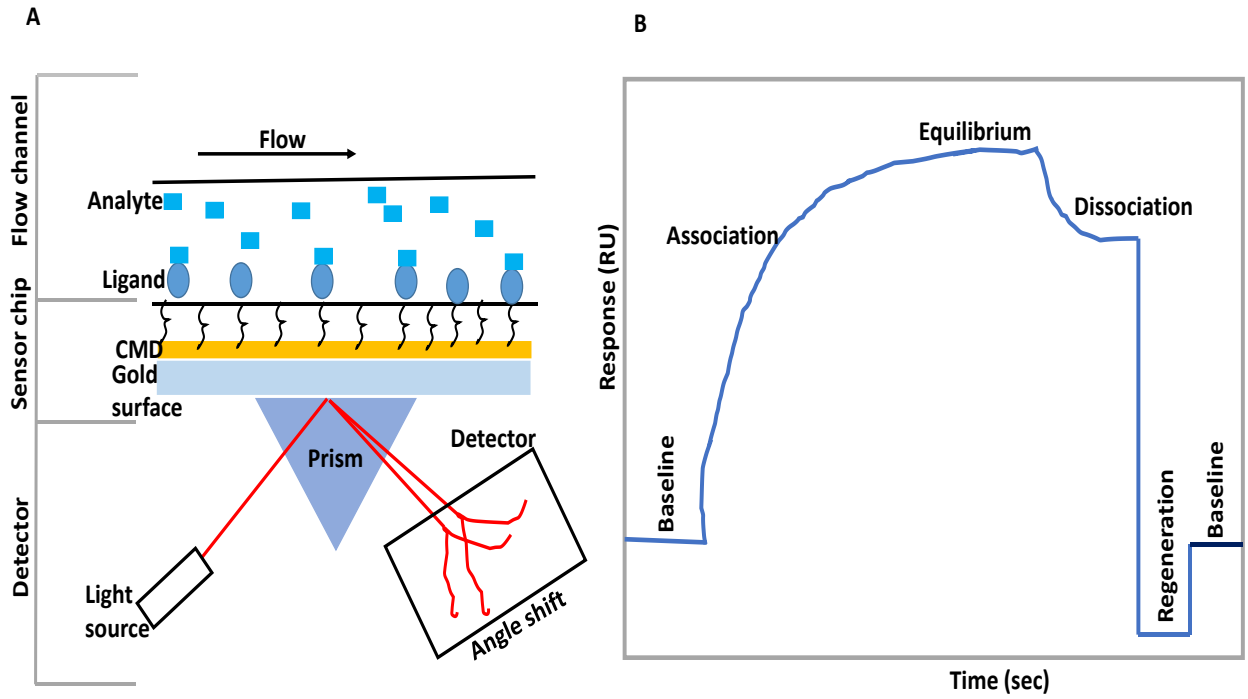

Figure 2.2: Schematic diagrams showing the events taking place in an SPR assay (A) and an example of sensorgram data of an SPR (B). In A, ligand and analyte interaction is shown and in B, baseline, association, equilibrium, dissociation and regeneration are shown in a SPR curve.

SPR assay was conducted in order to validate the observations obtained from the ELISA. SPR was conducted using Bionavis MP-SPR Navi 420A ILVES system. All buffers used in this assay were filter-sterilized using 0.45 µM membrane filters and de-gassed for 1 hour at 25 °C. For immobilization of proteins, the proteins were immobilized onto a carboxymethyl dextran (CMD 3-D) gold sensor chip. Briefly, the sensor chip was activated prior to protein immobilization by amine coupling. To activate the sensor chip, aliquots of 0.1 M (3-dimethylaminopropyl)-3-

ethylcarbodiimide (EDC) and 0.05 M of N-hydroxysuccinimide (NHS) were mixed at a ratio of 1:1 and injected onto the sensor chip at a flow rate of 50 µl/min. After activation, protein solution (100 µg/ml) was prepared in 5 mM sodium acetate buffer pH=4.0 and was also injected at a flow rate of 50 µl/min in one channel only and the second channel was injected with running buffer. This was followed by deactivation to both channels using 1 M ethanolamine in order to remove any free amine. The last step for immobilization was washing. A combination of 2 M sodium chloride (NaCl) and 0.01 M sodium hydroxide (NaOH) was injected into both channels.

As analyte, varying concentrations of PfHop were prepared at 0, 125, 250, 500, 1000 and 2000 nM in PBS buffer at pH=7.0 and injected at a flow rate of 50 µl/min. After each injection, a regeneration step was employed using 0.1 M glycine-hydrochloride pH=2.0. The effect of nucleotides on the interaction of PfHsp70-1 and PfHop was also assessed. The assay was repeated in the absence and presence of 5 mM ATP/ ADP. Data analysis was generated after double referencing with buffer blank and the chip without protein. The corrected sensorgrams were then further analysed using a bivalent fit model which determines the association rate constant (ka) and dissociation rate constant (kd). The affinity constant (KD) is determined by ka and kd, which equals to kd/ka.

To determine the binding affinity of colistin sulfate and pifithrin µ for PfHsp70-1, the assay was repeated in the presence of variable concentrations (0, 1.25, 2.5, 5, 10 and 20 nM) of colistin sulfate or pifithrin µ. Aliquots of EGCG and PMB (Zininga *et al*., 2017a; b) were used as positive controls in this assay. Each inhibitor with varying concentrations was injected over the immobilized PfHsp70-1 at a flow rate of 50 µl/min. The association was allowed for 8 minutes and dissociation was allowed for 5 minutes.

Data obtained was double referenced using a buffer blank (without any inhibitor) and a channel without any active protein. Steady-state equilibrium constant (KD) was generated. To determine the effects of colistin sulfate and pifithrin µ on the protein-protein interaction, the assay was repeated in the presence of 10 nM colistin sulfate or pifithrin µ. The data was analysed as previously described. All SPR data were generated using Trace Drawer software version 1.8 (Ridgeview Instruments; Sweden) and further analysed by GraphPad prism 6.05 (GraphPad Software, USA.

CHAPTER 3: RESULTS

3.1. Confirmation of the pQE30/PfHsp70-1 plasmid

The integrity of the pQE30/PfHsp70-1 plasmid construct was confirmed by restriction digest analysis using restriction enzymes *Bam*HI and *Hind*III (Figure 3.1). Restriction with either *Bam*HI or *Hind*III resulted in linearized plasmid 5459 bp (Figure 3.1B). Double restriction digest with both *Bam*HI and *Hind*III resulted in two distinct separate bands, the plasmid at 3424 bp and an insert at 2035 bp.

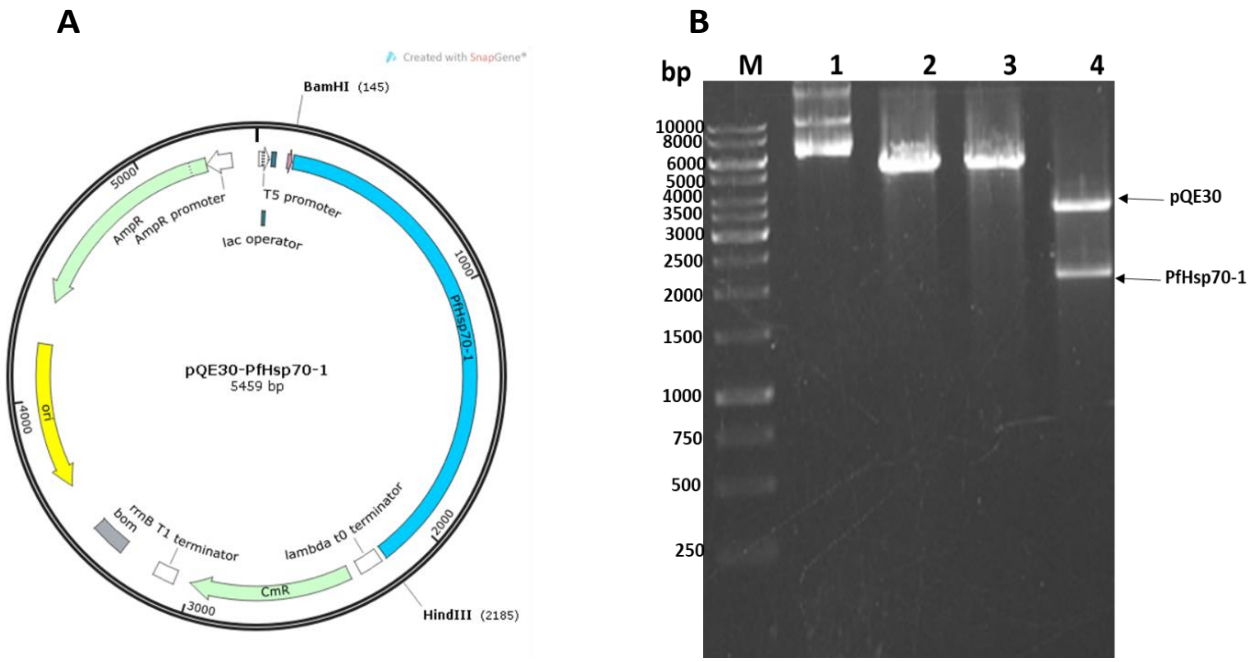

Figure 3.1: pQE30/PfHsp70-1 restriction plasmid map and restriction agarose gel.
Restriction analysis of pQE30/PfHsp70-1 DNA plasmid (**A**) Restriction map of pQE30/PfHsp70-1 showing the *Bam*HI and *Hind*III restriction sites. (**B**) Agarose gel electrophoresis of pQE30/PfHsp70-1, samples were loaded as follows: M, molecular weight maker; lane 1, unrestricted pQE30/PfHsp70-1; lane 2, pQE30/PfHsp70-1 restricted with *Bam*HI; lane 3, pQE30/PfHsp70-1 restricted with *Hind*III; lane 4, pQE30/PfHsp70-1 restricted with both *Bam*HI and *Hind*III.

3.2. Confirmation of the pQE30/PfHop plasmid

The pQE30/PfHop plasmid construct was confirmed by restriction digest analysis using *Sph*I and *Pst*I restriction enzymes (Figure 3.2). Single restriction digest with either *Sph*I or *Pst*I resulted in linearized plasmid of 5134 bp (Figure 3.2B). Double digest with both *Sph*I and *Pst*I resulted in two

separate bands of 3461 bp and 1695 bp, corresponding to pQE30 vector and pQE30/PfHop insert, respectively.

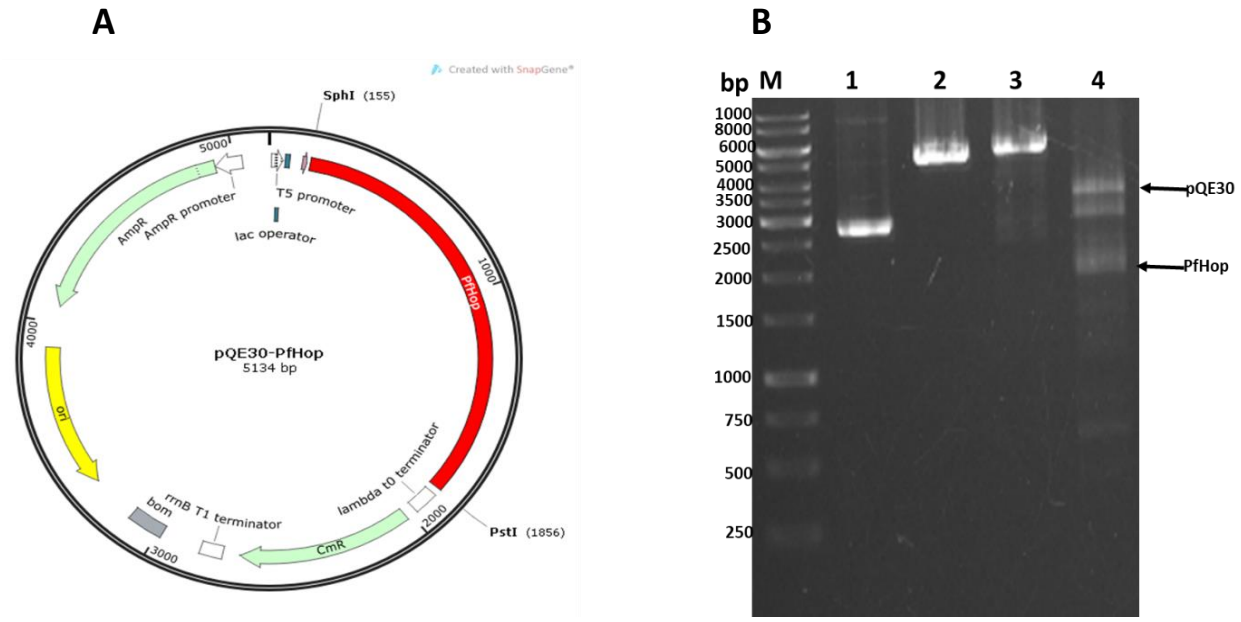

Figure 3.2: pQE30/PfHop plasmid map and restriction agarose gel.
Restriction analysis of pQE30/PfHop (**A**) Restriction map of pQE30/PfHop showing the *Sph*I and *Pst*I restriction sites. (**B**) Agarose gel electrophoresis of PQE30/PfHop, samples were loaded as follows: M, molecular weight maker; lane 1, unrestricted pQE30/PfHop; lane 2, pQE30/PfHop restricted with *Sph*I; lane 3, pQE30/PfHop restricted with *Pst*I; lane 4, pQE30/PfHop restricted with both *Sph*I and *PstI*.

3.3. Expression and purification of recombinant PfHop protein

Recombinant PfHop was successfully expressed in *E. coli* XL1 Blue cells transformed with pQE30/PfHop plasmid. As a negative control, *E. coli* XL1 Blue cells transformed with pQE30 vector without the DNA insert were used. As expected, there was no PfHop expression observed (Figure 3.3). PfHop expression was analyzed by SDS-PAGE and confirmed by Western blot analysis using specific antibody raised against PfHop (Figure 3.3A, lower panel). All proteins used in this study have N-terminus polyhistidine-tag. In addition, PfHop expression was also confirmed by α-His antibody. Recombinant PfHop expression was induced by IPTG. It was observed that PfHop migrated as a band on the gel at 66 kDa. This suggests that the protein was successfully expressed. Another species of 55 kDa was observed and it had the same trend of expression as PfHop at 66 kDa.). The expressed PfHop was successfully confirmed by α-PfHop and α-His

antibodies (Figure 3.3A, lower panel). The band that was initially picked by α-PfHop antibody did not appear when α-His antibody was used which confirms breakdown products.

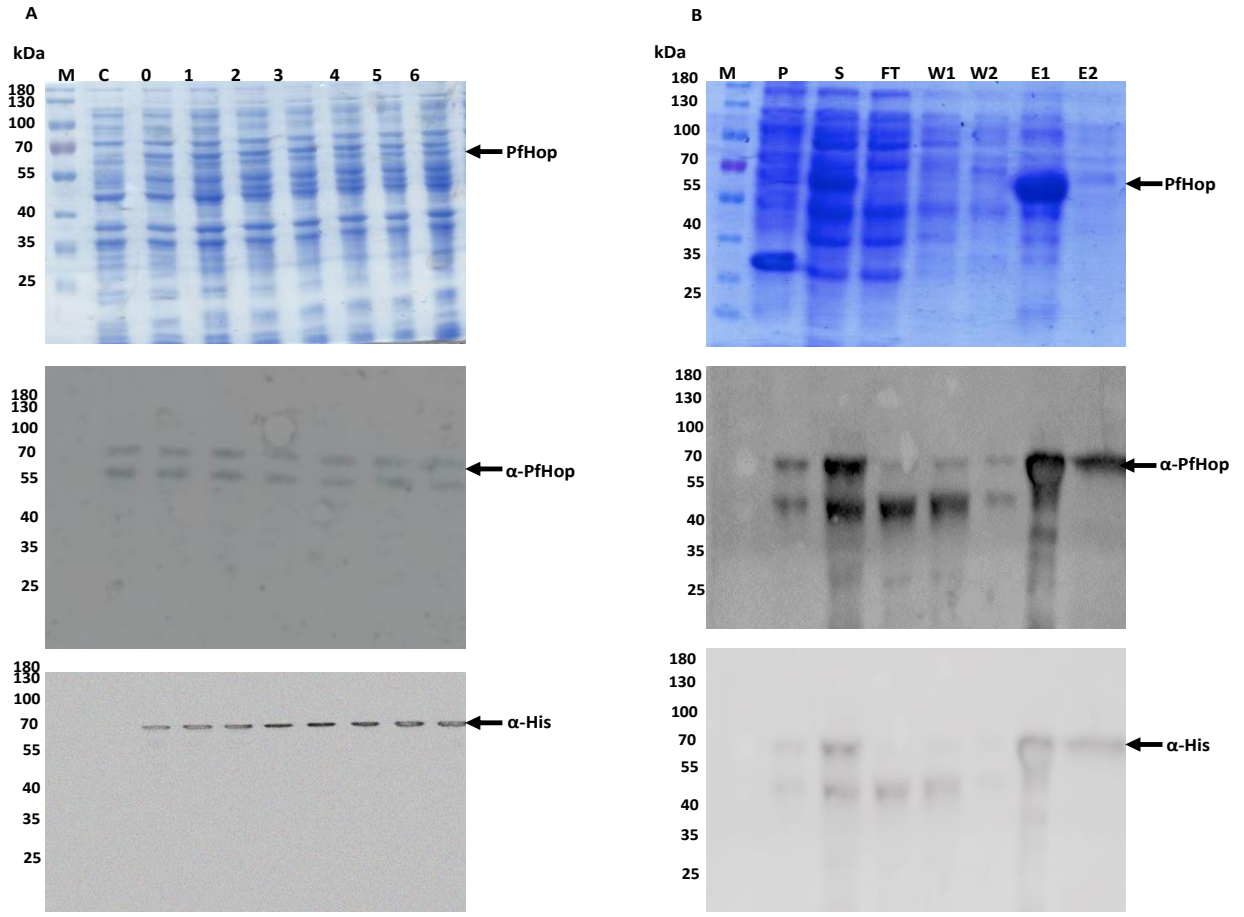

Figure 3.3: Analysis of the expression and purification of PfHop. (**A**) Analysis of the expression of PfHop in *E. coli* XL1 Blue cells using SDS-PAGE. Lane M: represents molecular weight maker (in kDa); Lane C: represents total extract of cells transformed with pQE30; lane 0: represents total extract of cells transformed with pQE30/PfHop before induction with IPTG; lanes 1-6; represents total extract of cells transformed with pQE30/PfHop after IPTG induction. (**B**) Purification of expressed PfHop using nickel affinity chromatography. Lane S: soluble fraction; lane P: insoluble fraction; lane FT: flow through; lane W: samples collected after washing steps and lane E represents elution fractions of PfHop. Lower panels: represents confirmation of the purified PfHop by Western blot using α-PfHop and α-His antibodies.

The His-tag PfHop was further purified by native nickel affinity chromatography. The purification was analyzed by SDS-PAGE (Figure 3.3B) and confirmed by Western blot analysis using both α-PfHop and α-His antibodies (Figure 3.3B, lower panel). SDS-PAGE of PfHop purification showed that some of the proteins were in the flow through, some were lost in the washes but successfully eluted at approximately 66 kDa with a yield of 9.6 mg per 1 L of culture. The purified PfHop was confirmed by Western blot using α-PfHop and α-His antibodies.

3.4. Expression and purification of recombinant PfHsp70-1 protein

The recombinant PfHsp70-1 was successfully expressed in *E. coli* XL1 Blue cells transformed with pQE30/PfHsp70-1 construct. The over-production of PfHsp70-1 was analyzed by SDS-PAGE (Figure 3.4A) and confirmed by Western blot analysis using specific antibody raised against PfHsp70-1 and α-His antibody (Figure 3.4, lower panel). The cells expressed PfHsp70-1 as a species of 74 kDa as seen on SDS-PAGE. An increase in band thickness was observed as we move from 1 hour to 5 hours after induction with IPTG. The expression of PfHsp70-1 was further confirmed by Western blot analysis using α-PfHsp70-1 and α-His antibodies respectively.

PfHsp70-1 was purified using nickel affinity chromatography (Figure 3.4B). The purification was analyzed by SDS-PAGE and confirmed by a Western blot (Figure 3.4A, B). PfHsp70-1 was purified under native conditions. PfHsp70-1 was soluble as seen in Figure 3.4B. PfHsp70-1 was successfully purified even though a small fraction of the protein was washed away as seen in the wash fractions. Overall, more protein was eluted in the elution fractions at approximately 74 kDa with a yield of 7.2 mg per 1 L of culture. The purification was further confirmed by Western blot analysis using both α-PfHsp70-1 and α-His antibodies.

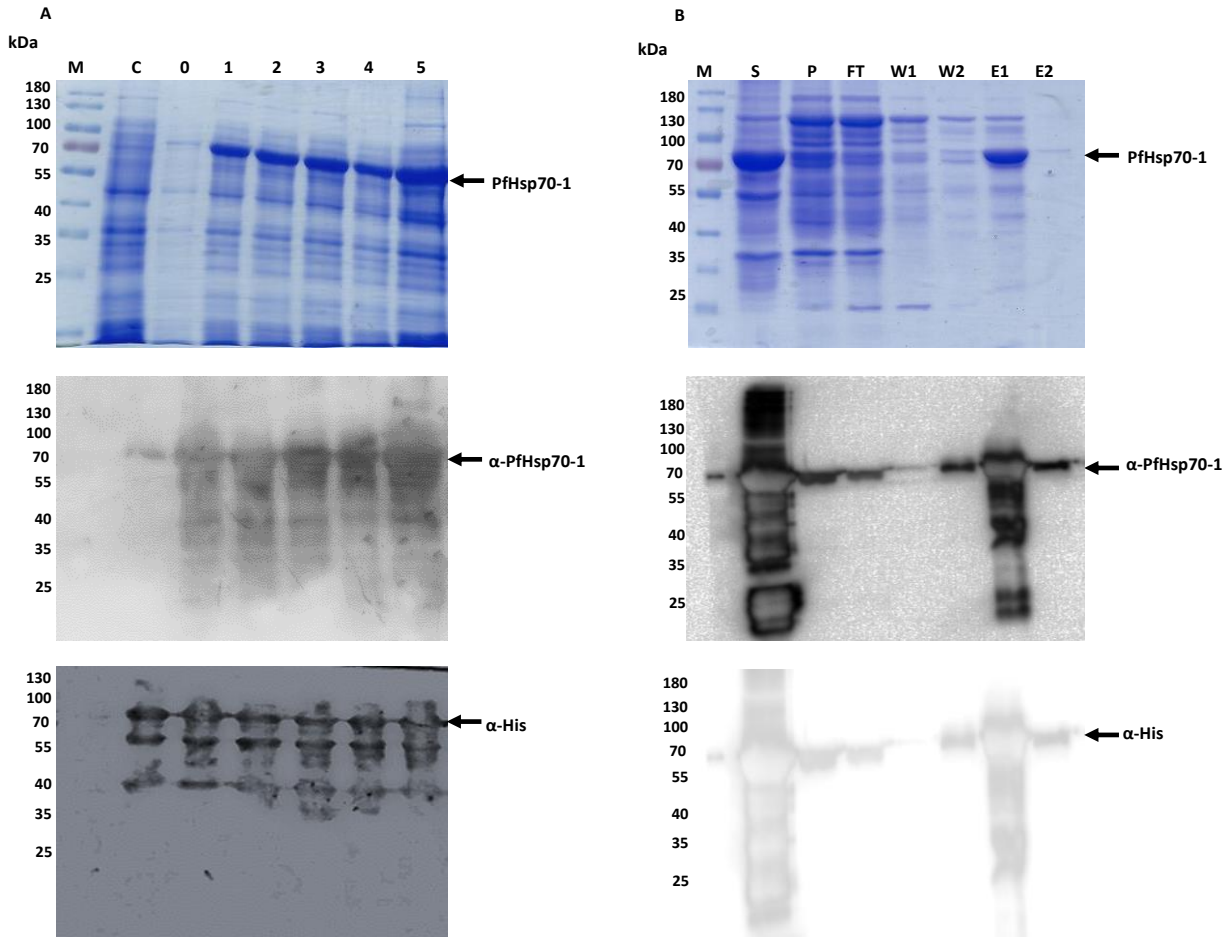

Figure 3.4: Analysis of the expression and purification of PfHsp70-1. (**A**) Analysis of the expression of PfHsp70-1 in *E. coli XL1* Blue cells using SDS-PAGE. Lane M: represents molecular weight maker (in kDa); Lane C: represents total extract of cells transformed with pQE30; lane 0: represents total extract of cells transformed with pQE30/PfHsp70-1 before induction with IPTG; lanes 1-5; represents total extract of cells transformed with pQE30/PfHsp70-1 after IPTG induction. (**B**) Purification of expressed PfHsp70-1 using nickel affinity chromatography. Lane S: soluble fraction; lane P: insoluble fraction; lane FT: flow through; lane W: samples collected after washing steps and lane E represents elution fractions of PfHsp70-1. Lower panels: represent confirmation of the purified PfHsp70-1 by Western blot using α-PfHsp70-1 and α-His antibodies.

3.5. Analysis of interaction of PfHsp70-1 and PfHop using ELISA

After successful expression and purification of recombinant PfHop and PfHsp70-1, both proteins were further dialyzed and quantified for use in the in vitro assays. To validate the interaction of PfHsp70-1 with PfHop, ELISA was used. PfHsp70-1 was noncovalently immobilized on the 96 well plate as ligand, and varying concentrations of PfHop as analyte were overlaid onto the immobilized ligand (PfHsp70-1). The ELISA showed that the interaction of PfHop and PfHsp70-1 occurred in the absence of nucleotides (Figure 3.5A). In addition, the interaction of PfHop with

PfHsp70-1 was specific, and this was further validated by the presence of a BSA control (non-chaperone) which does not bind to PfHsp70-1 (Figure 3.5). Overall, this confirms that the observed signal was not based on a random protein-protein interaction.

PfHop and PfHsp70-1 interaction is nucleotide dependent, therefore, to investigate the effect of nucleotides (ADP, ATP), the assay was repeated in the presence of 5 mM ATP / ADP (Figure 3.5B, C, and D). Interestingly, the ELISA data seem to obey this principle. The ADP and no nucleotide (NN) scenario were generally the same (Figure 3.5.1A, B, and D), and on the other hand ATP suppressed the interaction (Figure 3.5C, D, and E).

In addition, the titration curve fitted against the log scale (Figure 3.5D) provided the kinetics on the interaction of PfHsp70-1 with PfHop (Appendix C4). The kinetics showed that ADP had higher affinity and ATP had less affinity for the interaction (Appendix C4). Overall, differences in the PfHsp70-1 and PfHop interaction were observed both in the presence of ADP and ATP (Figure 3.5E). Taken together, the ELISA data supported that PfHsp70-1 and PfHop interact, and that their interaction is also influenced by the presence of nucleotides.

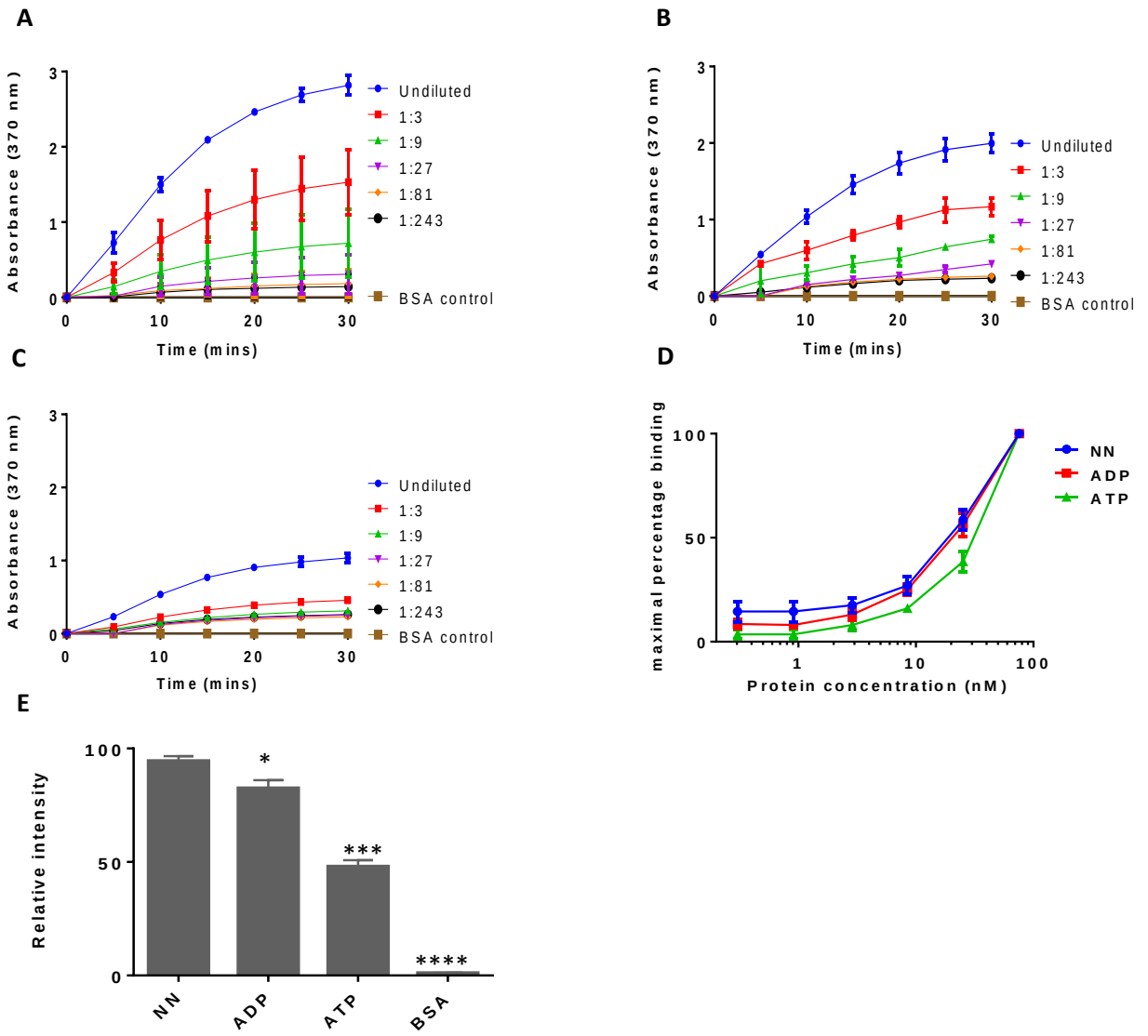

Figure 3.5: Analysis of PfHsp70-1 and PfHop interaction by ELISA. PfHsp70-1 was immobilized onto the ELISA plate and variable concentrations of PfHop were passed over the immobilized chaperone. BSA was used as a negative control. Representative interaction curves generated from ELISA analysis of PfHsp70-1 and PfHop interaction in the absence of nucleotide (NN) (**A**). The assay was repeated in the presence of 5 mM ADP (**B**) and in the presence 5 mM ATP (**C**). The 50 % maximal binding of the PfHop to the immobilized PfHsp70-1 is represented in (**D**). The relative binding affinities under different conditions were normalized to the maximum absorbance value obtained at the highest concentration of PfHop used (**E**). The error bars represent the standard deviations obtained for at least three assays conducted independently. The reference for One-way ANOVA was the interaction of PfHsp70-1 versus PfHop in the absence of nucelotides. Statistical significance of differences is indicated by asterisks positioned above the bar graphs ($p< 0.05$*; $p<0.001$***; $p<0.0001$****).

The ELISA was repeated by swapping the ligand and analyte status to validate the pattern of interaction. Swapping of ligand and analyte was done to ensure that the interaction between two or more molecules is reproducible with some expected variations since the molecule that is

immobilized has different orientation compared to the molecule in solution (analyte). The immobilization was reversed as follows, PfHop was immobilized onto a 96 well plate and varying concentrations of PfHsp70-1 were overlaid onto the PfHop (Figure 3.6).

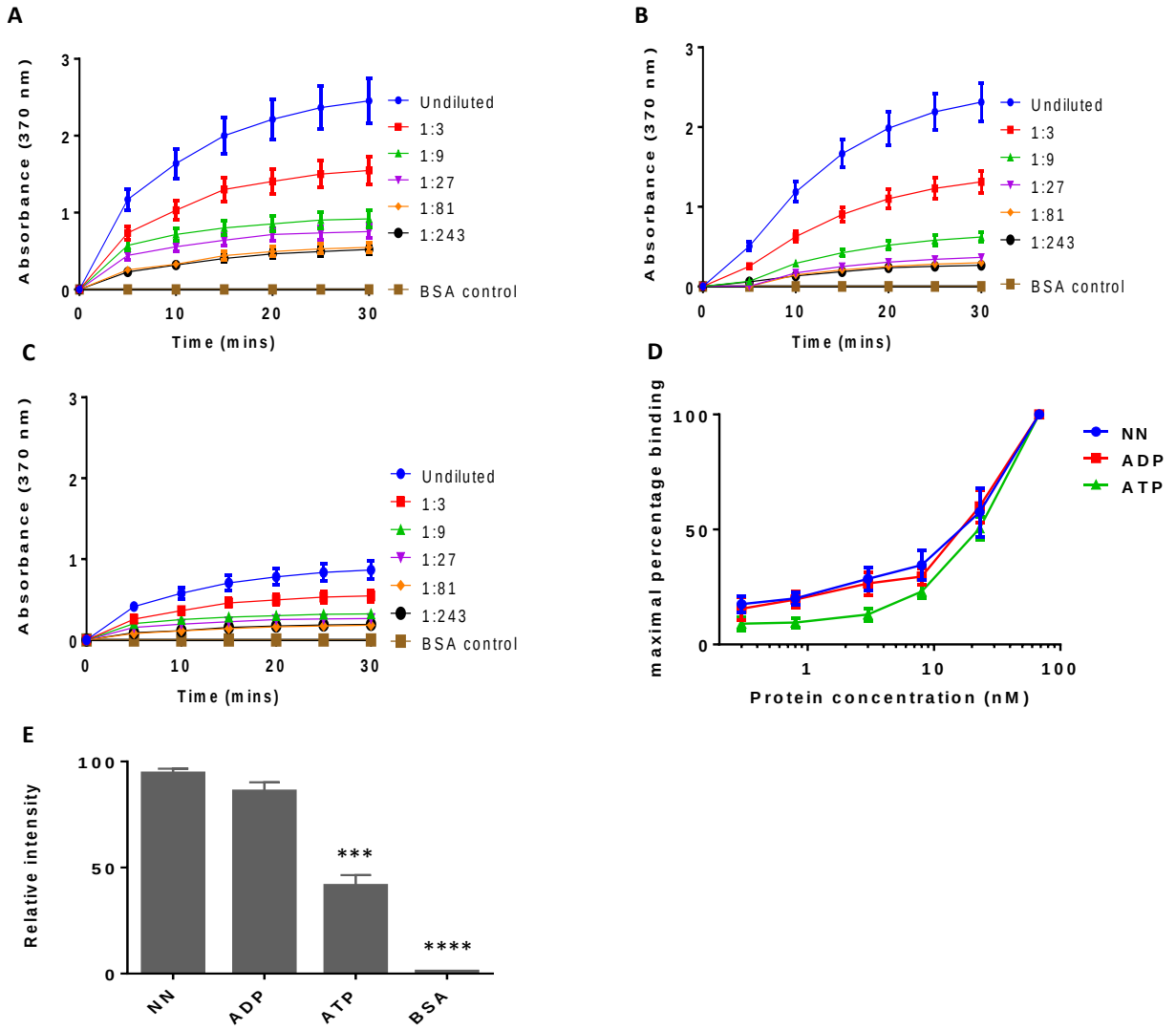

Figure 3.6: Analysis of PfHsp70-1 and PfHop interaction by ELISA. PfHop was immobilized onto the ELISA plate and variable concentrations of PfHsp70-1 were passed over the immobilized chaperone. BSA was used as a negative control. Representative interaction curves generated from ELISA analysis of PfHsp70-1 and PfHop interaction in the absence of nucleotide (NN) (**A**). The assay was repeated in the presence of 5 mM ADP (**B**) and in the presence 5 mM ATP (**C**). The 50 % maximal binding of the PfHsp70-1 to the immobilized PfHop is represented in (**D**). The relative binding affinities under different conditions were normalized to the maximum absorbance value obtained at the highest concentration of PfHsp70-1 used **(E**). The error bars represent the standard deviations obtained for at least three assays conducted independently. The reference for One-way ANOVA was the interaction of PfHsp70-1 versus PfHop in the absence of nucelotides. Statistical significance of differences is indicated by asterisks positioned above the bar graphs ($p<0.001$***; $p<0.0001$****).

The interaction of PfHsp70-1 with PfHop after swapping the status of ligand and analyte showed some minor variations (Figure 3.6). The ELISA data showed that PfHsp70-1 interacts with PfHop in a concentration dependent manner (Figure 3.6). The ELISA data also showed that the interaction of these two proteins occurs in the absence and presence of nucleotides (Figure 3.6A, B, C) as also observed in Figure 3.5A, B, C. Evidently, the current ELISA data supported the observations made before swapping the ligand and analyte status (Figure 3.5). Furthermore, it was noted that the interaction of PfHsp70-1 with PfHop in the presence of ADP showed no significant difference compared to the interaction in the absence of nucleotide (Appendix C4). Overall, both ELISA data (Figure 3.5. and Figure 3.6) confirmed the interaction of PfHsp70-1 with PfHop. Despite all the minor variations in the interaction of PfHsp70-1 with PfHop, the general observed affinities of all the ELISA data sets were comparable as shown (Appendix C, Table C4 and C6).

3.6. Analysis of the effects of colistin sulfate and pifithrin μ on the interaction of PfHsp70-1 with PfHop

The effects of both colistin sulfate and pifithrin μ on the interaction of PfHsp70-1 with PfHop was investigated using ELISA. The ELISA developed here confirmed the interaction of PfHsp70-1 with PfHop. The ELISA was again used to screen for inhibitors that target the PfHop –PfHsp70-1 functional complex. PfHsp70-1 was immobilized on the 96 well plate as ligand, and PfHop was in buffer that was supplemented with varying concentration of colistin sulfate or pifithrin μ as analytes. BSA (5 μg/ml) and DMSO (0.5 %) were used as controls and as such, their signals were used as baseline. Known inhibitors EGCG and PMB were also included as positive controls. As expected, both EGCG and PMB suppressed the interaction of PfHsp70-1 with PfHop (Figure 3.7A, B) respectively. Low signals of absorbance were observed as the concentration of colistin sulfate increases in the interaction between PfHsp70-1 and PfHop (Figure 3.7C). This suggest that colistin sulfate suppressed PfHop-PfHsp70-1 interaction. In addition, reduction of absorbance was also observed in the interaction of PfHsp70-1 with PfHop in the presence of pifithrin μ (Figure 3.7D), suggesting suppressed interaction. Furthermore, both colistin sulfate and pifithrin μ suppressed the interaction of PfHsp70-1 with PfHop in a concentration-dependent manner (Figure 3.7C, D).

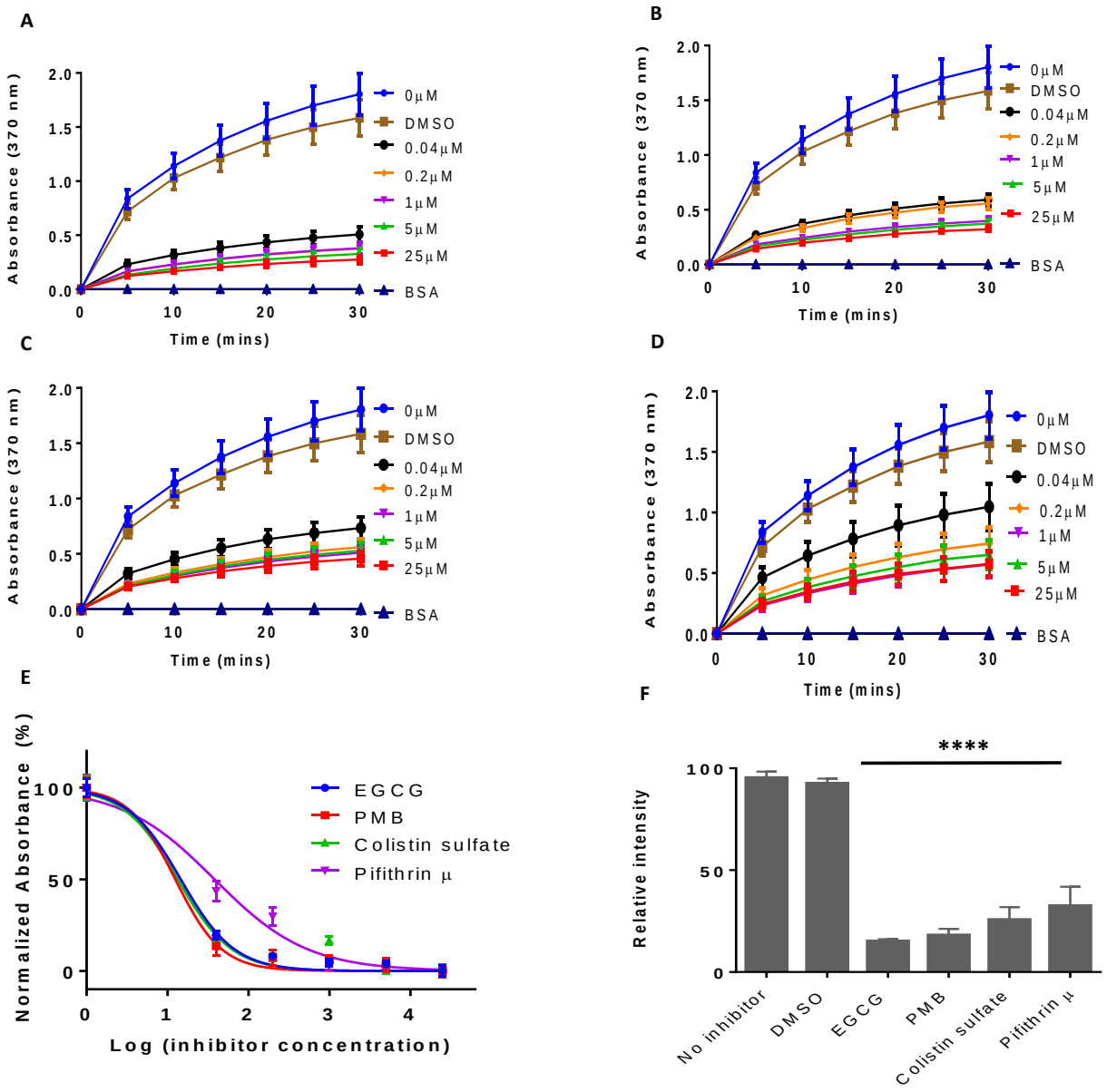

Figure 3.7: The effects of colistin sulfate and pifithrin µ on the interaction of PfHsp70-1 and PfHop by ELISA. PfHsp70-1 was immobilized as ligand and variable concentrations of inhibitors with PfHop were passed over the immobilized chaperone. DMSO and BSA were used as controls. Representative curves of PfHsp70-1 and PfHop in the presence of positive controls: epigallocatechin-3-gallate (EGCG) (**A**) and polymyxin B (PMB) (**B**) respectively, colistin sulfate (**C**) and pifithrin µ (**D**). The dose response curve of the the IC_{50} values of inhibitors is shown (E). Bar graph showing the comparative effects of the inhibitors on the interaction of PfHsp70-1 and PfHop are shown (**F**). The error bars represent the standard deviations obtained for at least three assays conducted independently. The reference for One-way ANOVA was the interaction of PfHsp70-1 versus PfHop in the absence of an inhibitor. Statistical significance of differences is indicated by asterisks positioned above the bar graphs ($p<0.0001$****).

To further validate the inhibition of the interaction of PfHsp70-1 with PfHop, the absorbances obtained from the titration curves were used to fit a dose response curve which determines the IC_{50} values of inhibitors (Appendix C5). The dose response curve showed that both colistin sulfate and pifithrin μ inhibited 50 % of PfHsp70-1 and PfHop interaction as evidenced by the reduction of response units upon increase of inhibitor concentrations (Figure 3.7E). Colistin sulfate had an IC_{50} of 1.187 nM and pifithrin μ registered an IC_{50} of 1.427 nM (Appendix C7). Based on these IC_{50} values, colistin sulfate was more effective than pifithrin μ (Figure 3.7E, Appendix C7). In addition, significant differences were observed for the activity of colistin sulfate versus that of pifithrin μ (Figure 3.7F). For example, relative to control, colistin sulfate suppressed the interaction by 74 % while pifithrin μ registered 67 % suppression of interaction (Figure 3.7F). Overall, both colistin sulfate and pifithrin μ are effective inhibitors of PfHop-PfHsp70-1 interaction.

The roles of colistin sulfate and pifithrin μ on PfHsp70-1 and PfHop interaction was investigated further by swapping the ligand and analyte status (Figure 3.8). PfHop was immobilized as ligand and PfHsp70-1 in buffer supplemented with varying concentration of inhibitors as analytes. The controls used after swapping the ligand and analyte status remained the same, and data was analysed as previously described. The events observed before swapping the status of ligand and analyte were also observed in Figure 3.8. Lower signals of absorbances were observed in the presence of both colistin sulfate and pifithrin μ as compared to the interaction in the absence of both colistin sulfate and pifithrin μ (Figure 3.8C, D). This suggests suppression of interaction of PfHsp70-1 with PfHop as previously observed in Figure 3.7C, D. In addition, EGCG and PMB showed greater suppression of interaction than colistin sulfate and pifithrin μ between PfHsp70-1 and PfHop interaction. The suppression of interaction of PfHsp70-1 with PfHop by both colistin sulfate and pifithrin μ occurred in a concentration-dependent manner (Figure 3.8C, D). Furthermore, colistin sulfate and pifithrin μ IC_{50} values were comparable with those that were found before swapping the ligand and analyte status (Figure3.8E, Appendix C5). Overall colistin sulfate had a greater inhibition compared to pifithrin μ. However, ANOVA test showed that there was no significant differences between the two inhibitors (Figure 3.8F, Appendix C7). Taken together, ELISA data showed that colistin sulfate and pifithrin μ suppressed the functional PfHsp70-1-PfHop pathway.

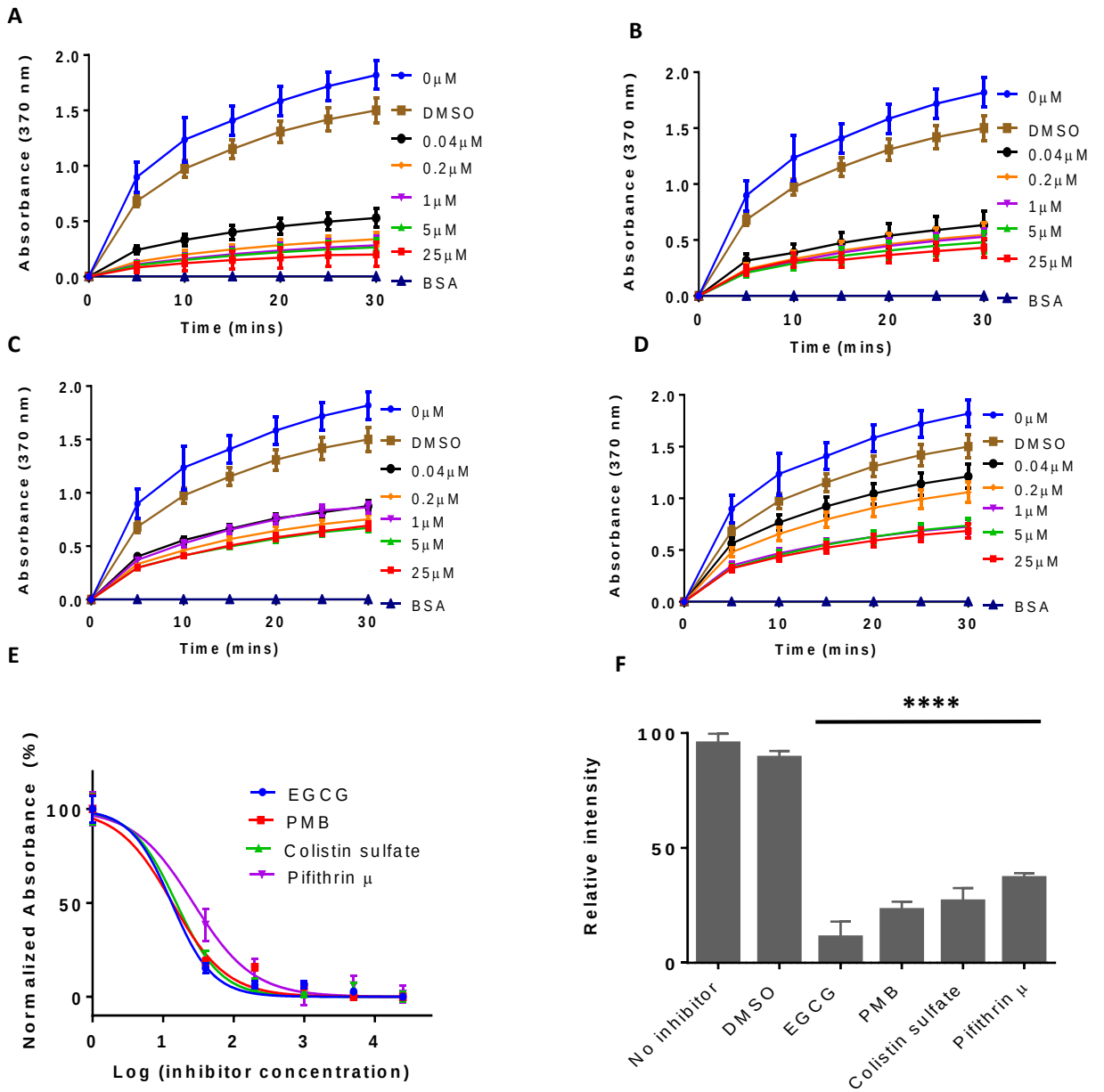

Figure 3.8: The effects of colistin sulfate and pifithrin µ on the interaction of PfHsp70-1 and PfHop by ELISA. PfHop was immobilized as ligand and variable concentrations of inhibitors with PfHsp70-1 were passed over the immobilized ligand. DMSO and BSA were used as controls. Representative curves of PfHsp70-1 and PfHop in the presence of positive controls: epigallocatechin-3-gallate (EGCG) (**A**) and polymyxin B (PMB) (**B**) respectively. Curves for data obtained in the presence of colistin sulfate (**C**) and pifithrin µ (**D**), respectively are shown. The dose response curve of the the IC_{50} values of inhibitors is shown (**E**). Bar graph showing the comparative effects of the inhibitors on the interaction of PfHsp70-1 and PfHop are shown (**F**). The error bars represent the standard deviations obtained for at least three assays conducted independently. The reference for One-way ANOVA was the interaction of PfHsp70-1 versus PfHop in the absence of an inhibitor. The statistical significance of differences is indicated by asterisks positioned above the bar graphs ($p<0.0001$****).

3.7. Analysis of the interaction of PfHsp70-1 with PfHop using SPR assay

The association of PfHsp70-1 with PfHop was further validated by SPR analysis. SPR analysis quantifies the interaction kinetics and the affinity of two or more molecules based on bivalent fit model (Gelinsky-Wersing *et al*., 2017). PfHsp70-1 was immobilised on the CMD sensor chip through covalent coupling and variable concentrations of PfHop (analyte) were injected over the immobilised ligand. The ATPase subdomain of PfHsp70-1 (PfHsp70-1_{NBD}) was used as a negative control as previously recommended (Zininga *et al*., 2015a). As expected, no interaction between PfHsp70-1_{NBD} and PfHop was observed as the response of interaction was too low to be quantified (Table 3.1). Representative sensorgrams were generated in the absence of nucleotide, or presence of 5 mM ADP/ ATP (Figure 3.9A, B, C). SPR data showed that the interaction of PfHsp70-1 with PfHop occurred in a concentration dependent manner as evidenced by the increase in response units as the concentration of analyte increases (Figure 3.9A). As expected, ADP favored the interaction of PfHsp70-1 with PfHop, while ATP showed less interaction (Figure 3.9 B, C, D).

The sensorgrams generated were used to determine the kinetics of the interaction of PfHsp70-1 with PfHop (Table 3.1). The SPR kinetics data showed that the interaction of PfHsp70-1 with PfHop occurred within nanomolar range, suggesting high affinity interaction. The association and dissociation rate constants were determined towards estimating the binding affinity at equilibrium state (Table 3.1; Appendix C8). Based on the binding affinity of PfHsp70-1 and PfHop interaction, low KD value was observed in the presence of ADP which denotes high binding affinity for the interaction while in the presence of ATP, the affinity for PfHsp70-1 with PfHop interaction was reduced by one order of magnitude (Figure 3.9D; Table 3.1). Overall, SPR data confirmed the interaction between PfHsp70-1 and PfHop.

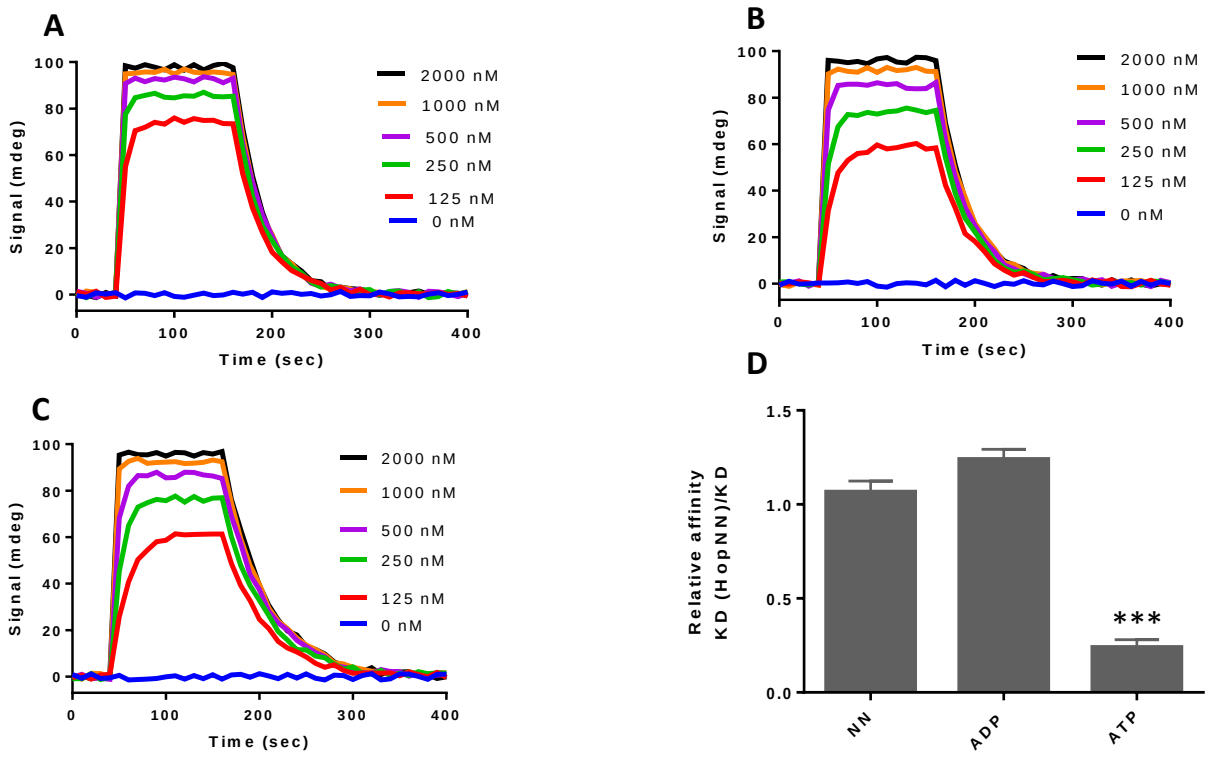

Figure 3.9: SPR analysis for the interaction of PfHsp70-1 with PfHop. PfHsp70-1 was immobilised on the CMD sensor chip and variable concentrations of PfHop were injected over the immobilised PfHsp70-1. Shown are the representative sensorgrams representing interaction of PfHsp70-1 and PfHop conducted in the absence of nucleotide (NN) (**A**), or presence of 5 mM ADP (**B**), and 5mM ATP (**C**). The relative affinities for PfHop towards PfHsp70-1 were determined and presented as bar graphs (**D**). Standard errors represent three independent assays conducted using independent protein batches. The reference for One-way ANOVA was the interaction of PfHsp70-1 versus PfHop in the absence of nucelotides. The statistical significance of differences is indicated by asterisks positioned above the bar graphs ($p<0.001$***).

The order of immobilization was reversed and PfHop was immobilized and varying concentrations of PfHsp70-1 were injected over the immobilized PfHop (Figure 3.10). The assay was again repeated in the presence of 5 mM ADP / ATP (Figure 3.10B, C). Minor variations were observed in the affinity of the PfHsp70-1 and PfHop interactions (Table 3.1). However, as previously demonstrated by SPR data before alternating ligand and analyte status (Figure 3.9), the interaction of PfHsp70-1 and PfHop was more enhanced in the presence of ADP than ATP (Figure 3.10; Table 3.1). In addition, the affinities derived in the presence or absence of nucleotides exhibited the same order of magnitude (Table 3.1). Taken together, SPR data confirmed the interaction of PfHsp70-1 and PfHop.

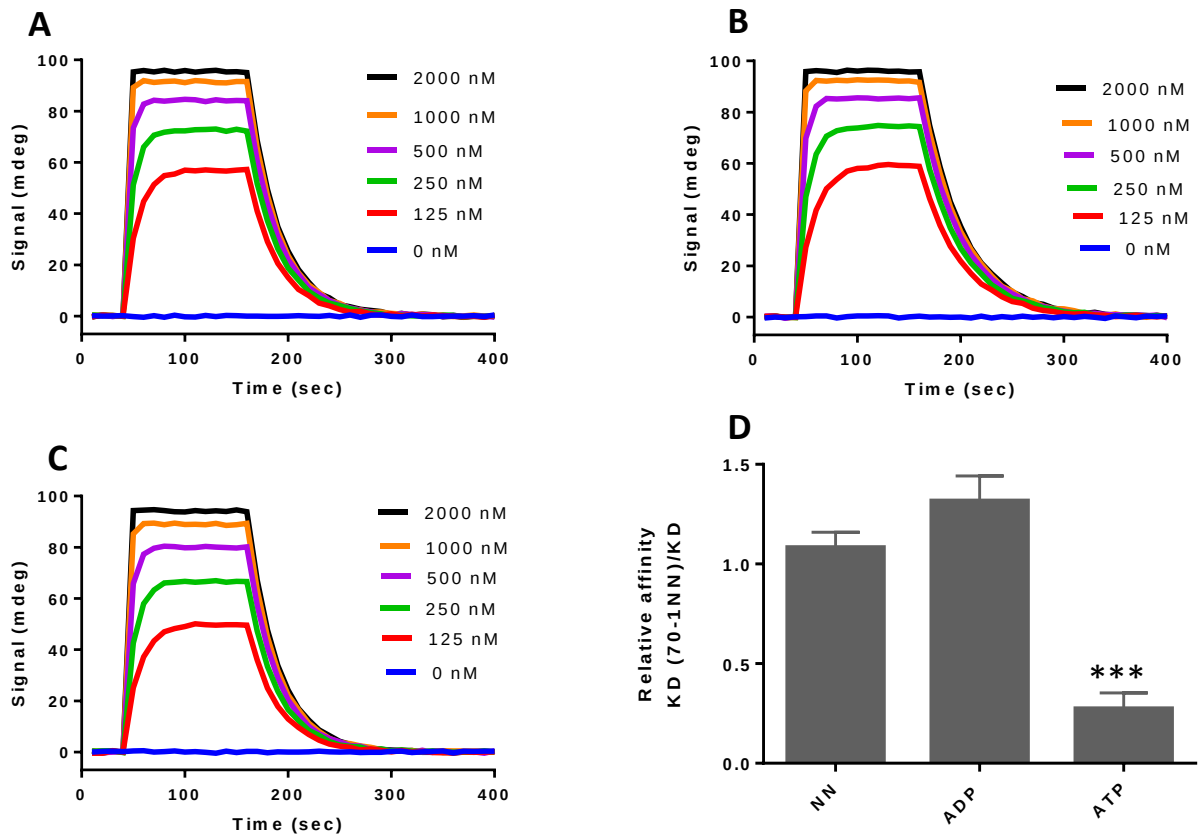

Figure 3.10: SPR analysis for the interaction of PfHsp70-1 with PfHop. PfHop was immobilised on the CMD sensor chip and variable concentrations of PfHsp70-1 were injected over the immobilised PfHop. Shown are the representative sensorgrams representing interaction of PfHsp70-1 and PfHop conducted in the absence of nucleotide (NN) (**A**), or presence of 5 mM ADP (**B**), and 5mM ATP (**C**). The relative affinities for PfHsp70-1 towards PfHop were determined and presented as bar graphs (**D**). Standard errors represent three independent assays conducted using independent protein batches. The reference for One-way ANOVA was the interaction of PfHsp70-1 versus PfHop in the absence of nucelotides.The statistical significance of differences is indicated by asterisks positioned above the bar graphs ($p<0.001$***).

Table 3.1: Kinetics evaluation of the interaction of PfHsp70-1 and PfHop

Ligand	Analyte	Nucleotide	Ka (1/Ms)	Kd (1/s)	KD (M)	χ^2
PfHsp70-1	PfHop	NN	7.67 (+/- 0.07) e^{5}	3.25 (+/- 0.05) e^{-3}	4.24 (+/- 0.04) e^{-9}	0.91
		ADP	7.81 (+/- 0.01) e^{5}	3.08 (+/- 0.08) e^{-3}	3.08 (+/- 0.08) e^{-9}	0.75
		ATP	2.59 (+/- 0.09) e^{5}	2.07 (+/- 0.07) e^{-2}	7.98 (+/- 0.08) e^{-8***}	2.12
PfHop	PfHsp70-1	NN	7.60 (+/- 0.6) e^{6}	3.41 (+/- 0.01) e^{-2}	4.49 (+/- 0.09) e^{-9}	0.19
		ADP	8.07 (+/- 0.07) e^{6}	2.50 (+/- 0.5) e^{-2}	3.10 (+/- 0.1) e^{-9}	0.10
		ATP	2.66 (+/- 0.06) e^{5}	2.15 (+/- 0.05) e^{-2}	8.09 (+/- 0.09) e^{-8***}	1.67
PfHsp70-1_{NBD}	PfHop	NN	ND	ND	ND	-
		ADP or ATP	ND	ND	ND	-

Table legends: ka-association rate constant, kd-dissociation rate constant, KD-equilibrium constant, ND-not determined (interaction too low to be determined), NN -no nucleotide, X^2 values indicate the goodness of fit for SPR sensorgrams fitting to the bivalent fit model. Three independent analyses were conducted during the SPR assay alternating the status of ligand and analyte. Standard errors are shown in brackets. Statistical analysis was done using one-way ANOVA. $p < 0.05$ represents statistically significant differences in affinities. The asterisk (*) represents significant differences.

3.8. Determination of binding affinities of colistin sulfate and pifithrin μ to PfHsp70-1 using SPR assay

To determine if colistin sulfate and pifithrin μ have the capability to directly bind the recombinant PfHsp70-1, SPR based assay was conducted. PfHsp70-1 was immobilized as ligand onto the chip and variable levels of colistin sulfate or pifithrin μ were prepared and injected as analytes (Figure 3.11). In addition, PfHsp70-1_{NBD} was also immobilized and variable concentrations of either colistin sulfate or pifithrin μ were injected over the immobilized ligand. As positive controls, known inhibitors EGCG and PMB were used (Figure 3.11). Nucleotides (ATP/ADP) were also used as controls to validate the specific binding (Table 3.2; Appendix C2). The interaction between ligand and analyte was quantified at equilibrium state (Figure 3.11). The SPR data showed that colistin sulfate and pifithrin μ bind to PfHsp70-1. In addition, both colistin sulfate and pifithrin μ bind to PfHsp70-1 in a concentration-dependent manner.

The binding affinities generated at equilibrium suggest that both colistin sulfate and pifithrin μ bind to PfHsp70-1 in a nanomolar range, suggesting high affinity interaction (Table 3.2). In addition, the affinity of both colistin sulfate and pifithrin μ for PfHsp70-1 were within the same order of magnitude (Table 3.2). Furthermore, the binding affinities also showed that colistin sulfate binds to PfHsp70-1_{NBD} with high affinity (Table 3.2; Appendix C3), suggesting that NBD is the minimal domain required for colistin sulfate binding. On the other hand, pifithrin μ had less affinity for the NBD of PfHsp70-1 (PfHsp70-1_{NBD}) compared to colistin sulfate (Table 3.2; Appendix C C3).

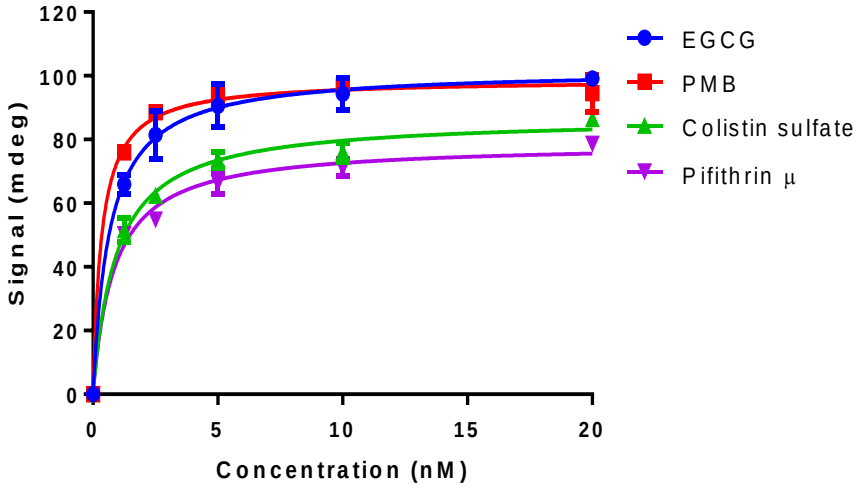

Figure 3.11: Both colistin sulfate and pifithrin μ directly bind to PfHsp70-1. The ligand PfHsp70-1 was immobilized at a concentration 100 μg/mL. The assay was conducted in the presence of variable levels of epigallocatechin-3-gallate (EGCG), polymyxin B (PMB), colistin sulfate and pifithrin μ. The interaction between ligand and analyte was determined using equilibrium SPR analysis. Standard errors represent three independent assays conducted using independent protein batches.

In addition, PfHop was also immobilized and variable levels of colistin sulfate and pifithrin μ were injected as analytes (Figure 3.12; Table 3.2). ATP was also included as a control (Appendix C2).

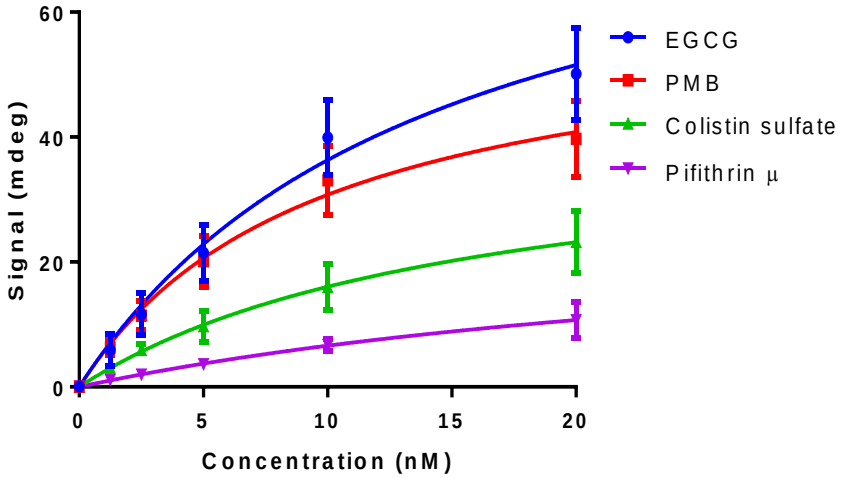

Figure 3.12: The capability of colistin sulfate and pifithrin μ to bind to PfHop chaperone. The ligand PfHop was immobilized at a concentration 100 μg/mL. The assay was conducted in the presence of variable levels of epigallocatechin-3-gallate (EGCG), polymyxin B (PMB), colistin sulfate and pifithrin μ. The interaction between ligand and analyte was determined using equilibrium SPR analysis. Standard errors represent three independent assays conducted using independent protein batches.

The SPR binding affinities showed that colistin sulfate and pifithrin μ bind to PfHop with a KD of 0.849 μM and 0.707 μM respectively, suggesting less affinity binding of colistin sulfate and pifithrin μ as compared to PfHsp70-1 (Table 3.2). The affinity of both colistin sulfate and pifithrin μ for PfHop was reduced by one order of magnitude compared to the full length PfHsp70-1. Overall, colistin sulfate and pifithrin μ bind to PfHsp70-1 with high affinity, and on the other hand less affinity binding was observed for PfHop in comparison with PfHsp70-1.

Table 3.2: Comparative affinities for ATP, colistin sulfate and pifithrin μ binding to PfHsp70-1/ PfHsp70-1$_{NBD}$ and PfHop at equilibrium phase

Ligand	Analyte	KD (M)	χ^2
PfHsp70-1	EGCG	1.47 (+/- 0.07) e^{-9}	1.21
	PMB	5.73 (+/- 0.03) e^{-9}	8.39
	Colistin sulfate	5.19 (+/- 0.09) e^{-8}	4.67
	Pifithrin μ	6.92 (+/- 0.02) e^{-8}	1.70
	ATP	5.37 (+/- 0.07) e^{-7}	1.73
PfHop	EGCG	4.52 (+/- 0.02) e^{-8}	4.93
	PMB	5.79 (+/- 0.09) e^{-8}	1.99
	Colistin sulfate	8.49 (+/- 0.09) e^{-7}	5.72
	Pifithrin μ	7.07 (+/- 0.07) e^{-7}	7.31
	ATP	8.61 (+/- 0.01) e^{-7}	6.90
PfHsp70-1$_{NBD}$	EGCG	1.20 (+/- 0.2) e^{-8}	5.33
	PMB	3.17 (+/- 0.07) e^{-9}	4.84
	Colistin sulfate	3.38 (+/- 0.08) e^{-9}	1.10
	Pifithrin μ	7.39 (+/- 0.09) e^{-6}	9.14
	ATP	2.23 (+/- 0.03) e^{-8}	1.01

Table legends: KD-equilibrium constant, EGCG-epigallocatechin-3-gallate, PMB-polymyxin B, X^2 values indicate the goodness of fit for SPR sensorgrams. Three independent analyses were conducted during the SPR assay. Standard errors are shown in brackets.

3.9. Analysis of the effects of colistin sulfate and pifithrin μ on PfHop-PfHsp70-1 interaction using SPR assay

The effect of inhibitors on the interaction of PfHsp70-1 with PfHop was investigated using SPR analysis. Previously, a direct PfHsp70-1-PfHop interaction was demonstrated by ELISA and SPR. It was also shown that their interaction is modulated by the presence of nucleotides. Therefore, it was interesting to determine the effect of inhibitors on these interactions. SPR assay was then used to determine the effects of colistin sulfate and pifithrin μ on the interaction between PfHsp70-1 with PfHop (Figure 3.13). PfHsp70-1 was immobilized as ligand and varying concentrations of PfHop were injected as analytes in the absence or presence of nucleotides and 10 nM colistin sulfate and pifithrin μ (Figure 3.13). As positive controls, EGCG and PMB were used. The

reduction in the affinities of interaction in the presence of EGCG and PMB was observed (Table 3.3).

The SPR data showed that the response of interaction between PfHsp70-1 and PfHop was decreased in the presence of colistin sulfate and pifithrin μ (Figure 3.13C, D), suggesting inhibition of interaction by both colistin sulfate and pifithrin μ. A more pronounced decrease in response of the interaction was observed in the presence of colistin sulfate (Figure 3.13C). In addition, abrogation of this interaction occurred in a concentration-dependent manner, meaning that more inhibition was observed as we move from the lowest to highest concentration of PfHop.

The binding affinity for each inhibitor was determined and summarized in a table below (Table 3.3). The affinity of PfHsp70-1 and PfHop in the presence of colistin sulfate was reduced by two order of magnitude (Table 3.3), suggesting that colistin sulfate inhibited PfHsp70-1 and PfHop interaction. Similarly, the affinity of PfHsp70-1 and PfHop interaction was also reduced by two order of magnitude in the presence of pifithrin μ. Overall, both colistin sulfate and pifithrin μ inhibited the interaction between PfHsp70-1 with PfHop.

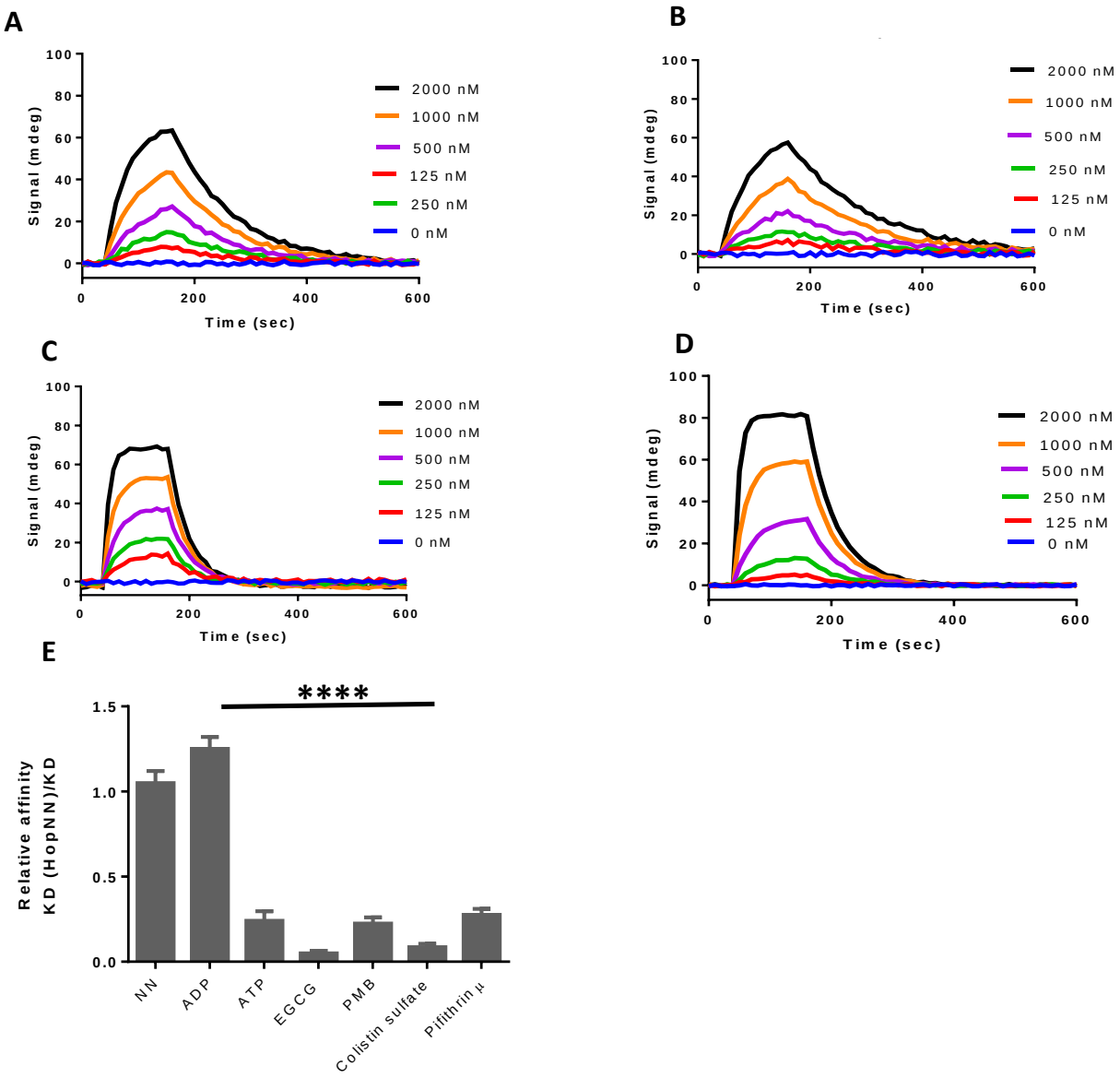

Figure 3.13: SPR analysis to confirm roles of colistin sulfate and pifithrin μ in abrogating PfHsp70-1-PfHop interaction. PfHsp70-1 was immobilised on the CMD sensor chip and variable concentrations of PfHop in the presence of inhibitors were injected over the immobilised PfHsp70-1 Representative sensorgrams conducted in the presence of epigallocate-3-gallate (EGCG) (**A**), polymyxin B (PMB) (**B**), colistin sulfate (**C**), and pifithrin μ (**D**) are shown. The relative affinities of the interaction in the absence or presence of ADP or ATP and inhibitors are shown in (**E**). Standard errors represent three independent assays conducted using independent protein batches. The reference for One-way ANOVA was the interaction of PfHsp70-1 versus PfHop in the absence of an inhibitor.The statistically significant of differences is indicated by asterisks above the bar graphs ($p<0.0001$****).

To further validate the inhibition of PfHsp70-1 and PfHop interaction, ligand and analyte were swapped, and the assay was repeated (Figure 3.14). As previously shown, a decrease in response

was observed on the interaction of PfHsp70-1 with PfHop in the presence of both colistin sulfate and pifithrin μ.

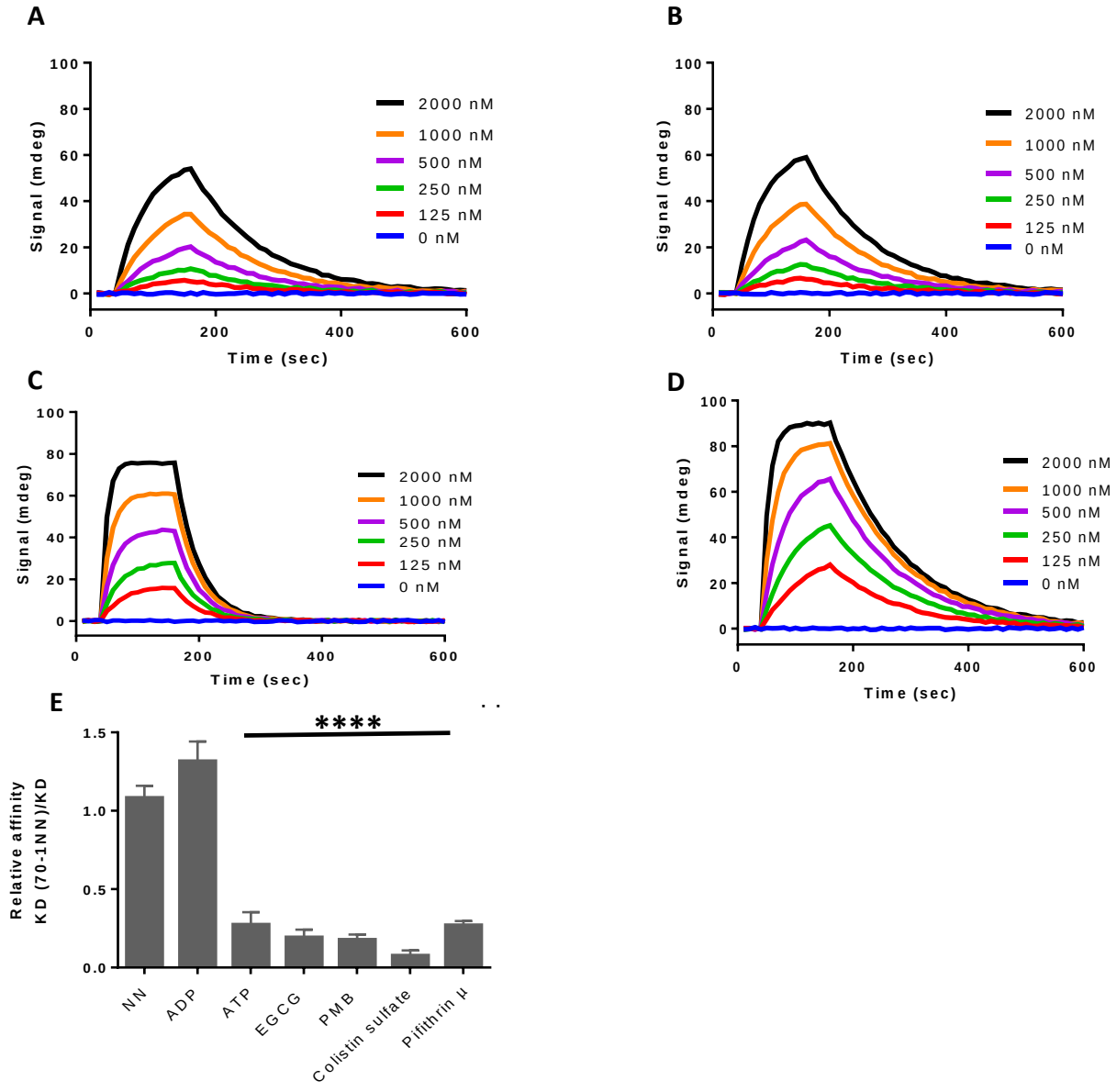

Figure 3.14: SPR analysis to confirm roles of colistin sulfate and pifithrin μ in abrogating PfHsp70-1-PfHop interaction. PfHop was immobilised on the CMD sensor chip and variable concentrations of PfHsp70-1 in the presence of inhibitors were injected as analytes over the immobilised PfHop. Representative sensorgrams conducted in the presence of of epigallocate-3-gallate (EGCG) (**A**), polymyxin B (PMB) (**B**), colistin sulfate (**C**), and pifithrin μ (**D**) are shown. The relative affinities of the interaction in the absence or presence of ADP or ATP and inhibitors are shown in (**E).** Standard errors represent three independent assays conducted using independent protein batches. The reference for One-way ANOVA was the interaction of PfHsp70-1 versus PfHop in the absence of an inhibitor. The statistically significant of differences is indicated by asterisks above the bar graphs ($p<0.0001$****).

The binding affinities for PfHsp70-1 with PfHop in the presence of both colistin sulfate and pifithrin μ were within the same order of magnitude after swapping ligand and analyte (Table 3.3). The differences in the relative affinities observed upon swapping ligand and analyte in the presence of colistin sulfate and pifithrin μ were not significant (Figure 3.14E; Appendix C9). Taken together, the SPR data revealed that both colistin sulfate and pifithrin μ bind to PfHsp70-1 with high affinity and abrogate the interaction with its functional partner PfHop.

Table 3.3: Relative affinities for the interaction of PfHsp70-1 with PfHop in the presence of nucleotides, colistin sulfate and pifithrin μ

Ligand	Analyte	Nucleotide	Ka (1/Ms)	Kd (1/s)	KD (M)	χ^2
PfHsp70-1	PfHop	NN	7.67 (+/-0.07) e^5	3.25 (+/- 0.05) e^{-3}	4.24 (+/- 0.04) e^{-9}	0.91
		ADP	7.81 (+/- 0.01) e^5	3.08 (+/- 0.08) e^{-3}	3.08 (+/- 0.08) e^{-9}	0.75
		ATP	2.59 (+/- 0.09) e^5	2.07 (+/- 0.07) e^{-2}	7.98 (+/- 0.08) e^{-8***}	2.12
		EGCG	6.31 (+/- 0.01) e^3	1.30 (+/- 0.3) e^{-1}	2.07 (+/- 0.07) e^{-5****}	0.51
		PMB	6.80 (+/- 0.8) e^3	6.96 (+/- 0.06) e^{-3}	1.02 (+/- 0.02) e^{-6****}	0.55
		Colistin sulfate	3.69 (+/- 0.09) e^4	2.84 (+/- 0.04) e^{-2}	7.70 (+/- 0.7) e^{-7****}	2.01
		Pifithrin μ	1.25 (+/- 0.05) e^5	2.66 (+/- 0.06) e^{-2}	2.14 (+/- 0.04) e^{-7****}	0.13
PfHop	PfHsp70-1	NN	7.60 (+/- 0.6) e^6	3.41 (+/- 0.01) e^{-2}	4.49 (+/- 0.09) e^{-9}	0.19
		ADP	8.07 (+/- 0.07) e^6	2.50 (+/- 0.5) e^{-2}	3.10 (+/- 0.1) e^{-9}	0.10
		ATP	2.66 (+/- 0.06) e^5	2.15 (+/- 0.05) e^{-2}	8.09 (+/- 0.09) e^{-8***}	1.67
		EGCG	6.71 (+/- 0.01) e^3	9.14 (+/- 0.04) e^{-3}	1.36 (+/- 0.06) e^{-6****}	0.12
		PMB	7.61 (+/- 0.01) e^3	8.58 (+/- 0.08) e^{-3}	1.13 (+/- 0.03) e^{-6****}	0.10
		Colistin sulfate	3.99 (+/- 0.09) e^4	2.52 (+/- 0.02) e^{-2}	6.31 (+/- 0.01) e^{-7****}	0.13
		Pifithrin μ	3.50 (+/- 0.5) e^4	8.11 (+/- 0.01) e^{-3}	2.32 (+/- 0.02) e^{-7****}	0.28

Table legends: ka-association rate constant, kd-dissociation rate constant, KD-equilibrium constant, EGCG-epigallocatechin-3-gallate, PMB-polymyxin B, X^2 values indicate the goodness of fit for SPR sensograms fitting to the bivalent fit model. Three independent analyses were conducted during the SPR assay alternating the status of ligand and analyte. Standard errors are shown in brackets. Statistical analysis was done using one-way ANOVA. $p < 0.05$ represents statistically significant differences in affinities. The asterisk (*) represents significant differences.

CHAPTER 4: DISCUSSION AND CONCLUSION

P. falciparum causes the most severe form of malaria. Unfortunately, the effectiveness of antimalarial drugs has been reduced due to emerging drug resistant parasite strains. As such, there is a need to explore novel drug targets for the treatment of malaria. PfHsp70-1 and PfHsp90 represent the main molecular chaperones that cooperate to facilitate the folding of other proteins that are essential for parasite survival (Pavithra *et al*., 2007; Shonhai *et al*., 2007). Both PfHsp70-1 and PfHsp90 are brought into proximity by PfHop. The three proteins form a functional complex within the parasite cytosol (Gitau *et al*., 2012; Zininga *et al*., 2015a). Both PfHsp70-1 and PfHsp90 are essential for the parasite survival. As such, they are potential drug targets in the design of novel antimalarials towards treatment and possible eradication of malaria disease. Therefore, this study sought to screen and identify inhibitors that target the PfHsp70-1 and PfHop complex formation. The findings from this study show that both colistin sulfate and pifithrin μ abrogate PfHop-PfHsp70-1 functional association.

The recombinant forms of PfHop and PfHsp70-1 were successfully expressed in *E. coli* XL1 Blue cells (Figure 3.3; Figure 3.4) respectively. Both PfHop and PfHsp70-1 expressions were further confirmed by Western blot using α-PfHop, α-His and α-PfHsp70-1 respectively. PfHop was confirmed as a species of approximately 66 kDa while PfHsp70-1 was confirmed as a species of 74 kDa. However, there was a species noticed below PfHop expression at approximately 55 kDa. Interestingly, these observations are line with previous expression of PfHop in *E. coli* XL1 Blue cells (Gitau *et al*., 2012). Furthermore, recombinant PfHsp70-1 and PfHop were successfully purified using nickel affinity chromatography (Figure 3.3; Figure 3.4) and further dialyzed. It was also very important to determine the solubility of each protein prior to their purification. Both PfHsp70-1 and PfHop were found to be in a soluble state and their soluble fractions were then used for purification. The final yield product of PfHsp70-1 was 7.2 mg per 1 L of culture and for PfHop was 9.6 mg per 1 L of culture suggesting a high yield production.

ELISA based analysis of the interaction between PHsp70-1 and PfHop was optimized. It was important to confirm the interaction between PfHsp70-1 and PfHop before introducing colistin

sulfate and pifithrin μ in the assay. Based on ELISA data, a direct interaction between PHsp70-1 and PfHop was observed (Figure 3.5 and Figure 3.6). Notably, PfHop and PfHsp70-1 interaction is nucleotide dependent, with ATP known to suppress the interaction while ADP does not seem to suppress the interaction that much (Gitau *et al*., 2012; Zininga *et al*., 2015a). Interestingly, the binding kinetics for the interaction showed that PfHop had a stronger affinity for PfHsp70-1 in the presence of ADP as compared to ATP (Appendix C4). These findings were in agreement with previous studies suggesting that Hop affinity for Hsp70 is enhanced by ADP (Ebonga *et al*., 2011; Gitau *et al*., 2012; Zininga *et al*., 2015a).

Furthermore, the ELISA was again used to determine the effects of colistin sulfate and pifithrin μ on the interaction of PfHsp70-1 with PfHop. EGCG and PMB were included as positive controls as they have been shown to disrupt PfHsp70-1 and PfHop interaction (Zininga *et al*., 2017a, b). The ELISA data showed that both colistin sulfate and pifithrin μ suppressed the interaction of PfHsp70-1 with PfHop (Figure 3.7 and Figure 3.8). Colistin sulfate was more effective at abrogating the interaction as compared to pifithrin μ (Figure 3.7 and Figure 3.8). To further validate the effectiveness of each inhibitor, IC_{50} values were determined from a dose response curve. Colistin sulfate had an IC_{50} of 1.187 nM and pifithrin μ had an IC_{50} of 1.427 nM (Appendix C7). Overall, both colistin sulfate and pifithrin μ abrogate the PfHsp70-1 and PfHop interaction and this suggest that both inhibitors are promising antiplasmodial agents targeting the Hsp70-Hop protein folding pathway of the malaria parasite.

SPR analysis was used to validate the ELISA data for the interaction of PfHsp70-1 with PfHop. The SPR data validated that the interaction between PfHsp70-1 and PfHop exist. The SPR data also confirmed that the interaction occurred in a concentration dependent manner (Figure 3.9 and Figure 3.10). As a negative control, the NBD of PfHsp70-1 was used. As expected, no interacton between PfHsp70-1_{NBD} and PfHop occurred (Table 3.1). The analysis showed that the interaction between PfHsp70-1_{NBD} and PfHop was too low to be determined. This was in line with the previous findings, where there was no interaction observed between PfHsp70-1_{NBD} and PfHop (Zininga *et al*., 2015a). PfHsp70-1_{NBD} lacks the EEVD motif which is important for interaction with co-chaperones containing TPR domains (Mabate *et al*., 2018; Zininga *et al*., 2015a). The SPR data further confirmed that the interaction between PfHsp70-1 and PfHop also occurred in the presence of nucleotides (Figure 3.9 and Figure 3.10). In addition, The SPR kinetics data confirmed that the

interaction of PfHsp70-1 with PfHop was more favored by ADP compared with ATP (Table 3.1). The interaction in the presence of ATP was reduced by one order of magnitude (Table 3.1), suggesting a more affinity binding in the presence of ADP and less binding in the presence of ATP (Table 3.1). Overall, these findings were in line with previous findings (Gitau *et al*., 2012; Zininga *et al* 2015a).

Furthermore, the SPR assay was used to determine the capability of colistin sulfate and pifithrin μ to bind to Hsp70 chaperone. In this case, nucleotides (ATP/ADP) were used as controls to validate the specificity of binding. For the first time, this study demonstrated that colistin sulfate binds to PfHsp70-1 (Figure 3.11; Table 3.2). In addition, pifithrin μ also binds to PfHsp70-1 (Figure 3.11; Table 3.2). Both colistin sulfate and pifithrin μ bind to PfHsp70-1 with high affinity compared to ATP (Figure 3.11; Table 3.2). The binding affinities for both colistin sulfate and pifithrin μ to PfHsp70-1 were in the same range of magnitude (Table 3.2). The study further established that colistin sulfate binds to PfHsp70-1_{NBD} with higher affinity that the full length PfHsp70-1 while pifithrin μ did not show high binding affinity (Table 3.2). These findings are in agreement with previously reported data on colistin sulfate's derivative (PMB) (Zininga *et al*., 2017a). In addition, colistin sulfate was initially known to bind to the NBD of Hsp90 (Minagawa *et al*., 2012), while pifithrin μ has been reported to bind to the C-terminal SBD of human Hsp70 in cancer cells (Liu *et al*., 2009; Kaiser *et al*., 2011; Leu *et al*., 2014).

This study also assessed the capability of these inhibitors to bind to PfHsp70-1 interacting partner PfHop using SPR assay. As a positive control, ATP was used. Studies have reported that PfHop possesses a nucleotide binding domain motif and its affinity for ATP was found to be comparable with affinities for PfHsp70-1 and PfHsp70-1_{NBD} (Yamamoto *et al*., 2014; Makumire, 2019). The SPR data showed that colistin sulfate and pifithrin μ bind to PfHop with less affinity compared to full length PfHsp70-1 (Table 3.2).

Furthermore, the SPR assay was used to determine effect of colistin sulfate and pifithrin μ on the interaction of PfHsp70-1 with PfHop. EGCG and PMB were used as positive controls. As expected, their data showed that the affinity of PfHsp70-1 and PfHop interaction was greatly reduced by four order of magnitude for EGCG and three order of magnitude for PMB compared to the interaction in the absence of an inhibitor. This was in line with previously reported data

(Zininga *et al*., 2017a, b). The SPR analysis confirmed that ADP enhances the interaction of PfHsp70-1 with PfHop as compared to ATP (Figure 3.9 and Figure 3.10). However, when colistin sulfate was introduced into the reaction mixture, reduction of affinity of PfHsp70-1 for PfHop was noted (Figure 3.13 and Figure 3.14; Table 3.3). This suggests that colistin sulfate disrupted the interaction (Table 3.3). In addition, the same phenomenon was observed when pifithrin μ was introduced into the reaction mixture (Figure 3.13 and Figure 3.14). The relative affinities of the inhibition by both colistin sulfate and pifithrin μ were within the same range of magnitude (Table 3.3). Overall, both colistin sulfate and pifithrin μ are capable of disrupting the PfHsp70-1 and PfHop functional pathway. This will eventually lead to the degradation of client proteins that solely depend on this pathway to fold and perform biological functions.

In conclusion, this was the first study to establish that colistin sulfate and pifithrin μ directly bind to PfHsp70-1 to inhibit its association with its interacting partner, PfHop. Altogether, these findings contribute to the possibility of both colistin sulfate and pifithrin μ as antiplasmodial agents. In the future, it will be important to investigate the effect of colistin sulfate and pifithrin μ on malaria parasite cells and further investigate if colistin sulfate and pifithrin μ are capable of inhibiting the parasite PfHsp70-1-PfHop pathway without affecting the human Hsp70-Hop pathway.

REFERENCES

Achan, J., Talisuna, A.O., Erhart, A., Yeka, A., Tibenderana, J.K., Baliraine, F.N., Rosenthal, P.J., D'Alessandro, U. (2011). Quinine, an old anti-malarial drug in a modern world: role in the treatment of malaria. *Malar J*, **1**: 144.

Acharya, P., Kumar, R., Tatu, U. (2007). Chaperoning a cellular upheaval in malaria: heat shock proteins in *Plasmodium falciparum*. *Mol Biochem Parasitol*, **153**: 85-94.

Acharya, P., Kumar, R., Tatu, U. (2007). Chaperoning a cellular upheaval in malaria: heat shock proteins in *Plasmodium falciparum*. *Mol Biochem Parasitol*. **153**: 85–94.

Ahmad, A., Bhattacharya, A., McDonald, R.A., Cordes, M., Ellington, B., Bertelsen, E.B., Zuiderweg, E.R. (2011). Heat shock protein 70 kDa chaperone/DnaJ cochaperone complex employs an unusual dynamic interface. *Proc Natl Acad Sci* **108**: 18966-18971.

Ashton, M., Sy, N.D., Van Huong, N., Gordi, T., Hai, T.N., Huong, D.X., Niêu, N.T., Công, L.D., (1998). Artemisinin kinetics and dynamics during oral and rectal treatment of uncomplicated malaria. *Clin Pharmacol* Ther, **63**: 482-493.

Banumathy, G., Singh, V., Pavithra, S. R, and Tatu, U. (2003). Heat shock protein 90 is essential for *Plasmodium falciparum* growth in human erythrocytes. *J Biol Chem*, **278**: 18336–18345.

Barends, T.R., Werbeck, N.D., Reinstein, J. (2010). Disaggregases in 4 dimensions. *Curr Opin Struct Biol*. **20**: 46-53.

Bergen, P.J., Li, J., Rayner, C.R., Nation, R.L. (2006). Colistin methanesulfonate is an inactive prodrug of colistin against *Pseudomonas aeruginosa*. *Antimicrob Agents Chemother*, **50**: 1953-1958.

Birnbaum, J., Scharf, S., Schmidt, S., Jonscher, E., Hoeijmakers, W.A.M., Flemming, S., Toenhake, C.G., Schmitt, M., Sabitzki, R., Bergmann, B., Fröhlke, U. (2020). A Kelch13-defined endocytosis pathway mediates artemisinin resistance in malaria parasites. *Sciences*, **367**: 51-59.

Bonnet, M., Roper, C., Félix, M., Coulibaly, L., Kankolongo, G.M., Guthmann, J.P. (2007). Efficacy of antimalarial treatment in Guinea: in vivo study of two artemisinin combination therapies in Dabola and molecular markers of resistance to sulphadoxine-pyrimethamine in N'Zerekore. *Malar J*, **6**: 54.

Borges-Walmsley, M.I., Mckeegan, K.S., Walmsley, A.R. (2003). Structure and function of efflux pumps that confer resistance to drugs. *Biochem J*, ***376***: 313-338.

Bosl, B., Grimminger, V., Walter, S. (2006). The molecular chaperone Hsp104-a molecular machine for protein disaggregation. *J Struct Biol*, **156**: 139–148.

Botha, M., Chiang, A.N., Needham, P.B., Stephens, L.L., Hoppe, H.C., Külzer, S., Przyborski, J.M., Lingelbach, K., Wipf, P., Brodsky, J.L., Shonhai, A., Blatch, G.L. (2011). *Plasmodium falciparum* encodes a single cytosolic type I Hsp40 that functionally interacts with Hsp70 and is upregulated by heat shock. *Cell Stress Chaperones*, **16**: 389-401.

Botha, M., Pesce, E.R., Blatch, G.L. (2007). The Hsp40 proteins of Plasmodium *falciparum* and other apicomplexa: regulating chaperone power in the parasite and the host. *Int J Biochem Cell Biol*, **39**: 1781-803.

Boyle, M.J., Richards, J.S., Gilson, P.R., Chai, W., Beeson, J.G. (2010). Interactions with heparin-like molecules during erythrocyte invasion by *Plasmodium falciparum* merozoites. *Blood*, **115**: 4559-68.

Brodsky, J.L., Bracher, A. (2007). Nucleotide exchange factors for Hsp70 molecular chaperones. In *Networking of Chaperones by Co-chaperones*, 1-12. Springer, New York, NY.

Bukau, B., Weissman, J., Horwich, A. (2006). Molecular chaperones and protein quality control. *Cell*, **125**: 443–451.

Butler, N.S., Schmidt, N.W., Harty, J.T. (2010). Differential effector pathways regulate memory CD8 T cell immunity against *Plasmodium berghei* versus *P. yoelii* sporozoites. *J Immunol*, **184**: 2528-2538.

Chakafana, G., Zininga, T., Shonhai, A. (2019). Comparative structure-function features of Hsp70s of *Plasmodium falciparum* and human origins. *Biophys Rev*, 1-12.

Chang, H.C.J., Nathan, D.F., Lindquist, S. (1997). In vivo analysis of the Hsp90 cochaperone Sti1 (p60). *Mol Cell Biol*, **17**: 318–325.

Charnaud, S.C., Dixon, M.W., Nie, C.Q., Chappell, L., Sanders, P.R., Nebl, T., Hanssen, E., Berriman, M., Chan, J.A., Blanch, A.J., Beeson, J.G. (2017). The exported chaperone Hsp70-x supports virulence functions for *Plasmodium falciparum* blood stage parasites. *PLoS One*, **12**: e0181656.

Chen, Y., Murillo-Solano, C., Kirkpatrick, M., Antoshchenko, T., Park, T., Pizarro, J. (2018). Repurposing drugs to target the malaria parasite unfolding protein response. *Sci Rep*. **8**: 10333–10350.Chen, Y., Murillo-Solano, C., Kirkpatrick, M.G., Antoshchenko, T., Park, H.W., Pizarro, J.C., (2018). Repurposing drugs to target the malaria parasite unfolding protein response. *Sci R*, **8**: 1-12.

Ciglia, E., Vergin, J., Reimann, S., Smits, S.H.J., Schmitt, L., Groth, G., Holger, G. (2014). Resolving hot spots in the C-terminal dimerization domain that determine the stability of the molecular chaperone Hsp90. *PLoS One*, **9**: e96031.

Cobb, D.W., Florentin, A., Fierro, M.A., Krakowiak, M., Moore, J.M., Muralidharan, V. (2017). The exported chaperone PfHsp70x is dispensable for the *Plasmodium falciparum* intraerythrocytic life cycle. *MSphere*, ***2***.

Cockburn, I.L., Boshoff, A., Pesce, E.R., Blatch, G.L. (2014). Selective modulation of plasmodial Hsp70s by small molecules with antimalarial activity. *Biol Chem*, **395**: 1353–1362.

Cockburn, I.L., Pesce, E.-R., Pryzborski, J.M., Davies-Coleman, M.T., Clark, P.G., Keyzers, R.A., Stephens, L.L., Blatch, G.L. (2011). Screening for small molecule modulators of Hsp70 chaperone activity using protein aggregation suppression assays: Inhibition of the plasmodial chaperone PfHsp70-1. *Biol Chem*., **392**: 431–438.

Cowman, A.F., Karcz, S., Galatis, D., Culvenor, J.G. (1991). A P-glycoprotein homologue of *Plasmodium falciparum* is localized on the digestive vacuole. *J Cell Biol*, **113**: 1033-1042.

Cui, L., Mharakurwa, D.N., Ndiaye, D., Rathod, P.K., Rosenthai, P.J. (2015). Antimalarial drug resistance: Literature review and activities and findings of the ICEMR Network, **93**: 57-68.

Cunico, W., Ferreira, M.D.L.G., Ferreira, T.G., Penido, C., Henriques, M.G., Krettli, L.G., Varotti, F.P., Krettli, A.U. (2008). Synthesis and antimalarial activity of novel hydroxyethylamines, potential aspartyl protease inhibitors. *Lett Drug Des Discov*, **5**: 178-181.

Curd, F.H.S., Davey, D.G., Rose, F.L. (1945). Studies on synthetic antimalarial drugs: ii.—General chemical considerations. *Ann Trop Med Parasitol*, **39**: 157-164.

Daniyan, M.O., Przyborski, J.M. and Shonhai, A. (2019). Partners in mischief: functional networks of heat shock proteins of *Plasmodium falciparum* and their influence on parasite virulence. *Biomolecules*, **9**: 295.

De Maio, A., Santoro, M.G., Tanguay, R.M., Hightower, L.E. (2012). Ferruccio Ritossa's scientific legacy 50 years after his discovery of the heat shock response: a new view of biology, a new society, and a new journal. *Cell Stress Chaperones*, **17**: 139-143.

Demand, J., Alberti, S., Patterson, C., Höhfeld, J. (2001). Cooperation of a ubiquitin domain protein and an E3 ubiquitin ligase during chaperone/proteasome coupling. *Curr Biol*, **11**: 1569-1577.

Dragovic, Z., Broadley, S.A., Shomura, Y., Bracher, A., Hartl, F.U. (2006). Molecular chaperones of the Hsp110 family act as nucleotide exchange factors of Hsp70s. EMBO J**, 25**: 2519-2528.

Ebonga, I., Morgnera, N., Zhoua, M., Saraivab, M.A., Daturpallib, S., Jacksonb, S.E., Robinsona, C.V. (2011). Heterogeneity and dynamics in the assembly of the heat shock protein 90 chaperone complexes. *Proc Natl Acad Sci*, **108**: 17939–17944.

El Bakkouri, M., Pow, A., Mulichak, A., Cheung, KL., Artz, JD., Amani, M., Fell, S., de Koning-Ward, TF., Goodman, CD., McFadden, GI., Ortega, J. (2010).The Clp chaperones and proteases of the human malaria parasite *Plasmodium falciparum*. *J Mol Biol*, **404**: 456-77.

Evans, C.G., Chang, L., Gestwicki, J.E. (2010). Heat shock protein 70 (hsp70) as an emerging drug target. *J Med Chem*. **53**: 4585-4602.

Fairhurst, R., McCutchan, T.F., Aravind, L. (2007). Molecular factors and biochemical pathways induced by febrile temperature in intra erythrocytic *Plasmodium falciparum* parasites. Infect Immun, **75**: 2012-2025.

Falagas, M.E., Kasiakou, S.K. and Saravolatz, L.D. (2005). Colistin: the revival of polymyxins for the management of multidrug-resistant gram-negative bacterial infections. *Clin Infec Dis*, **40**: 1333-1341.

Famin, O., Ginsburg, H. (2003). The treatment of *Plasmodium falciparum*-infected erythrocytes with chloroquine leads toaccumulation of ferriprotoporphyrin IX bound to particularparasite proteins and to the inhibition of the parasite's 6-phosphogluconate dehydrogenase. *Parasite*, **10**:39–50.

Feder, M.E., Hofmann, G.E. (1999). Heat-shock proteins, molecular chaperones, and the stress response: evolutionary and ecological physiology. *Annu Rev Physiol*, **61**: 243-282.

Feng, X., Carlton, J.M., Joy, D.A., Mu, J., Furuya, T., Suh, B.B., Wang, Y., Barnwell, J.W., Su, X.Z. (2003). Single-nucleotide polymorphisms and genome diversity in *Plasmodium vivax*. *Proc Natl Acad Sci,*, ***100***: 8502-8507.

Ferraris, M., Perero, S., Miola, M., Ferraris, S., Gautier, G., Maina, G., Fucale, G., Verne, E. (2010). Chemical, mechanical, and antibacterial properties of silver nanocluster–silica composite coatings obtained by sputtering. *Adv Eng Mater*, **12**: B276-B282.

Fitch CD. (1989). Ferriprotoporphyrin IX: role in chloroquine susceptibility and resistance in malaria. *Prog Clin Biol Res*, **313**:45–52.

Flom, G., Weekes, J., Williams, J.J., Johnson, J.L. (2006). Effect of mutation of the tetratricopeptide repeat and asparatate-proline 2 domains of Sti1 on Hsp90 signaling and interaction in Saccharomyces cerevisiae. *Genetics*, **172**: 41-51.

Fujioka, H., Aikawa, M. (2002). Structure and life cycle. In *Malaria Immunology*, **80**: 1-26.

Gavigan, C.S., Shen, M., Machado, S.G., Bell, A. (2007). Influence of the *Plasmodium falciparum* P-glycoprotein homologue 1 (pfmdr1 gene product) on the antimalarial action of cyclosporin. *J Antimicrob Chemother*, **59:** 197-203.

Gelinsky-Wersing, D., Wersing, W. and Pompe, W. (2017). Bivalent kinetic binding model to surface plasmon resonance studies of antigen-antibody displacement reactions. *Anal Biochem*, **518**: 110-125.

Gitau, G.W., Mandal, P., Blatch, G.L., Przyborski, J., Shonhai, A. (2012). Characterization of the *Plasmodium falciparum* Hsp70-Hsp90 organising protein (PfHop). *Cell Stress Chaperones*, **17**: 191-202.

Grigg, R., Lea, R., Sullivan, A.A., Curtain, R., MacMillian, J. Griffiths, L. (2000). Identification of a novel mutation C144F in the Notch3 gene in an Australian CADASIL pedigree. *Human mutation*, **16**: 449.

Hahn, J.S. (2009). The Hsp90 chaperone machinery: from structure to drug development. *BMB Rep*. **42**: 623-30.

Hartl, F.U., Hayer-Hartl, M. (2002). Molecular chaperones in the cytosol: from nascent chain to folded protein. *Sciences*, **295**: 1852-1858.

Hartl, F.U., Hayer-Hartl, M. (2009). Converging concepts of protein folding in vitro and in vivo. *Nat Struct Mol Biol*, **16**: 574.

Hennessy, F., Nicoll, W.S., Zimmermann, R., Cheetham, M.E., Blatch, G.L. (2005). Not all J domains are created equal: implications for the specificity of Hsp40-Hsp70 interactions. *Protein Sci*, **14**: 1697–1709.

Hobbs, C., Duffy, P. (2011). Drugs for malaria: something old, something new, something borrowed. *F1000 Biol Rep*, **3**, 24-32.

Hombach, A., Heuser, C., Sircar, R., Tillmann, T., Diehl, V., Pohl, C., Abken, H. (1998). An anti-CD30 chimeric receptor that mediates CD3-ζ-independent T-cell activation against Hodgkin's lymphoma cells in the presence of soluble CD30. *Cancer Res*, **58**: 1116-1119.

Jhaveri, K., Taldone, T., Modi, S., Chiosis, G. (2012). Advances in the clinical development of heat shock protein 90 (Hsp90) inhibitors in cancers. *Biochim Biophys Acta*, **1823**: 742–55.

J.M., Lingelbach, K., Wipf, P., Brodsky, J.L., Shonhai, A., & Blatch, G.L. (2011). *Plasmodium falciparum* encodes a single cytosolic type I Hsp40 that functionally interacts with Hsp70 and is upregulated by heat shock. *Cell Stress Chaperones*, **16**: 389-401.

Jemal, A., Center, M.M., DeSantis, C., Ward, E.M. (2010). Global patterns of cancer incidence and mortality rates and trends. *Cancer Epidemiol Biomarkers Prev*, **19**: 1893-1907.

Jiang, J., Maes, E.G., Taylor, A.B., Wang, L., Hinck, A.P., Lafer, E.M. and Sousa, R. (2007). Structural basis of J cochaperone binding and regulation of Hsp70. *Molecular Cell*, **28**: 422-433.

Johnson, J.L., Brown, C. (2009). Plasticity of the Hsp90 chaperone machine in divergent eukaryotic organisms. *Cell Stress Chaperones*, **14**: 83-94.

Kabani, M., Martineau, C.N. (2008). Multiple hsp70 isoforms in the eukaryotic cytosol: mere redundancy or functional specificity?. *Curr Genomics*, **9**: 338-348.

Kaiser, M., Kühnl, A., Reins, J., Fischer, S., Ortiz-Tanchez, J., Schlee, C., Mochmann, L.H., Heesch, S., Benlasfer, O., Hofmann, W.K., Thiel, E. (2011). Antileukemic activity of the HSP70 inhibitor pifithrin-μ in acute leukemia. *Blood Cancer J*, **1**: e28-e28.

Kampinga, H.H., Craig, E.A. (2010). The HSP70 chaperone machinery: J proteins as drivers of functional specificity. *Nat reviews Mol Cell Biol*, **11**: 579-592.

Kampinga, H.H., Hageman, J., Vos, M.J., Kubota, H., Tanguay, R.M., Bruford, E.A., Cheetham, M.E., Chen, B., Hightower, L.E. (2009). Guidelines for the nomenclature of the human heat shock proteins. *Cell Stress Chaperones*, **14***:* 105-111.

Karagöz, G.E., Rüdiger, S.G. (2015). Hsp90 interaction with clients. *Trends Biochem Sci*, **40**: 117-125.

Kaur, K., Jain, M., Reddy, R.P., Jain, R. (2010). Quinolines and structurally related heterocycles as antimalarials. *Eur J Med Chem*, **45**: 3245-3264.

Komura, S., Kurahashi, K. (1979). Partial purification and properties of L-2,4-diaminobutyric acid activating enzyme from a polymyxin E producing organism, *J Biochem*, **86**: 1013-21.

Krukenberg, K.A., Street, T.O., Lavery, L.A., Agard, D.A. (2011). Conformational dynamics of the molecular chaperone Hsp90. *Q Rev Biophys*, **44**: 229-255.

Kudyba, H.M., Cobb, D.W., Fierro, M.A., Florentin, A., Ljolje, D., Singh, B., Lucchi, N.W., Muralidharan, V. (2019). The endoplasmic reticulum chaperone PfGRP170 is essential for asexual development and is linked to stress response in malaria parasites. *Cellular Microbiol*, **21**: e13042.

Külzer, S., Charnaud, S., Dagan, T., Riedel, J., Mandal, P., Pesce, E.R., Blatch, G.L., Crabb, B.S., Gilson, P.R., Przyborski, J.M. (2012). *Plasmodium falciparum*-encoded exported Hsp70/Hsp40 chaperone/co-chaperone complexes within the host erythrocyte. *Cell Microbiol*, **14**: 1784-1795.

Kumar, N., Koski, G., Harada, M., Aikawa, M., Zheng, H. (1991). Induction and localization of *Plasmodium falciparum* stress proteins related to the heat shock protein 70 family. *Mol Biochem Parasitol*, **48**: 47–58.

Kumar, R., Musiyenko, A., Barik, S. (2003). The heat shock protein 90 of *Plasmodium falciparum* and antimalarial activity of its inhibitor, geldanamycin. *Malar J*, **2**: 30.

Kusnezow, W., Hoheisel, J.D. (2003). Solid supports for microarray immunoassays. *J Mol Recognit*, **16**: 165-176.

Lacroix, M., Toillon, R.A., Leclercq, G. (2006). p53 and breast cancer, an update. *Endocrine-related Cancer*, **13**: 293-325.

Lebepe, C.M., Matambanadzo, P.R., Makhoba, X.H., Achilonu, I., Zininga, T., Shonhai, A. (2020). Comparative Characterization of *Plasmodium falciparum* Hsp70-1 Relative to *E. coli* DnaK Reveals the Functional Specificity of the Parasite Chaperone. *Biomolecules*, **10**: 856.

Li, D., Marchenko, N.D., Schulz, R., Fischer, V., Velasco-Hernandez, T., Talos, F., Moll, U.M. (2011). Functional inactivation of endogenous MDM2 and CHIP by HSP90 causes aberrant stabilization of mutant p53 in human cancer cells. *Mol Cancer Res*, **9**: 577-588.

Liu, F., Cui, S.J., Hu, W., Feng, Z., Wang, Z.Q., and Han, Z.G. (2009). Excretory/secretory proteome of the adult developmental stage of human blood fluke, *Schistosoma japonicum. Mol Cell Proteomics*, **8**: 1236-1251.

Liu, H.H., He, J.Y., Chi, C.F., Shao, J. (2014). Differential HSP70 expression in Mytilus coruscus under various stressors. *Gene*, **54***:* 166-173.

Lu, Z., Cyr, D.M. (1998). Protein folding activity of Hsp70 is modified differentially by the hsp40 co-chaperones Sis1 and Ydj1. *J Biol Chem*, **273**: 27824-27830.

Mabate, B., Zininga, T., Ramatsui, L., Makumire, S., Achilinou, I., Dirr, H., Shonhai, A. (2018). Structural and biochemical characterization of *Plasmodium falciparum* Hsp70-x reveals functional versatility of its C-terminal EEVN motif. *Proteins*: *Structure Function and Bioinformatics*, **86**: 1189-1201.

Makumire, S. (2019). Investigation of the role of the GGMP motif of *Plasmodium falciparum* Hsp70-1 on the chaperone function of the protein and its interaction with a co-chaperone, *PfHop* (Doctoral dissertation, University of Venda).

Makumire, S., Zininga, T., Vahokoski, J., Kursula, I., Shonhai, A. (2020). Biophysical analysis of *Plasmodium falciparum* Hsp70-Hsp90 organising protein (PfHop) reveals a monomer that is characterised by folded segments connected by flexible linkers. *PloS One*, **15**: e0226657.

Matambo, T. S., Odunuga, O. O., Boshoff, A., Blatch, G. L. (2004). Overproduction, purification, and characterization of the *Plasmodium falciparum* heat shock protein 70. *Protein Expr Purif*, **33**: 214–222.

Mayer, M.P., Bukau B. (2005). Hsp70 chaperones: cellular functions and molecular mechanism. *Cell Mol Life Sci*, **62**: 670–684.

McDonough, H., Patterson, C., (2003). CHIP: a link between the chaperone and proteasome systems. *Cell Stress Chaperones*, **8**: 303.

McHaourab, H.S., Godar, J.A., Stewart, P.L. (2009). Structure and mechanism of protein stability sensors: chaperone activity of small heat shock proteins. *Biochemistry*. **48**: 3828-37.

Minagawa, S., Kondoh, Y., Sueoka, K., Osada, H. and Nakamoto, H. (2012). Cyclic lipopeptide antibiotics bind to the N-terminal domain of the prokaryotic Hsp90 to inhibit the chaperone activity. *Biochem J*, **435**: 237-246.

Miotto, O., Amato, R., Ashley, E.A., MacInnis, B., Almagro-Garcia, J., Amaratunga, C., Lim, P., Mead, D., Oyola, S.O., Dhorda, M., Imwong, M. (2015). Genetic architecture of artemisinin-resistant *Plasmodium falciparum*. *Nat Genet*, **47**: 226.

Mishra, N., Kaitholia, K., Srivastava, B., Shah, N.K., Narayan, J.P., Dev, V., Phookan, S., Anvikar, A.R., Rana, R., Bharti, R.S., Sonal, G.S. (2014). Declining efficacy of artesunate plus sulphadoxine-pyrimethamine in northeastern India. *Malar J*, **13**: 284.

Mogk, A., Kummer, E., Bukau, B. (2015). Cooperation of Hsp70 and Hsp100 chaperone machines in protein disaggregation. *Front Mol Biosci*, **2**: 22.

Morishima, Y., Kanelakis, K.C., Murphy, P.J., Lowe, E.R., Jenkins, G.J., Osawa, Y., Sunahara, R.K. and Pratt, W.B. (2003). The hsp90 cochaperone p23 is the limiting component of the multiprotein hsp90/hsp70-based chaperone system in vivo where it acts to stabilize the client protein· hsp90 complex. *J Biol Chem*, **278**: 48754-48763.

Muralidharan, V., Oksman, A., Pal, P., Lindquist, S., Goldberg, D.E. (2012). *Plasmodium falciparum* heat shock protein 110 stabilizes the asparagine repeat-rich parasite proteome during malarial fevers. *Nat Commun*, **3**: 1310.

Nation, R.L., Li, J. (2009). Colistin in the 21st century. *Curr Opin Infect Dis*, **22**: 535.

Nicolet, C.M., Craig, E.A. (1989). Isolation and characterization of STI1, a stress-inducible gene from Saccharomyces cerevisiae. *Mol Cell Biol*, **9**: 3638-3646.

Njunge, J.M., Ludewig, M.H., Boshoff, A., Pesce, E.R., and Blatch, G.L. (2013). Hsp70s and J proteins of *Plasmodium* parasites infecting rodents and primates: structure, function, clinical relevance, and drug targets. *Curr Pharm Des*, **19**: 387-403.

Njunge, J.M., Mandal, P., Przyborski, J.M., Boshoff, A., Pesce, E.R., Blatch, G.L. (2015). PFB0595w is a *Plasmodium falciparum* J protein that co-localizes with PfHsp70-1 and can stimulate its in vitro ATP hydrolysis activity. *Int J Biochem Cell Biol*, **62**: 47-53.

Nowicki, Ł., Leźnicki, P., Morawiec, E., Litwińczuk, N., Liberek, K. (2012). Role of a conserved aspartic acid in nucleotide binding domain 1 (NBD1) of Hsp100 chaperones in their activities. *Cell Stress Chaperones*, **17**: 361–373.

Nyakundi, D.O., Vuko, L.A., Bentley, S.J., Hoppe, H., Blatch, G.L., Boshoff, A. (2016). *Plasmodium falciparum* Hep1 is required to prevent the self-aggregation of PfHsp70-3. *PLoS One*, **11**: e0156446.

Oakley, M.S.M., Kumar, S., Anantharaman, V., Zheng, H., Mahajan, B., Haynes, J.D., Moch, J.K., Shahinas, D., Folefoc, A., Taldone, T., Chiosis, G., Crandall, I., Pillai, D.R. (2013). A purine analog synergizes with chloroquine (CQ) by targeting *Plasmodium falciparum* Hsp90 (PfHsp90). *PLoS One*, **8**: 9.

Odunuga, O.O., Hornby, J.A., Bies, C., Zimmermann, R., Pugh, D.J., Blatch, G.L. (2003). Tetratricopeptide repeat motif-mediated Hsc70-mSTI1 interaction molecular characterization of the critical contacts for successful binding and specificity. *J Biol Chem*, **278**: 6896-6904.

Odunuga, O.O., Longshaw, V.M., Blatch, G.L. (2004). Hop: more than an Hsp70/Hsp90 adaptor protein. *Bioessays*, **26**: 1058-1068.

O'Neill, P.M., Amewu, R.K., Nixon, G.L., Bousejra ElGarah, F., Mungthin, M., Chadwick, J., Shone, A.E., Vivas, L., Lander, H., Barton, V., Muangnoicharoen, S. (2010). Identification of a 1, 2, 4, 5-tetraoxane antimalarial drug-development candidate (RKA 182) with superior properties to the semisynthetic artemisinins. *Angew Chem Int Ed*, **49**: 5693-5697.

Pallavi, R., Acharya, P., Chandran, S., Daily, J.P., Tatu, U. (2010). Chaperone expression profiles correlate with distinct physiological states of *Plasmodium falciparum* in malaria patients. *Malar J*, **9**: 236.

Pavithra, S.R., Kumar, R., Tatu, U. (2007). Systems analysis of chaperone networks in the malarial parasite *Plasmodium falciparum*. *PLoS Comput Biol*, **3***:* 9.

Pesce, E. R., Acharya, P., Tatu, U., Nicoll, W. S., Shonhai, A., Hoppe, H. C., Blatch, G. L. (2008). The *Plasmodium falciparum* heat shock protein 40, Pfj4, associates with heat shock protein 70 and shows similar heat induction and localization patterns. *J Biochem Cell Biol*, **40**: 2914-2926.

Posfai, D., Sylvester, K., Reddy, A., Ganley, J.G., Wirth, J., Cullen, Q.E., Dave, T., Kato, N., Dave, S.S., Derbyshire, E.R. (2018). *Plasmodium* parasite exploits host aquaporin-3 during liver stage malaria infection. *PLoS Pathog*, **14**: 100-7057.

Prodromou, C., Siligardi, G., O'Brien, R., Woolfson, D.N., Regan, L., Panaretou, B., Ladbury, J.E., Piper, P.W., Pearl, L.H. (1999). Regulation of Hsp90 ATPase activity by tetratricopeptide repeat (TPR)-domain co-chaperones. *EMBO J*, **18**: 54-762.

R Teixeira, R., W de M Carneiro, J., T de Araujo, M., G Taranto, A. (2012). A critical view on antimalarial endoperoxide QSAR studies. *Mini Rev Med Chem*, ***12***: 562-572.

Ratzke, C., Mickler, M., Hellenkamp, B., Buchner, J., Hugel, T. (2010). Dynamics of heat shock protein 90 C-terminal dimerization is an important part of its conformational cycle. *Proc Natl Acad Sci*, **107**: 16101-16106.

Reed, M.B., Saliba, K.J., Caruana, S.R., Kirk, K., Cowman, A.F. (2000). Pgh1 modulates sensitivity and resistance to multiple antimalarials in *Plasmodium falciparum*. *Nature*, **403**: 906-909.
Ritossa, F. (1996). Discovery of the heat shock response. *Cell Stress Chaperones*, **1**: 97-8.

Rosser, M.F., Cyr, D.M. (2007). Do Hsp40s act as chaperones or co-chaperones? In *Networking of Chaperones by Co-Chaperones*, 38-51. Springer, New York, NY.

Rubio, J.P., Cowman, A.F. (1996). The ATP-binding cassette (ABC) gene family of *Plasmodium falciparum*. *Parasitol Today*, **12**: 135-140.

Saibil, H. (2013). Chaperone machines for protein folding, unfolding and disaggregation. *Nat Rev Mol Cell Biol*, **14**: 630-642.

Sargeant, T.J., Marti, M., Caler, E., Carlton, J.M., Simpson, K., Speed, T. P., Cowman, A. F. (2006). Lineage-specific expansion of proteins exported to erythrocytes in malaria parasites. *Genome Biol*, **7**: R12.

Sato, S., Wilson, R.J.M. (2005). The plastid of *Plasmodium* spp.: a target for inhibitors. In *Malaria: Drugs, Disease and Post-genomic Biology*, 251-273.

Scheufler, C., Brinker, A., Bourenkov, G., Pegoraro, S., Moroder, L., Bartunik, H., Hartl, F.U., Moarefi, I. (2000). Structure of TPR domain–peptide complexes: critical elements in the assembly of the Hsp70–Hsp90 multichaperone machine. *Cell*, **101**: 199-210.

Schmid, A.B., Lagleder, S., Gräwert, M.A., Röhl, A., Hagn, F., Wandinger, S.K., Cox, M.B., Demmer, O., Richter, K., Groll, M., Kessler, H. (2012). The architecture of functional modules in the Hsp90 co-chaperone Sti1/Hop. *EMBO J*, **31**: 1506-1517.

Seo, Y.H. (2015). Organelle-specific Hsp90 inhibitors. *Arch Pharm Res*, **38**: 1582-1590.

Seraphim, T.V., Ramos, C.H. and Borges, J.C. (2014). The interaction networks of Hsp70 and Hsp90 in the *Plasmodium* and *Leishmania* parasites. In *The molecular chaperones interaction networks in protein folding and degradation*, 445-481.

Sharma, D., Masison, D.C. (2009). Hsp70 structure, function, regulation and influence on yeast prions. *Protein Pept Lett*, **16**: 571–581.

Sharma, Y.D. (1992). Structure and possible function of heat-shock proteins in *Plasmodium falciparum*. *Comp Biochem Physiol*, **102**: 437–444.

Shiber, A., Ravid, T. (2014). Chaperoning proteins for destruction: diverse roles of Hsp70 chaperones and their co-chaperones in targeting misfolded proteins to the proteasome. *Biomolecules*, **4**: 704-724.

Shonhai, A. (2010). Plasmodial heat shock proteins: targets for chemotherapy. *FEMS Immunol Med Microbiol*, **58**: 61-74.

Shonhai, A., Boshoff, A., Blatch, G. L. (2005). *Plasmodium falciparum* heat shock protein 70 is able to suppress the thermosensitivity of an *Escherichia coli* DnaK mutant strain. *Mol Genet Genomic*s, **274**: 70–78.

Shonhai, A., Boshoff, A., Blatch, G.L. (2007). The structural and functional diversity of Hsp70 proteins from *Plasmodium falciparum*. *Protein Sci*, **16:** 1803-1818.

Shonhai, A., Botha, M., de Beer, T.A., Boshoff, A., Blatch, G.L. (2008). Structure-function study of a *Plasmodium falciparum* Hsp70 using three dimensional modelling and invitro analyses. *Protein Pept Lett*, **15**: 1117-1125.

Shonhai, A., G Maier, A., M Przyborski, J., L Blatch, G. (2011). Intracellular protozoan parasites of humans: the role of molecular chaperones in development and pathogenesis. *Protein Pept Lett*, **18**: 143-157.

Shonhai, A., G Maier, A., M Przyborski, J., L Blatch, G. (2011). Intracellular protozoan parasites of humans: the role of molecular chaperones in development and pathogenesis. *Protein Pept Lett*, **18**: 143-157.

Silva, M.D., Cooke, B.M., Guillotte, M., Buckingham, D.W., Sauzet, J.P., Scanf, C.L., Contamin, H., David, P., Mercereau-Puijalon, O., Bonnefoy, S. (2005). A role for the *Plasmodium falciparum*

RESA protein in resistance against heat shock demonstrated using gene disruption. *Mol Microbiol*, **56**: 990-1003.

Staines, H.M., Krishna, S. eds. (2012). Treatment and prevention of malaria: antimalarial drug chemistry, action and use. *Springer Science and Business Media.*

Stankiewicz, M., Nikolay, R., Rybin, V., Mayer, M.P. (2010). CHIP participates in protein triage decisions by preferentially ubiquitinating Hsp70-bound substrates. *FEBS J*, **277**: 3353-3367.

Strom, E., Sathe, S., Komarov, P.G., Chernova O.B., Pavlovska, I. (2006). Small-moleculae inhibitor of p53 binding to mitochondria protects mice from gamma radiation. *Nat Chem Biol*, **2**: 474–479.

Szabo, A., Langer, T., Schröder, H., Flanagan, J., Bukau, B., Hartl, F.U. (1994). The ATP hydrolysis-dependent reaction cycle of the *Escherichia coli* Hsp70 system DnaK, DnaJ, and GrpE. *Proc Natl Acad Sci*, **91**: 10345-10349.

Taipale, M., Jarosz, D.F., Lindquist, S. (2010). HSP90 at the hub of protein homeostasis: emerging mechanistic insights. *Nat Rev Mol Cell Biol*, **11**: 515-528

Terasawa, K., Minami, M., Minami, Y. (2005). Constantly updated knowledge of Hsp90. *J Biochem*, **137**: 443-447.

Tuteja, R. (2007). Malaria—an overview. FEBS J, **18**: 4670–4679.

Vos, M.J., Hageman, J., Carra, S., Kampinga, H.H. (2008). Structural and functional diversities between members of the human HSPB, HSPH, HSPA, and DNAJ chaperone families. *Biochemistry*, **47**: 7001-7011.

Walsh, P., Bursać, D., Law, Y.C., Cyr, D., Lithgow, T. (2004). The J-protein family: modulating protein assembly, disassembly and translocation. *EMBO Rep*, **5**: 567-571.

Wang, W., Vinocur, B., Shoseyov, O., Altman, A. (2004). Role of plant heat-shock proteins and molecular chaperones in the abiotic stress response. *Trends Plant Sci*, ***9*:** 244-252.

Wayne, N., Bolon, D.N. (2007). Dimerization of Hsp90 is required for in Vivo Function design and analysis of monomers and dimers. *J Biol Chem*, **282**: 35386-35395.

Wayne, N., Mishra, P. and Bolon, D.N. (2011). Hsp90 and client protein maturation. "In *Mol Chaperones"*. *Humana Press*, 33-44.

Wen, N., Wang, Y., Wen, L., Zhao, S.H., Ai, Z.H., Wang, Y., Wu, B., Lu, H.X., Yang, H., Liu, W.C. and Li, Y. (2014). Overexpression of FOXM1 predicts poor prognosis and promotes cancer cell proliferation, migration and invasion in epithelial ovarian cancer. *J Transl Med*, **12**: 134.

Whitesell, L., Lindquist, S.L. (2005). HSP90 and the chaperoning of cancer. *Nat RevCancer*, **5**: 761-772.

Wichmann, O., Jelinek, T., Peyerl-Hoffmann, G., Mühlberger, N., Grobusch, M.P., Gascon, J., Matteelli, A., Hatz, C., Laferl, H., Schulze, M., Burchard, G. (2003). Molecular surveillance of the antifolate-resistant mutation I164L in imported African isolates of *Plasmodium falciparum* in Europe: sentinel data from TropNetEurop. *Malar J*, **2**: 17.

Witkowski, B., Lelièvre, J., Barragán, M.J.L., Laurent, V., Su, X.Z., Berry, A., Benoit-Vical, F. (2010). Increased tolerance to artemisinin in *Plasmodium falciparum* is mediated by a quiescence mechanism. *Antimicrob Agents Chemother*, **54**: 1872-1877.

Woods, I.G., Wilson, C., Friedlander, B., Chang, P., Reyes, D.K., Nix, R., Kelly, P.D., Chu, F., Postlethwait, J.H., Talbot, W.S. (2005). The zebrafish gene map defines ancestral vertebrate chromosomes. *Genome Res*, **15**: 1307-1314.

World Health Organization. (2015). *World Malaria Report.* Available on: *https://www.who.int/malaria/publications/world-malaria-report-2015/report/en/.*

World Health Organization. (2019). *World Malaria Report.* Available on: *https://www.who.int/malaria/publications/world-malaria-report-2019/en/.*

World Health Organization. (2016). *World Malaria Report.* Available on: *https://www.who.int/malaria/media/world-malaria-report-2016/en/.*

Xiao, J., Kim, L.S., Graham, T.R. (2006). Dissection of Swa2p/auxilin domain requirements for cochaperoning Hsp70 clathrin-uncoating activity in vivo. *Mol Cell Biol*, **17**: 3281-3290.

Yamamoto, S., Subedi, G.P., Hanashima, S., Satoh, T., Otaka, M., Wakui, H., Sawada, K.I., Yokota, S.I., Yamaguchi, Y., Kubota, H., Itoh, H. (2014). ATPase activity and ATPdependent conformational change in the co-chaperone Hsp70/Hsp90-organizing protein (HOP). *J Biol Chem*, **289**: 9880-9886.

Yang, J., Nune, M., Zong, Y., Zhou, L., Liu, Q. (2015). Close and allosteric opening of the polypeptide-binding site in a human Hsp70 chaperone, BiP. *Structure*, **23**: 2191-203.

Young, J.C., Agashe, V.R., Siegers, K., Hartl, F.U. (2004). Pathways of chaperone-mediated protein folding in the cytosol. *Nat Rev Mol Cell Biol*, **5**: 781–791.

Zhang, J., Schröder, G.F., Douglas, N.R., Reissmann, S., Jakana, J., Dougherty, M., Fu, C.F., Levitt, M., Ludtke, S.J., Frydman, J., Chiu, W. (2010). Mechanism of folding chamber closure in a group II chaperonin. *Nature*, **463**: 379–383.

Zininga, T., Achilonu, I., Hoppe, H., Prinsloo, E., Dirr, H.W., Shonhai, A. (2015b) Overexpression, Purification and Characterization of the *Plasmodium falciparum* Hsp70-z (PfHsp70-z) Protein, *PLoS One*, **10**: e0129445.

Zininga, T., Achilonu, I., Hoppe, H., Prinsloo, E., Dirr, H.W., Shonhai, A. (2016). *Plasmodium falciparum* Hsp70-z, an Hsp110 homolog, exhibits independent chaperone activity and interacts with Hsp70-1 in a nucleotide-dependent fashion. *Cell Stress Chaperones*, **21**:499-513.

Zininga, T., Makumire, S., Gitau, G.W., Njunge, J. M., Pooe, O. J., Klimek, H., Scheurr, R., Raifer, H., Prinsloo, E., Przyborski, J.M., Hoppe, H., Shonhai, A. (2015a). Plasmodium *falciparum* Hop (PfHop) interacts with the Hsp70 chaperone in a nucleotide-dependent fashion and exhibits ligand Selectivity. *PLoS One*, **10**: e0135326.

Zininga, T., Pooe, O.J., Makhado, P.B., Ramatsui, L., Prinsloo, E., Achilonu, I., Dirr, H., Shonhai, A. (2017a). Polymyxin B inhibits the chaperone activity of *Plasmodium falciparum* Hsp70. *Cell Stress Chaperones*, **22**: 707-715.

Zininga, T., Ramatsui, L., Makhado, P.B., Makumire, S., Achilinou, I., Hoppe, H., Dirr, H.W., Shonhai, A. (2017b). (-)-Epigallocatechin-3-Gallate inhibits the chaperone activity of *Plasmodium falciparum* Hsp70 chaperones and abrogates their association with functional partners. *Molecules*, **22**: 2139.

Zininga, T., Shonhai, A. (2014). Are heat shock proteins druggable candidates? *Am J Biochem Biotechnol*, **10**: 211- 213.

Zininga, T., Shonhai, A. (2019). Small molecule inhibitors targeting the heat shock protein system of human obligate protozoan parasites. *Int J Mol Sci*, **20**: 5930.

APPENDICES

Appendix A: Additional materials

A1: Table A1. List of reagents used

Reagent	Supplier
Acetic acid	Merck, Germany
Adenosine triphosphate (ATP)	Sigma-Aldrich, USA
Agarose	Merck, Germany
Ammonium persulfate	Sigma-Aldrich, USA
Ampicillin	Melford, UK
Bovine serum albumin	Melford, UK
Bromophenol blue	Merck, Germany
Calcium chloride	Merck, Germany
Chemiluminescence Western blotting Kit	Amersham, USA
Nitrocellulose membrane	Thermo Scientific, USA
Immobilon-P transfer Membrane	Merck, Germany
Coomasie brilliant blue R250	Merck, Germany
Ethidium bromide	Merck, Germany
Glacial acetic acid	Merck, Germany
Glycerol	Merck, Germany
Glycine	Merck, Germany
Imidazole	Merck, Germany
Isopropyl-1-thio-D-galacopyranoside	Sigma-Aldrich, USA
GeneRuler 1kb DNA ladder	Thermo Scientific, USA
Lysozyme	Merck, Germany
Magnesium chloride	Merck, Germany
Methanol	Merck, Germany
Phenylmethylsufonyl fluoride	Merck, Germany
Amicin® Ultra-15 10K centrifuge filter device	Merck, Germany
Sodium chloride	Merck, Germany
Sodium dodecyl sulphate	Merck, Germany
TEMED	Sigma-Aldrich, USA
Tris-HCL	Merck, Germany
Tryptone	Merck, Germany
Tween 20	Melford, UK
Yeast extract	Merck, Germany
Page ruler prestained protein ladder	Thermo Scientific, USA
Nutrient agar	Merck, Germany

Appendix B: Methodology

B1: Preparation of *E. coli* JM109/XL1 Blue competent cells

A single of *E. coli* JM109/ XL1-Blue cells was picked and inoculated into 5 ml of 2 x YT media broth (1.6 % tryptone, 1 % yeast extract, 0.5 % NaCl) containing 100 µg/ml ampicillin (final concentration) and incubated for overnight at 37 ° C incubator with shaking. The following day the overnight culture was transferred into fresh 2 x YT broth (45 ml) containing 100 µg/ml ampicillin and grown to OD_{600}= 0.4-0.6. The culture was centrifuged at 5000 g for 10 minutes at 4 ° C. The supernatant was discarded and the pellet was resuspended with 0.1 M $MgCl_2$ and then incubated on ice for 30 minutes. The suspension was then centrifuged at 5000 g for 10 minutes at 4 ° C. The supernatant was discarded and the remaining pellet was resuspended 0.1 M $CaCl_2$ and incubated on ice for 5 hours. The suspension was then centrifuged at 5000 g for 10 minutes at 4 ° C. After discarding the supernatant, the pellet was resuspended with equal amounts of $CaCl_2$ and 30 % glycerol and incubated on ice for 15-20 minutes before aliquoted. After incubation period, the cells were then aliquoted into 2 ml Eppendorf tubes that were pre-chilled on ice. The cells were then stored at -80 ° C.

B2: Transformation of plasmid DNA

The constructs pQE30/PfHop and pQE30/PfHsp70-1 plasmid were transformed with *E. coli* JM109 competent cells towards DNA extraction and the same constructs were transformed with *E. coli* XL1 Blue competent cells towards expression of each plasmid to produce recombinant proteins (PfHop and PfHsp70-1) respectively. Plasmid DNA (2µl) was added into 100 µL of competent cells. A mixture of cells and DNA was then incubated on ice for 30 minutes. The cells were heated at 42 ° C for 45 seconds and placed back on ice for additional 10 minutes. A volume of 900 µL of fresh 2 x YT broth was added and placed in a shaking incubator at 37 ° C for 1 hour. A volume of 100 µL of cells were streaked onto 2 x YT media (1.6 % tryptone, 1 % yeast extract, 0.5 % NaCl, 1.5 % agar bacteriological) plates containing 100 µg/ml ampicillin. The plates were then incubated overnight at 37 ° C incubator (No shaking).

B3: DNA Extraction

Single colonies of pQE30/PfHop and pQE30/PfHsp70-1 plasmids transformed with *E. coli* JM109 Competent cells were inoculated into 5 ml 2 x YT broth containing 100 µg/ml ampicillin (final concentration) and incubated in a shaking incubator at 37 ° C for overnight. DNA extraction was carried out using GeneJet Plasmid Miniprep Kit from Thermo Scientific. All steps were performed according to the manufacturer's instructions.

Table B1: Restriction digest reaction mixture

Components	**Tube 1 uncut**	**Tube 2 *BamHI***	**Tube 3 *HindIII***	**Tube 4 *BamHI + HindIII***
Deionised water	16	15	14	13
10 x fast digest green buffer	2	2	2	2
DNA	2	2	2	2
Fast digest enzymes	0	1	2	3
Total volumes in (µL)	20	20	20	20

B4: Agarose gel electrophoresis

Agarose gel was used to verify successful restriction digest. Agarose powder (0.8 %) was prepared in 150 ml TAE buffer (400 mM Tris, 0.1 % glacial acetic acid, 10 mM EDTA). The dissolved agarose was heated in a microwave for 2 minutes until the solution becomes clear. The agarose solution was then allowed to cool at room temperature, 10 % ethidium bromide was added and mixed. The gel was then poured into the gel casting tray. The combs were then place immediately in order to create wells. The gel was allowed to solidify at room temperature. Prior to loading the samples, the combs were removed and the gel casting tray was placed in the buffer tank (electrophoresis chamber). The gel was run at 100 v for 1 hour. The gel was visualized using ChemiDoc Imaging System (Bio-Rad, USA).

B5: SDS-PAGE analysis of proteins

Expressions and purifications were analyzed by SDS-PAGE. PfHop and PfHsp70-1 expression and purification samples were prepared with SDS sample buffer (0.25 % Coomasie Brilliant blue (R250); 2 % SDS; 10 % glycerol; 100 mM Tris, 1 % β-mercaptoethanol) in a ratio 4:1. The samples were boiled at 100 ° C for 10 minutes and resolved by 12 % acrylamide resolving gel. Pre-stained protein molecular marker was loaded first (Thermofischer Scientific, USA) followed by samples in respective wells. The gel was then run for 1 hour 20 minutes at 120 v using the Bio-Rad Mini protein electrophoresis system (Bio-Rad, USA) Table A2 and A3 show how running and stacking gels were prepared.

Table B2: 12 % SDS-PAGE running gel (X2)

Reagents	**X2**
Bis (ml)	4.16
1.5 M Tris pH 8.8 (ml)	2.5
10 % SDS (ml)	0.1
H_20 (ml)	3.16
APS (ml)	0.050
TEMED (µl)	20

Table B3: 12 % SDS-PAGE stacking gel (X2)

Reagents	**X2**
Bis (ml)	0.47
0.5 M Tris pH 6.8 (ml)	0.875
10 % SDS (ml)	0.035
H_20 (ml)	2.1
APS (ml)	0.017
TEMED (µl)	20

B6: Western blot analysis of proteins

Western blot analysis was used to confirm all the expression and purification of proteins analyzed by SDS-PAGE (Appendix A7). After completion of SDS-PAGE analysis, the gels were removed from the glasses and immersed in the buffer to equilibrate at 8 ° C for 15-20 minutes. The following were also added, the Whatman filter papers, the two scotchbrite fiber pads and the nitrocellulose membrane. The sandwhich was prepared as follows; filter papers were placed on a scotch brite pad; the gel was placed onto the filter paper carefully to avoid air bubbles; nitrocellulose was placed on top of the gel; additional filter paper was placed on the nitrocellulose and an additional scotch brite was placed on top.The sandwhich was then placed in a eletrophoresis chamber with Western transfer buffer. The transfer was run for one hour at 100 v. The membrane was removed from the tank and rinsed with transfer buffer to ensure no adhering gel left. The membrane was blocked with 5 % non-fat milk made in TBS for 1 hour on a shaker. The membrane was washed three times for a total of 10 minutes using TBS-Tween. The membrane was then incubated with primary antibody for 1 hour followed by washing three times for 10 minutes each to ensure that all unbound primary antibody is removed. The membrane was incubated with secondary antibody for 1 hour followed by washing three times using TBS-Tween. The membrane was visualized using Enhanced chemiluminescence (ECL) according to manufacturer's instructions and further viewed by ChemiDoc Imaging system (Bio-Rad, USA).

B7: Quantification of proteins using Bradford assay

The quantity of proteins was determined by Bradford's assay (Bradford, 1976). BSA concentrations were prepared with concentrations ranging from 0-100 µg/ml in 0.15 M NaCl using a 96-well plate. A volume of 200 µl of Bradford reagents (Sigma-Aldrich, USA) was added to 10 µl of protein. The reaction mixture was incubated at room temparure for 5-10 minutes. The absorbance was measured at 595 nm using a SpectaMax M3 (Molecular devices, USA). The protein samples were treated similarly. All the readigs were prepared in triplets and average for each was determined. The protein concentration was determined from the standard curve.

Appendix C: Supplementary data

C1: Bradford's assay standard curve

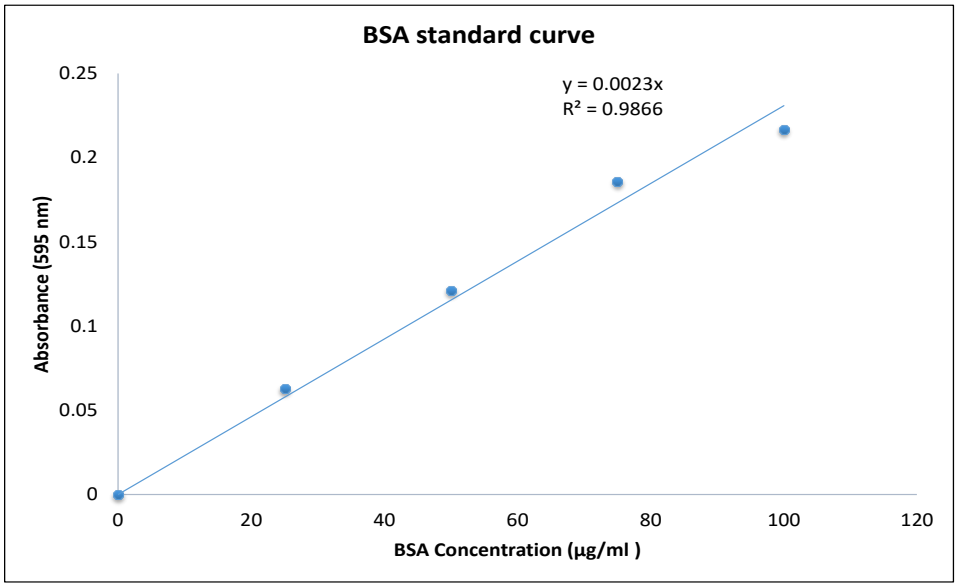

Figure C1. BSA standard curve for protein determination. Protein (PfHop/ PfHsp70-1) concentrations were determined by bradford's reagents. The equation Y= 0.00023x; R^2= 0.9866 was used to calculate the concentration of protein in mg/ml.

C2. Nucleotide equilibrium binding of PfHsp70-1/ PfHsp70-1$_{NBD}$ and PfHop

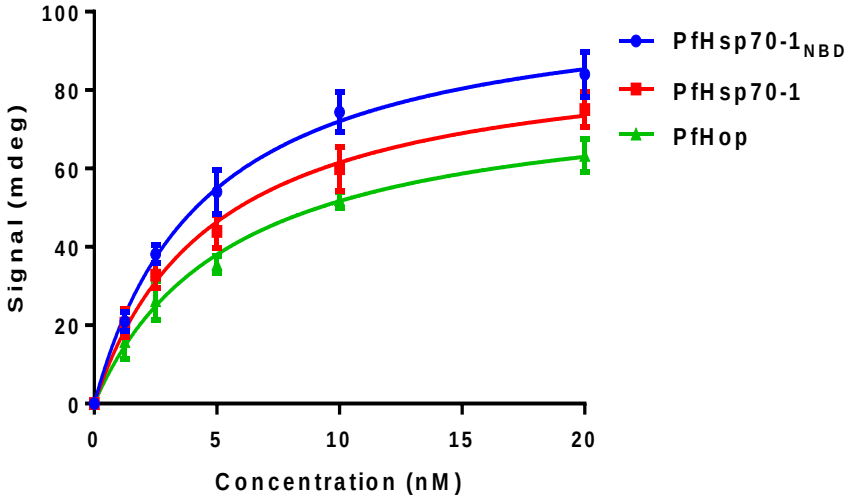

Figure C2: Equilibrium analysis of ATP binding by PfHsp70-1/ PfHsp0-1$_{NBD}$ and PfHop. The data represents equilibrium analysis of ATP binding contants for all three proteins. The interaction between ligand and analyte was determined using equilibrium SPR analysis. Standard errors represent three independent assays conducted using independent protein batches.

C3. Analysis of inhibitors binding to PfHsp70-1$_{NBD}$

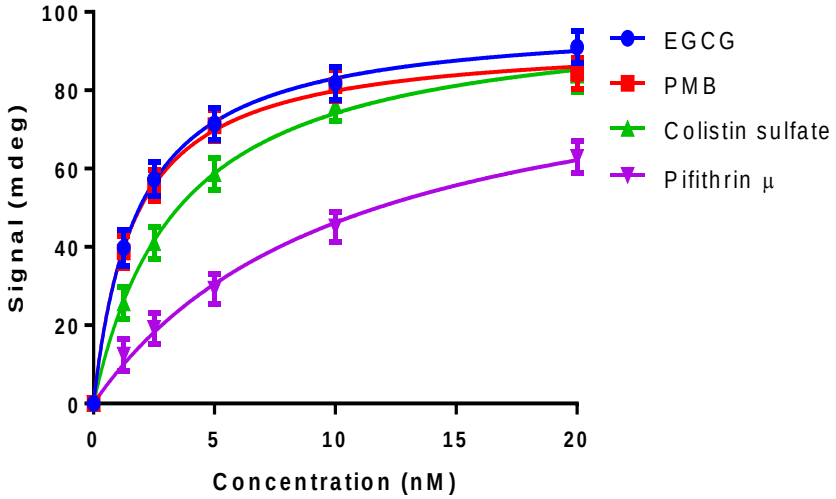

Figure C3: Equilibrium analysis of colistin sulfate and pifithrin μ binding to PfHsp70-1$_{NBD}$. PfHsp70-1$_{NBD}$ was immobilized as ligand at a concentration 100 µg/mL. The assay was conducted in the presence of variable levels of EGCG, PMB, colistin sulfate and pifithrin µ. The interaction between ligand and analyte was determined using equilibrium SPR analysis. Standard errors represent three independent assays conducted using independent protein batches.

C4. Table C1: Binding kinetics obtained from ELISA analysis for the interaction of PfHsp70-1 with PfHop (in the presence and absence of nucleotides) interchanging the status of ligand and analyte respectively

Ligand	Analyte	Nucleotides	Kd (nM)	R^2
PfHsp70-1	PfHop	NN	15.85 (+/- 0.05)	0.97
		ADP	13.07 (+/- 0.7)*	0.99
		ATP	47.01 (+/- 0.1)***	0.98
PfHop	PfHsp70-1	NN	18.81 (+/- 0.01)	0.89
		ADP	21.58 (+/- 0.08)	0.92
		ATP	55.65 (+/- 0.05)***	0.98

Table legends: Kd dissociation rate constant, R^2 represents the goodness of the fit model. The standard errors are shown in the brackets. Three independent analyses were conducted during an ELISA assay alternating the status of ligand and analyte. Standard errors are shown in brackets. Statistical analysis was done using one-way ANOVA ($p < 0.05$) represents statistically significant differences in affinities. The asterisk (*) represents significant differences.

C5. Table C2: The half maximal inhibitory concentration (IC_{50}) of colistin sulfate and pifithrin μ obtained from ELISA analysis for the interaction of PfHsp70-1 with PfHop interchanging the status of ligand and analyte respectively

Ligand	Analyte	Name of the inhibitor	$LogIC_{50}$	IC50 (nM)	R^2
PfHsp70-1	PfHop	EGCG	1.122	13.23	0.97
		PMB	1.131	13.53	0.96
		Colistin sulfate	1.187	15.39	0.96
		Pifithrin μ	1.427	6.72	0.92
PfHop	PfHsp70-1	EGCG	1.164	14.57	0.98
		PMB	1.097	12.50	0.96
		Colistin sulfate	1.127	13.39	0.94
		Pifithrin μ	1.581	38.13	0.95

Table legends: IC50 represents half maximal inhibitory concentration, R^2 represents the goodness of the fit model. Three independent analyses were conducted during an ELISA assay alternating the status of ligand and analyte. Standard errors are shown in brackets.

C6. Table C3: ELISA statistical analysis for the interaction of PfHsp70-1 and PfHop (in the presence and absence of nucleotides) interchanging the status of ligand and analyte respectively

Ligand/ analyte	Comparison datasets	Significant? (Yes/No)	Summary (*/ ns)	P value
PfHsp70-1/ PfHop	NN vs. ADP	Yes	*	0.0290
	NN vs. ATP	Yes	***	0.0002
	ADP vs. ATP	Yes	***	0.0006
PfHop/ PfHsp70-1	NN vs. ADP	No	ns	0.2028
	NN vs. ATP	Yes	***	0.0004
	ADP vs. ATP	Yes	***	0.0007

Table legends: ns- Not significant

C7. Table C4: ELISA statistical analysis for the effect of colistin sulfate and pifithrin μ on the interaction of PfHsp70-1 and PfHop interchanging status of ligand and analyte respectively

Ligand/ analyte	Comparison datasets	Significant? (Yes/No)	Summary (*/ ns)	P value
PfHsp70-1/ PfHop	No inhibitor vs. EGCG	Yes	****	< 0.0001
	No inhibitor vs. PMB	Yes	****	< 0.0001
	No inhibitor vs. Colistin sulfate	Yes	****	< 0.0001
	No inhibitor vs. Pifithrin μ	Yes	****	< 0.0001
	Colistin sulfate vs. Pifithrin μ	No	ns	0.5689
PfHop/ PfHsp70-1	No inhibitor vs. EGCG	Yes	****	< 0.0001
	No inhibitor vs. PMB	Yes	****	< 0.0001
	No inhibitor vs. Colistin sulfate	Yes	****	< 0.0001
	No inhibitor vs. Pifithrin μ	Yes	****	< 0.0001
	Colistin sulfate vs. Pifithrin μ	No	ns	0.1173

Table legends: ns- Not significant

C8. Table C5: SPR assay statistical analysis for the interaction of PfHsp70-1 and PfHop (in the presence and absence of nucleotides) interchanging the status of ligand and analyte respectively

Ligand/ analyte	Comparison datasets	Significant? (Yes/No)	Summary (*/ ns)	P value
PfHsp70-1/ PfHop	NN vs. ADP	Yes	*	0.0137
	NN vs. ATP	Yes	***	< 0.0001
	ADP vs. ATP	Yes	****	< 0.0001
PfHop/ PfHsp70-1	NN vs. ADP	No	ns	0.0570
	NN vs. ATP	Yes	***	0.0001
	ADP vs. ATP	Yes	****	< 0.0001

Table legends: ns- Not significant

C9. Table C6: SPR assay statistical analysis for the effect of colistin sulfate and pifithrin μ on the interaction of PfHsp70-1 and PfHop interchanging status of ligand and analyte respectively

Ligand/ analyte	Comparison datasets	Significant? (Yes/No)	Summary (*/ ns)	P value
PfHsp70-1/ PfHop	NN vs. EGCG	Yes	****	< 0.0001
	NN vs. PMB	Yes	****	< 0.0001
	NN vs. Colistin sulfate	Yes	****	< 0.0001
	NN vs. Pifithrin μ	Yes	****	< 0.0001
	Colistin sulfate vs. Pifithrin μ	No	ns	0.0519
PfHop/ PfHsp70-1	NN vs. EGCG	Yes	****	< 0.0001
	NN vs. PMB	Yes	****	< 0.0001
	NN vs. Colistin sulfate	Yes	****	< 0.0001
	NN vs. Pifithrin μ	Yes	****	< 0.0001
	Colistin sulfate vs. Pifithrin μ	Yes	*	0.0490

Table legends: ns- Not significant